

Performance Analysis of Digital Modulation Schemes used in Mobile Radio

by

Bassam Mohamed Hashem

A Thesis Presented to the

FACULTY OF THE COLLEGE OF GRADUATE STUDIES

KING FAHD UNIVERSITY OF PETROLEUM & MINERALS

DHAHRAN, SAUDI ARABIA

In Partial Fulfillment of the
Requirements for the Degree of

MASTER OF SCIENCE

In

ELECTRICAL ENGINEERING

June, 1994

INFORMATION TO USERS

This manuscript has been reproduced from the microfilm master. UMI films the text directly from the original or copy submitted. Thus, some thesis and dissertation copies are in typewriter face, while others may be from any type of computer printer.

The quality of this reproduction is dependent upon the quality of the copy submitted. Broken or indistinct print, colored or poor quality illustrations and photographs, print bleedthrough, substandard margins, and improper alignment can adversely affect reproduction.

In the unlikely event that the author did not send UMI a complete manuscript and there are missing pages, these will be noted. Also, if unauthorized copyright material had to be removed, a note will indicate the deletion.

Oversize materials (e.g., maps, drawings, charts) are reproduced by sectioning the original, beginning at the upper left-hand corner and continuing from left to right in equal sections with small overlaps. Each original is also photographed in one exposure and is included in reduced form at the back of the book.

Photographs included in the original manuscript have been reproduced xerographically in this copy. Higher quality 6" x 9" black and white photographic prints are available for any photographs or illustrations appearing in this copy for an additional charge. Contact UMI directly to order.

UMI

University Microfilms International
A Bell & Howell Information Company
300 North Zeeb Road, Ann Arbor, MI 48106-1346 USA
313/761-4700 800/521-0600

Order Number 1360421

**Performance analysis of digital modulation schemes used in
mobile radio**

Hashem, Bassam Mohamed, M.S.

King Fahd University of Petroleum and Minerals (Saudi Arabia), 1994

U·M·I
300 N. Zeeb Rd.
Ann Arbor, MI 48106



PERFORMANCE ANALYSIS OF DIGITAL MODULATION
SCHEMES USED IN MOBILE RADIO

BY

BASSAM MOHAMED HASHEM

A Thesis Presented to the
FACULTY OF THE COLLEGE OF GRADUATE STUDIES
KING FAHD UNIVERSITY OF PETROLEUM & MINERALS
DHAHRAN, SAUDI ARABIA

In Partial Fulfillment of the
Requirements for the Degree of

MASTER OF SCIENCE

In

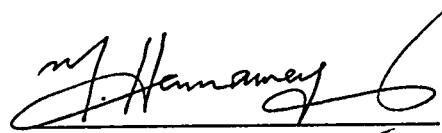
ELECTRICAL ENGINEERING

JUNE 1994

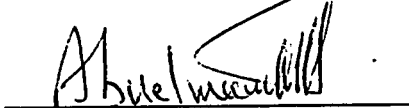
King Fahd University of Petroleum & Minerals
College of Graduate Studies

This thesis, written by **BASSAM MOHAMED HASHEM** under the direction of his Thesis Advisor and approved by his Thesis Committee, has been presented to and accepted by the Dean of the college of Graduate Studies, in partial fulfillment of the requirements for the degree of **MASTER OF SCIENCE** in **ELECTRICAL ENGINEERING**.

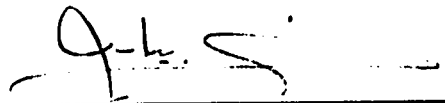
Thesis Committee




Dr. M. S. El-Hennawey (Advisor)



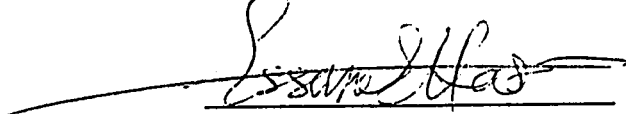
Dr. M. Abuelma'atti (Member)



Dr. Khaled Biyari (Member)




Dr. Hussein Baher (Member)



Dr. Essam Hassan (Member)


Department Chairman


Dean, College of Graduate Studies

18.6.94
Date



Dedicated to

My Parents who taught me how to give.

Acknowledgement

Praise be to Allah for helping me in finishing this thesis and in all my life aspects.

I wish to thank my thesis advisor Dr. Samy El-Hennaway for his continuous guidance and encouragement. I wish to thank all the members of my thesis committee for their help and valuable suggestions. I would like also to thank King Fahd University of Petroleum and Minerals for supporting me during my work.

Table of Contents

	page
List of Figures	vi
List of Tables	ix
Abstract (English)	x
Abstract (Arabic)	xi
1. Introduction	1
1.1 Overview	1
1.2 Literature Review	4
1.3 Problem Formulation	
1.4 Thesis Contribution	8
1.5 Thesis Organization	8
2. Limitations in Mobile Communications	10
2.1 Introduction	10
2.2 Digital Communication	11
2.3 Transmission Media	14
2.4 Transmission Impairments	25
2.4.1 AWGN	25
2.4.2 Intersymbol Interference	27
2.4.2 Power Amplifier Nonlinearity	35
2.5 Summary	40
3. Analysis of $\pi/4$ -DQPSK, GMSK and QAM Systems	43
3.1 Introduction	43
3.2 Phase Shift Keying	44
3.3 Gaussian Minimum Shift Keying	50
3.4 Quadrature Amplitude Modulation	75
3.5 Summary	85

	page
4. Performance Evaluation of $\pi/4$-DQPSK, GMSK and QAM Systems Under Different Mobile Channel Impairments	86
4.1 Introduction	86
4.2 Baseband Representation	88
4.3 The $\pi/4$-Shifted-DQPSK	90
4.4 The GMSK System	94
4.5 QAM System	109
4.6 Summary	130
5. Conclusions and Recommendations for Future Work	132
5.1 Conclusions	132
5.2 Recommendations for Future Work	136
Appendix A	137
References	155

List of Figures

		Page
2.1	Pulse degradation and regeneration	13
2.2	Three basic forms of signaling binary information	13
2.3	Simplified illustration of multipath channel	19
2.4	Diffuse multipath model	19
2.5	Rayleigh distribution	23
2.6	Rician distribution	23
2.7	Ideal lowpass filter characteristic	29
2.8	Effect of channel distortion	30
2.9	Linear adaptive equalizer based on the LMS criterion	36
2.10	Characteristic of an Intelsat IV TWT	38
2.11	Power amplifier nonlinearities	41
3.1	QPSK modulation	45
3.2	QPSK and OQPSK signal constellations	49
3.3	$\pi/4$ -shifted-QPSK signal constellations	49
3.4	Minimum tone spacing for noncoherently detected orthogonal FSK	54
3.5	CPFSK signalling	55
3.6	MSK parallel type modulator	58
3.7	Timing diagrams for MSK modulators	59
3.8	Receiver for MSK	61
3.9	Normalized PSD for BPSK, QPSK, OQPSK and MSK	62
3.10	Fractional out of band power for OQPSK and MSK	64
3.11	Gaussian filter characteristics	68
3.12	Bandwidth filter characteristics	68
3.13	Power spectra of GMSK	70

	Page
3.14 Adjacent channel interference of GMSK	70
3.15 Normalized minimum signal distance of GMSK	72
3.16 Degradation of required E_b/N_0 for attaining BER of 10^{-3}	73
3.17 GMSK parallel type modulator	74
3.18 Gray encoding for 16 QAM	77
3.19 Differential encoding for 16 QAM	77
3.20 Signals used in the V32 modem	80
3.21 Gray encoding for star 16 QAM	83
3.22 Rings ratio optimization for Star QAM	84
4.1 $\pi/4$ -DQPSK under AWGN & Rayleigh fading channels ..	93
4.2 $\pi/4$ -DQPSK under frequency selective fading channels ..	93
4.3 Equalized performance of $\pi/4$ -DQPSK	95
4.4 Conventio MSK receiver	97
4.5 New proposed transmitter structure for the GMSK	97
4.6 PSD of GMSK system	98
4.7 The GMSK signal demodulated as an FM signal	100
4.8 GMSK under AWGN and Rayleigh fading channels	104
4.9 GMSK and MSK under frequency selective fading	107
4.10 Equalized performance of GMSK	108
4.11 Typical communication system	110
4.12 Different 16-QAM systems under AWGN	113
4.13 Nonlinearly amplified 16-QAM under AWGN	115
4.14 Nonlinearly amplified 16-QAM under AWGN	116

	Page
4.15 Nonlinearly amplified star 16-QAM at different backoffs	118
4.16 Nonlinearly amplified star 16-QAM at a fixed backoff	120
4.17 16-QAM under Rayleigh fading (backoff = 7 dB)	121
4.18 16-QAM under Rayleigh fading (backoff = 5 dB)	121
4.19 16-QAM under frequency selective fading ($u = .06$)	123
4.20 16-QAM under frequency selective fading ($u = .1$)	123
4.21 Nonlinearity amplified square 16-QAM under frequency selective fading	125
4.22 Nonlinearity amplified differential 16-QAM under frequency selective fading	126
4.23 Nonlinearity amplified differential star 16-QAM under frequency selective fading	126
4.24 Equalized square 16-QAM ($u = .1$)	127
4.25 Equalized differential square 16-QAM ($u = .1$)	127
4.26 Equalized star 16-QAM ($u = .1$)	128
4.27 Equalized differential star 16-QAM ($u = .1$)	128
5.1 Equalized performance of three systems	134

List of Tables

	Page
3.1 Phase of the $\pi/4$ -shifted-DQPSK signal	50
3.2 Implementation of 16 QAM	81
4.1 Different E_b/N_0 values to achieve a BER of 10^{-3} for different saturation backoff values	117
4.2 Optimum ratio for different saturation backoff values	119

Abstract

Name : Bassam Mohamed Hashem
Title: Performance Analysis of Digital Modulation Schemes used in
Mobile Radio
Major Field: Electrical Engineering
Date of Degree: June 1994

Mobile communication is becoming an important field where people need to communicate while moving to follow rapid changes occurring in the world. The mobile communication channel is considered as a multipath fading channel where frequency selective fading can occur. Also, in the mobile environment, the available bandwidth is limited and usually non-linear power amplifiers are used. Under all these severe conditions, many digital modulation schemes have been investigated to be used for mobile radio.

The Gaussian minimum shift keying (GMSK) is the modulation scheme used in the GSM system which is installed in Europe while the modulation scheme used in North America is the $\pi/4$ -shifted-DQPSK. The QAM system is being proposed for mobile communication because of its spectral efficiency but it suffers from employing non-constant envelope signals which creates problems when nonlinearity is present.

The aforementioned schemes are simulated in this thesis under different channel conditions and their bit error rate(BER) performance is evaluated. The effect of non-linear amplification to the signals on the QAM systems is also investigated. Linear equalization is employed to alleviate the effect of the frequency-selective fading channel.

Simulation results showed that both the GMSK & the $\pi/4$ -shifted-DQPSK have comparable BER performance. However, this BER increases in the case of QAM. To reduce this BER and make it comparable with the other two systems, the transmission rate has to be reduced giving only 20% bit rate advantage to the QAM system.

A new transmitter structure for the GMSK system is proposed. It is more spectrally efficient compared to the existing transmitter. This reduces the interference between adjacent channels which is an important property especially in the mobile radio.

خلاصة الرسالة

تقييم اداء طرق التضمين الرقمية المستخدمة في الراديو السيار

لقد أصبح مجال الاتصالات المتنقلة ذا أهمية كبرى لاحتياج مستخدميها للاتصال أثناء التنقل وذلك للمتابعة المباشرة لما يحدث في العالم. وتعتبر قناة الاتصال المتنقل إحدى القنوات متعددة المسارات المضمحلة حيث يمكن حدوث الاضمحلال الترددي. وتعتبر قنوات الاتصال المتنقلة محدودة من حيث حزم التردد المتاحة وتستخدم في اجهزتها مكبرات غير خطية. ويتم تحت هذه الظروف القاسية التحقق من ملائمة مختلف طرق التضمين الرقمية.

وتستخدم طريقة تفتيح الازاحة الصغرى الجاوسية-GMSK- في نظام ال GMS والذي تم تطبيقه في اوروبا بينما تستخدم طريقة ط/٤ -DQPSK المزاحة في أمريكا الشمالية. أما طريقة تضمين المقدار العمودي-QAM- فما تزال تحت التجربة وقد تم اقتراحها نتيجة لكفائتها من الناحية الطيفية وذلك بالرغم من استخدامها لموجات ذات غلاف غير ثابت.

وقد تم في هذه الرسالة محاكاة الانظمة سابقة الذكر تحت مختلف الظروف وقد تم ايضا قياس معدل الخطأ في الخانة الثنائية لكل نظام. بالاضافة الى ذلك تم التحقق من أهمية استخدام المعادل الخطي خصوصا تحت ظروف الاضمحلال الترددي.

وقد كانت النتائج المستخلصة من هذه الرسالة ان كلا من نظامي GMSK و ط/٤ -DQPSK المزاح لهما نفس معدل الخطأ بينما يزداد هذا المعدل اذا ما استخدم نظام QAM. ولكي يتم الحصول على نفس معدل الخطأ فقد اثبتت التجارب انه يلزم تخفيض معدل الارسال في نظام QAM بحيث تصل الزيادة الخاصة في هذا النظام الى عشرين بالمائة (٢٠٪) فقط.

وقد قمنا في هذه الرسالة باقتراح هيكل جديد للمرسل من خلال نظام GMSK والذي اثبتت كفائته الفعالة من الناحية الطيفية مما يقلل من التداخل بين الموجات قريبة التردد وذلك بالمقارنة مع المرسل المستخدم حاليا. وتعتبر هذه ميزة هامة خصوصا في مجال الاتصالات المتنقلة.

CHAPTER ONE

INTRODUCTION

1.1 Overview

Mobile communications have attracted the attention since the early days of introducing wireless communication because of the flexibility they give to the user enabling him to communicate from different locations and even while he is moving around. There has been a rapid growth in the demand for new channels which is faced by the limited available spectrum. Also, digital communication systems outperform analog ones in terms of noise performance and flexibility. Hence, there has been a great deal of search for a digital communication system that is bandwidth efficient and has a low bit error rate (BER) at a relatively low signal-to-noise ratio (SNR).

Minimum shift keying (MSK) is a well-known modulation technique which is a special type of frequency shift keying (FSK). From the viewpoint of mobile radio use, the out-of-band radiation power in the adjacent channel should be generally suppressed by 60–80 dB below that in the desired channel [Hirade 1981]. MSK fails to satisfy this severe requirement. Thus, the MSK can be filtered to reduce the out-of-band power. However, this results in a higher BER. The used filter

is of Gaussian type which has almost a constant group delay. The filtered MSK is termed Gaussian MSK (GMSK). GMSK has been adopted as the modulation standard for the pan-European digital cellular network GSM [Lee 1989].

Phase shift keying (PSK) is a well-known digital modulation scheme where the phase of the carrier is keyed according to the incoming data. In quaternary phase shift keying (QPSK), every two bits (dibit) are combined together and the carrier is given a certain phase from four possible phases according to the dibit. The $\pi/4$ -shifted-QPSK is viewed as the superposition of two QPSK signals offset by 45 degrees relative to each other. By differentially encoding the data, the $\pi/4$ -shifted-differential QPSK ($\pi/4$ -shifted-DQPSK) system has robustness against phase ambiguity at the receiver. The $\pi/4$ -shifted-DQPSK has been adopted in North American Cellular network [Lee 1989].

Future mobile systems are supposed to provide data communications at high rates with addition to voice. This requires a higher order spectrally efficient digital modulation scheme. Quadrature amplitude modulation schemes are considered good candidates. QAM systems suffer from having a non-constant envelope and hence are considered inefficient when operating in non-linear environments. Such non-linearity is usually introduced by power amplifiers at the transmission stage.

Power amplifiers are usually used to amplify the transmitted signal. Ampli-

fiers need to be power efficient since the power sources are limited at subscriber radio units and hence the operating point is usually close to the saturation region. When operating near the saturation region, power amplifiers exhibit non-linear behavior both in the amplitude (AM/AM distortion) and in the introduced phase shift (AM/PM distortion). In such a non-linear environment, the magnitude and the phase of the output voltage are not a linear function of the input voltage [Abulma'atti 1984].

Mobile radio channels exhibit a phenomenon called fading. The transmitted signal is reflected by surrounding buildings and hence reaches the receiver via many different paths. These received signals can add constructively or destructively resulting in fluctuations in the magnitude of the received signal which is termed fading. The fading channel is usually modeled as a Rayleigh model where it is assumed that the signal amplitude is distributed according to the Rayleigh distribution [Haykin 1988]. Each channel has a coherence bandwidth which can be measured by known techniques. If the bandwidth of the transmitted signal is large compared to the coherence bandwidth of the channel, the channel is said to be frequency selective and the signal is severely distorted. The channel is called frequency non-selective when its coherence bandwidth is large compared to the bandwidth of the transmitted signal. The channel issue will be considered in chapter two.

Several techniques have been investigated in order to alleviate the effect of fading to decrease the BER in mobile radio . Those include diversity (space, frequency, time), channel coding, base-band waveform coding, spread spectrum and channel equalization. Equalizers are used to complement the effect of the channels in frequency-selective fading and can enhance the system performance considerably [Proakis 1989].

The performance of the three aforementioned systems under additive white Gaussian noise, Rayleigh fading and frequency selective fading channels will be investigated. The effect of non-linear power amplifiers on the QAM system will be examined too.

1.2 Literature Review

Minimum shift keying (MSK) is a special case of a frequency shift keying (FSK) technique with the minimum spacing required between signals to keep them orthogonal. MSK can be implemented as a binary FM signal [Hirade 1981] or it can be implemented in a similar way of implementing a QPSK signal with the difference that the modulating pulses are sinusoidal [Peebles 1991]. The performance of the MSK system in AWGN and Rayleigh fading is well known and the system performance when operating under a frequency selective channel has been reported

in the literature [Justin 1987]. The Gaussian MSK (GMSK) was introduced by Hirade in 1981. The system performance under AWGN and Rayleigh fading was investigated. The GMSK is used in Europe.

Phase shift keying (PSK) is a well-known bandwidth efficient digital modulation technique. The $\pi/4$ -shifted-DQPSK belongs to PSK systems. The $\pi/4$ -shifted-QPSK characteristics were reported in [Fung 1993]. The performance of the system under AWGN is equal to that of QPSK which is well reported in the literature [Haykin 1988]. The system performance when modeled as a frequency selective Rayleigh fading channel corrupted by AWGN and co-channel interference (CCI) is reported in [Lin 1991]. The system is used in North America.

Quadrature amplitude modulation techniques are used because of their high spectral efficiency. Many types of QAM systems (square, star, differential) are reported in literature. The recommendations of the CCITT for the V.32 modems use a 16 differential QAM (16 DQAM) for 9600 bit/s and 14.4 kbps. The performance of 16 QAM systems in AWGN is very well reported in literature. These systems performance under Rayleigh fading was reported in [Adachi 1992]. The performance of square 16 QAM under frequency selective fading with the *rms* delay spread as a parameter was investigated in [Justin 1989].

Other signal constellations suitable for mobile communication has been proposed

[Daido, Morais]. More detailed analysis of the three modulation schemes; GMSK, $\pi/4$ -shifted-DQPSK and 16 QAM is presented in Chapter Three.

Modeling the communication channel topic has received a considerable effort since the early days of mobile communication. In order to simulate a communication system, every system component should be represented by a mathematical model. The Rayleigh fading model is widely used to model the channel. However, in the mobile radio environment where the signal is delayed and received via different paths in a random manner, a more sophisticated model is required. One of such channel models is the multipath radio channel which is very well documented in [Shanmugan 1992]. More details about the channel modeling issue can be found in [Rummler, Garber, Seymour]. Specific channel models will be described in Chapter Two.

1.3 Problem Formulation

The mobile radio is a unique environment where the available spectrum is limited and the out-of-band radiation power in the adjacent channel should be kept at least 60 dB below that in the desired channel. This is to reduce the interference between adjacent channels. The mobile radio channel is also known to suffer from the multipath fading phenomenon which degrades the system performance

considerably.

The GMSK and the $\pi/4$ -shifted-DQPSK are already in use while the 16 QAM system performance is being proposed because of its spectral efficiency [Justin 1989]. The first two systems use waveforms that have a constant envelope while the 16 QAM uses waveforms with different magnitudes making it vulnerable when operating in a non-linear environment.

Non-linearity can be introduced by power amplifiers operating near saturation in order to achieve high power efficiency. Non-linear distortion can be in both the magnitude (AM/AM) and the introduced phase shift (AM/PM).

In this thesis, we find that the parallel GMSK modulator gives better performance over the one being used and suggested by [Hirade 1981]. Different types of 16 QAM (square, star and differential) will be simulated. The effect of (AM/AM) and (AM/PM) distortions introduced by power amplifiers effect on these non-constant envelope techniques is investigated. Linear equalization will be used to alleviate the effect of distortions introduced by the frequency selective channel. In the case of star QAM (SQAM), it will be investigated if there is an optimum ratio between the outer ring and the inner ring when the waveforms are non-linearly amplified. An optimum ratio of 1.8 was reported in [Chow 1992] in the case of AWGN.

The $\pi/4$ -shifted-DQPSK system performance under frequency selective fading is investigated, too. Linear equalization will be used to see its effect on the system performance.

The performance analysis will be made using computer simulation and the systems performance will be compared in terms of bit error rate (BER) and spectral efficiency.

1.4 Thesis Contribution

In this thesis, a thorough comparison will be made between the three aforementioned systems under different channel models. The objective will be to see to what extent the performance can be sacrificed in order to gain a reduction in the required bandwidth.

1.5 Thesis Organization

The thesis organization will be as follows. Chapter Two is devoted to the explanation of transmission impairments which include additive white Gaussian noise (AWGN), intersymbol interference (ISI) caused by both filtering and by frequency selective fading and power amplifiers non-linearity both in magnitude and phase. Channel equalization which is used to alleviate the effect of ISI will be

discussed too. Chapter three will consider the three systems under study, GMSK, $\pi/4$ -shifted-DQPSK and 16 QAM (square, star and differential). Minimum shift keying (MSK) properties and ways of implementing it are discussed. The Gaussian filters (both at the transmitter and the receiver) optimum bandwidth are discussed. Ways to implement the other two systems are investigated indicating the usefulness of differentially encoding the data before modulating the carrier.

Chapter Four will contain the results of computer simulation of the three systems operating under AWGN, Rayleigh fading and frequency selective fading. The effect of the non-linear power amplifiers on 16 QAM systems are also shown. Furthermore, the performance improvement due to equalization is evaluated. The simulation objective is to compare the performance of the three systems under different channel environments. The main results, conclusions and future work are presented in the last chapter.

CHAPTER TWO

LIMITATIONS IN MOBILE COMMUNICATION

2.1 Introduction

Although the earliest developments of radio and mobile communication technologies were aimed at specific applications, they were quickly adapted to suit the needs of professional organizations in a variety of fields. Current uses of land mobile communications are diverse and difficult to separate. Some common modes of use include:

Paging: A person is signaled that there is a message waiting to be received.

Dynamic Routing: A vehicle or a person is redirected after leaving their base of operation which reduces the response time.

Emergency Beaconing: Notification of a base station in case of emergency by specialized one-way beacon systems.

Data Transmission: Provision of data received on mobile printout devices.

Conversation: The verbal exchange of information for personal objectives.

In this chapter, digital communication is introduced. The effect of the trans-

mission media (channel) on the transmitted signals in a mobile environment is discussed. Also, a general review is presented for some transmission impairments like additive white Gaussian noise (AWGN), intersymbol interference (ISI) and nonlinear power amplifiers.

2.2 Digital Communication

There are many reasons to explain the conversion from analog to digital systems in both the military and commercial sectors. The main advantage of digital systems over analog ones is that digital signals can be reconstructed in a much easier way compared to analog signals. Fig. 2.1 shows a typical digital pulse propagating through a certain transmission media (channel). The shape of the pulse is affected by two factors. All practical channels have a nonideal transfer function causing distortion to the ideal pulse. Noise or other interference further distorts the pulse. Before the pulse degrades to an ambiguous state, it can be conditioned and amplified by a digital amplifier (repeater) and the original pulse shape is retransmitted.

Digital circuits operate in one of two states, fully-on or fully-off. To cause an error, the disturbance must be large enough to cause transition from one state to another. In contrast, analog signals can take an infinite number of shapes. With

analog signals a small disturbance can cause an unacceptable level of distortion to the reproduced signal. Moreover, this distortion can not be removed by amplification since the noise is irrevocably bound to the transmitted signal. Hence, using digital techniques, very low error rates are possible through some error detection and correction techniques which are not available with analog transmission.

Digital circuits are also more reliable and can be implemented at lower cost than analog circuits. The implementation of digital hardware is more flexible than analog hardware. The combining of digital signals using time division multiplexing (TDM) is simpler than the combining of analog signals using frequency division multiplexing (FDM). Also, digital techniques lend themselves naturally to functions that protect against interference and jamming or that provide encryption and privacy [Sclar 1988].

Digital transmission has some disadvantages compared to analog transmission. The major disadvantage of digital communication is the requirement of a greater bandwidth compared to analog transmission. Also, digital transmission requires more synchronization.

Digital Modulation:

When digital data is transmitted over a band-pass channel, it is necessary

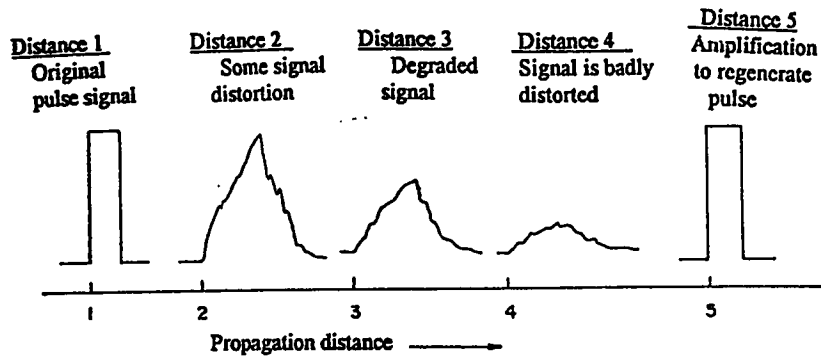


Fig 2.1 Pulse degradation and regeneration

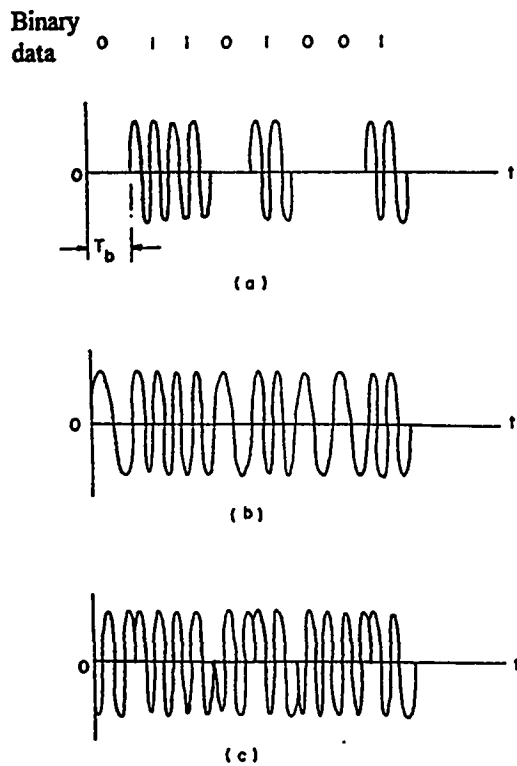


Fig 2.2 Three basic forms of signaling binary information
 (a) Amplitude-shift Keying
 (b) Frequency-shift Keying
 (c) Phase-shift Keying

to modulate the incoming data onto a carrier wave (usually sinusoidal) with fixed frequency limits determined by the channel. The channel may involve a microwave radio link, or satellite channel, etc. The modulation process involves switching or keying the amplitude, frequency or phase of the carrier according to the incoming data. Hence, there are three basic signaling techniques known as amplitude-shift keying (ASK), frequency-shift-keying (FSK) and phase shift keying (PSK), see Fig. 2.2. FSK and PSK signals have a constant envelope making them impervious to amplitude nonlinearities and hence they are more widely used in practice than ASK signals [Haykin 1988].

2.3 Transmission Media

2.3.1 Band Limited Channels

When the channel bandwidth is unrestricted (which is never the case), it only affects the transmitted signals by introducing an attenuation factor and a phase shift in addition to the additive white Gaussian noise (AWGN). When the channel is band-limited, its effect can still be modeled by a simple attenuation factor and a phase shift provided that the signal bandwidth is small compared to the channel bandwidth. However, in this case, the available channel bandwidth will not be utilized properly.

Let the channel transfer function be $C(f)$ with an equivalent impulse response of $c(t)$. Let the transmitted signal be [Proakis 1989]

$$s(t) = \text{Re} [v(t)e^{j2\pi ft}] \quad (2.1)$$

where $v(t)$ is the lowpass transmitted signal. The equivalent lowpass received signal will be

$$r(t) = \int_{-\infty}^{\infty} v(\tau)c(t - \tau)d\tau + n(t) \quad (2.2)$$

where $n(t)$ represents the AWGN and $c(t)$ is the lowpass impulse response of the channel.

If the channel bandwidth is limited to W Hz, then any component of $v(f)$ above $|f| = W$ will not pass through the channel and hence the bandwidth of the transmitted signal is restricted to W Hz also.

Within the bandwidth of the channel, the frequency response of the channel $C(f)$ can be expressed as

$$C(f) = |C(f)|e^{j\theta(f)} \quad (2.3)$$

where $|C(f)|$ is the amplitude response characteristic and $\theta(f)$ is the phase response characteristic. The delay response characteristic $\tau(f)$ is defined as

$$\tau(f) = -\frac{1}{2\pi} \frac{d\theta(f)}{df}. \quad (2.4)$$

The channel is ideal or distortionless if the amplitude response $|C(f)|$ is constant for all $|f| \leq W$ and $\theta(f)$ is a linear function of frequency or equivalently $\tau(f)$ is constant for all $|f| \leq W$. If $|C(f)|$ is not constant, then the signal is distorted in amplitude and if $\tau(f)$ is not constant, then the signal is distorted in delay. In the presence of such a distortion, a train of pulses transmitted through the channel are no longer identified at the receiver as well-defined pulses. Instead, they overlap resulting in the well known intersymbol interference (ISI) [Proakis 1989].

2.3.2 Multipath Channels

In many radio channels, there may be more than one path from the transmitter to the receiver. This multipath phenomenon is due to atmospheric reflection or reflections from buildings and other surroundings resulting in fluctuations in the level of the received signal. This characterization serves as a model for the signal transmission over many radio channels such as shortwave ionospheric radio communication in the 3-to-30 MHz frequency band (HF), tropospheric scatter (beyond-the-horizon) radio communications in the 300-to 3000-MHz frequency band (UHF) and 3000-to-30,000-MHz frequency band (SHF), and isospheric forward scatter in the 30-to-300-MHz frequency band (VHF) [Proakis 1989].

The different paths may consist of several discrete paths each with a distinct

time delay and attenuation or they may consist of a continuum of paths. The introduced delay and attenuation are usually time-varying. The ions in the ionospheric layer which reflect signals in the HF band are moving continuously resulting in a random change to the introduced delay and attenuation. The case is similar in the mobile radio situation where buildings reflect the transmitted signal. The vehicle is in continuous motion which means different reflected signals occur from buildings at different times. These fluctuations result in amplitude variations which is usually called fading. Depending upon the differential delay over all the paths, there can also be distortion which is called frequency selective multipath. Depending upon the number of received signals, there are two types of multipaths: discrete and diffuse [Shanmugan 1992].

Discrete Multipath:

A simple model for a discrete multipath channel has the form [Proakis 1989]

$$y(t) = \sum_n \alpha_n(t) s(t - \tau_n(t)) \quad (2.5)$$

where

$s(t)$ is the bandpass input signal.

$\alpha_n(t)$ is the attenuation factor for the signal received on the k -th path.

$\tau_n(t)$ is the corresponding propagation delay.

See Fig. 2.3.

From equation (2.5) it can be seen that the multipath channel can be modeled by a tapped delay line with time-varying coefficients. The differential delay is called delay-spread. It is the difference between the longest and the shortest path delays. It is considered an important channel characterization. The tapped delay line with appropriate coefficients can represent any arbitrary transfer function over a certain bandwidth which is the reciprocal of the tap spacing. If the delay spread is of the order of the reciprocal of the bandwidth (or larger), frequency selective effects over the bandwidth of the signal can occur [Shanmugan 1992].

Diffuse Multipath:

For some channels like the tropospheric scatter channel or mobile radio channel, it is more convenient to view the received signal as consisting of a continuum of multipath components. This is called the diffuse multipath channel and in this case the response given in equation (2.5) becomes

$$y(t) = \int_{-\infty}^{\infty} \alpha(\tau; t) s(t - \tau) d\tau \quad (2.6)$$

The low-pass time-varying impulse response becomes

$$\hat{h}(\tau; t) = \alpha(\tau; t) e^{-j2\pi f_c t} \quad (2.7)$$

If the signal is band-limited (which is always the case in practice), then the time-varying diffuse multipath channel can be represented by a tapped-delay line with time-varying coefficients and fixed tap spacing as shown in Fig. 2.4.

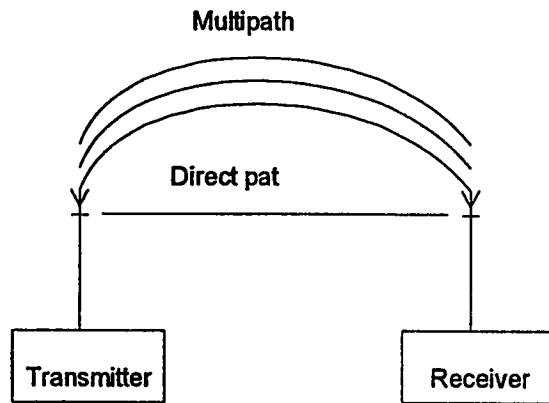


Fig 2.3 Simplified illustration of multipath channel

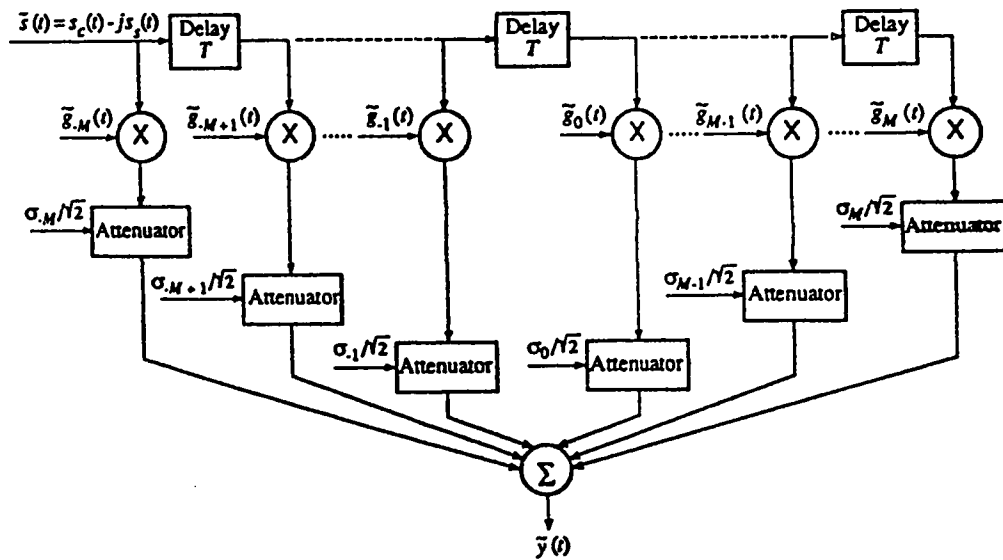


Fig 2.4 Diffuse multipath model (Shanmugan 1991)

If we write $s(t)$ as

$$s(t) = \text{Re}\{\hat{s}(t)e^{j2\pi f_c t}\} \quad (2.8)$$

where $s(t)$ is the input bandpass signal, then the received signal will be

$$\hat{y}(t) = \sum_m \hat{g}_m(t) \hat{s}\left(t - \frac{m}{W}\right) \quad (2.9)$$

where

$$\hat{g}_m(t) = \frac{1}{W} \hat{h}\left(\frac{m}{W}; t\right) \quad (2.10)$$

is the sampled complex equivalent low-pass impulse response and W is the bandwidth of the equivalent bandpass signal.

In principle, the index (m) in equation (2.9) is unbounded, i.e., $-\infty < m < \infty$. However, the number of taps has to be finite in order to be able to realize the model. The finite number of taps is a good approximation to the physical channels. The length of the tapped delay line is determined by the delay spread.

The next step will be to characterize the channel explicitly. The delay cross-power spectral density of the channel is given by [Shanmugan 1992]

$$R_c(\tau_1, \tau_2; t, \Delta t) = \frac{1}{2} E[\hat{h}^*(\tau_1; t) \hat{h}(\tau_2; t + \Delta t)] \quad (2.11)$$

Using the wide-sense stationary uncorrelated scattering (WSUS) assumption, equation (2.11) can be reduced to

$$R_c(\tau_1, \tau_2; \Delta t) = R_c(\tau_1; \Delta t) \delta(\tau_1 - \tau_2) = \frac{1}{2} E[\hat{h}^*(\tau, t) \hat{h}(\tau, t + \Delta t)]. \quad (2.12)$$

When $\Delta t = 0$, $R_c(\tau; \Delta t)$ will be equal to $R_c(\tau)$ which characterizes the average power as a function of delay. The function $R_c(\tau)$ is called the delay power spectrum or multipath intensity profile. The range of τ for which R_c is essentially nonzero is called the multipath delay spread, T_m . Referring to Fig. 2.4, the number of used taps in the delay line is $T_m W + 1$. If $(T_m W + 1)$ is not an integer, it is rounded up to the nearest integer [Shanmugan 1992].

Another important characterization of the channel is the scattering function which is the Fourier transform of $R_c(\tau; \Delta t)$ with respect to Δt

$$S(\tau; \nu) = \int_{-\infty}^{\infty} R_c(\tau; \Delta t) e^{-j2\pi\nu\Delta t} d(\Delta t) \quad (2.13)$$

When τ is fixed, the scattering function will describe the power spectral density in the frequency variable ν , which is often called the Doppler frequency.

To complete the characterization of the channel, another assumption is made about the distribution of $\hat{h}(\tau; t)$. The quantity $\hat{h}(\tau; t)$ is usually modeled as a complex-valued Gaussian process. If the process has a zero mean, the envelope $|\hat{h}(\tau; t)|$ at any instant is Rayleigh-distributed and the channel is called a Rayleigh fading channel. If there is a line of sight (LOS) between the transmitter and the receiver and part of the transmitted signal reaches the receiver directly while a part reaches the receiver as a continuum of multipath reflections, then the envelope will have a Rice distribution and the channel is called a Ricean channel [Proakis 1989].

The Rayleigh distribution in its normalized form is given by [Haykin 1988]

$$f_V(\nu) = \begin{cases} \nu \exp(-\frac{\nu^2}{2}), & \nu \geq 0 \\ 0, & \text{elsewhere} \end{cases} \quad (2.14)$$

which is plotted in Fig. 2.5.

The Rician distribution in the normalized form is given by [Haykin 1988]

$$f_V(\nu) = \nu \exp\left(-\frac{\nu^2 + \alpha^2}{2}\right) I_0(\alpha\nu) \quad (2.15)$$

where I_0 is the modified Bessel function of the first kind. A Rician distribution is shown in Fig. 2.6.

According to the preceding assumptions, the tapped-delay line model takes the following characteristics. The tap spacings are $(1/W)$ and the number of taps is $T_m W + 1$. The time-varying tap gain coefficients $\hat{g}_m(t)$ are complex-valued Gaussian processes with variance of each component equal to $\sigma_m^2 = (1/W)^2 R_c(m/W)$. The power spectral density of $\hat{g}_m(t)$ is given by $(1/W)^2 s(m/W; \nu)$. Furthermore, the various tap gain coefficients are independent processes [Shanmugan 1992]

Power Delay Profile:

The three common delay profiles are

$$R_c(\tau) = \begin{cases} \frac{1}{\sqrt{2\pi}\tau_0} \exp\left\{-\frac{\tau^2}{2\tau_0^2}\right\} & \text{Gaussian} \\ \frac{1}{2\tau_0} e^{-|\tau|/\tau_0} & \text{exponential} \\ \frac{\sqrt{\sigma}\tau_0 - |\tau|}{\sigma\tau_0^2}, \quad |\tau| \leq \sqrt{\sigma}\tau_0 & \text{triangular} \end{cases} \quad (2.16)$$

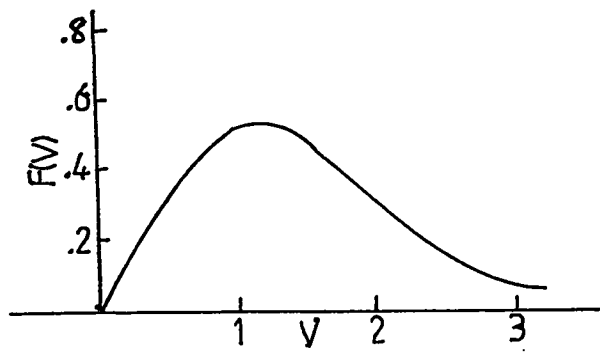


Fig 2.5 Rayleigh distribution

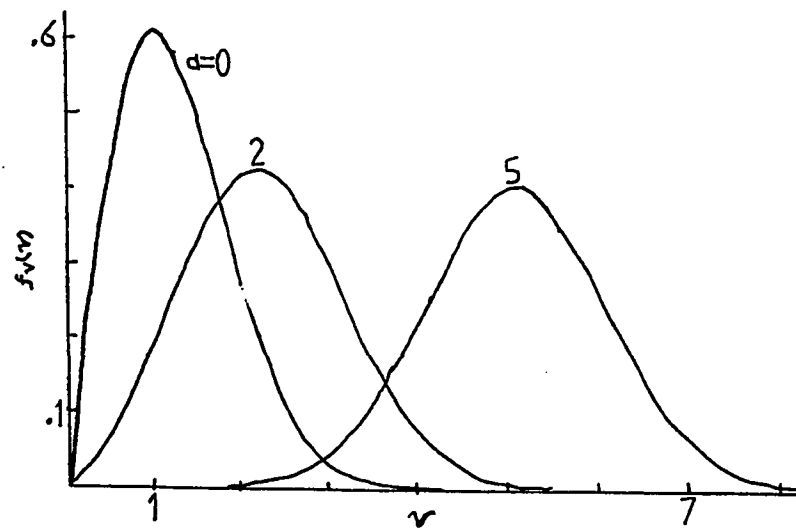


Fig 2.6 Rician distribution

The shape of the delay profile is found to be of secondary importance [Shanmugan 1992]. The BER performance of the QPSK and the MSK systems is also found to be dependent on the delay spread rather than the delay profile shape [Justin 1987]. The primary factor affecting the performance of a mobile or personal radio is the *rms* delay spread, which is expressed as [Shanmugan 1992]

$$\tau_{rms} = E[(\tau - \tau_0)^2] \quad (2.17)$$

where τ_0 is the mean delay.

Regardless of the chosen $R_c(\tau)$, it is truncated at some value $\tau = T_m$ beyond which $R_c(\tau)$ is negligible. For simulation purposes in this thesis, $R_c(m/W)$ is used to scale the various tap gains as mentioned earlier. The number of taps used is $L = T_m W + 1$, and τ_0 is determined by the physical environment. It ranges from about $1\mu s$ in a suburban-type environment to about $.1\mu s$ in urban environment [Shanmugan 1992].

The scattering function is difficult to measure. Instead, an approximation that assumes the power spectrum is the same at all tap gains is used. The assumed scattering function is given by [Shanmugan 1992]

$$s(v) = A \left\{ 1 - \left(\frac{v}{f_m} \right)^2 \right\}^{-1/2} \quad (2.18)$$

where $f_m = V/\lambda$, in which V is the velocity of the mobile, and λ is the wavelength of the transmitted carrier. Equation (2.18) can be derived under the assumptions that

a mobile is moving at constant velocity V and the omnidirectional receiver antenna receives N reflected waves at angles uniformly distributed on $[0, 2\pi]$. As $N \rightarrow \infty$, the received spectrum takes the form given in equation (2.18). [Shanmugan 1992] The normalized Doppler frequency ($f_m T$) used in this thesis is $1/300$. There are other factors beside the channel that degrade the performance which are presented below.

2.4 Transmission Impairments

There are many factors that degrade the performance of a communication system. Among these impairments are the additive white Gaussian noise (AWGN), the intersymbol interference (ISI) caused by both filtering and different delays introduced by the multipath channel and finally the nonlinear characteristic of the power amplifier which give rise to AM/PM and AM/AM conversion effects. In the following sections, these sources of performance degradation are briefly discussed.

2.4.1 Additive White Gaussian Noise (AWGN)

The noise analysis of communication systems is usually based on an idealized form of noise, the spectral density of which is independent of the operating frequency. The adjective white is used in the sense that white light contains equal

amounts of all frequencies within the visible band of electromagnetic radiation.

Strictly speaking, white noise has infinite mean power and, as such, it is not physically realizable. In order to assume the noise to be white, it has to have a constant spectrum over a frequency band that is greater than the system bandwidth.

In practical communication systems, the signal and the noise are usually processed by band-limited filters so that only those frequencies that lie inside the passband of the system will appear at the output. We are therefore considering white Gaussian noise when it is transmitted through a narrow-band filter. By narrow band we mean that the mid-band frequency f_c is large compared with the half bandwidth of the filter (B). The output $n(t)$ of such a filter in response to white Gaussian noise appears to be somewhat similar to a carrier wave of frequency f_c modulated by low-pass noise signal extending in frequency content effectively from 0 to B . It can be shown that Gaussian random noise in narrow band channels $n(t)$ can be represented by its in-phase and quadrature channel components [Haykin 1988]

$$n(t) = n_c(t) \cos w_c t + n_s(t) \sin w_c t \quad (2.19)$$

where the in-phase component $n_c(t)$ and quadrature component $n_s(t)$ are independent and Gaussian. We may, therefore, express their probability density functions

(PDFs) as

$$p(n_c) = \frac{1}{\sqrt{2\pi\sigma}} \exp\left(-\frac{n_c^2}{2\sigma^2}\right) \quad (2.20)$$

$$p(n_s) = \frac{1}{\sqrt{2\pi\sigma}} \exp\left(-\frac{n_s^2}{2\sigma^2}\right) \quad (2.21)$$

where σ^2 is the variance of the narrow-band noise $n(t)$ and equals the average noise power. In this thesis, the general noise had initially a unity variance and then scaled according to the desired signal to noise ratio (SNR).

2.4.2 Intersymbol interference

In digital communication systems, the information is carried by discrete pulses. A major criterion in determining the performance of communication system is the utilized bandwidth. The available spectrum is limited and very valuable. Hence, a filter is usually used at the transmitter. To limit the effect of the additive white Gaussian noise (AWG), another filter is used at the receiver.

Each filter distorts the shape of the pulse and, as a result, a trailing waveform appears at the output instead of a sharp pulse cutoff. This pulse trail interferes with the adjacent pulses. The trails produced from a series of signaling pulses, added together, can deform the next incoming pulse to an extent that the receiver may erroneously interpret the presence or absence of the signaling pulse. This type of interference is known as intersymbol interference (ISI).

An ideal low-pass filter with constant amplitude and linear phase characteristics is shown in Fig. 2.7. The impulse response of this filter has $\sin x/x$ characteristics. The zero crossings of the impulse response occur at $t = \pm nT$ where n is an integer and is not equal to zero. This means that if impulses are transmitted, the filter output consists of one impulse response waveform for each input pulse. Each impulse response's main lobe peak will occur at the zero crossing of all other impulse responses. The impulse response peaks occur every $t = \pm nT$. In other words, if the ideal low-pass filter cutoff frequency is $\frac{1}{2T}$, the channel will process data with a rate $R = \frac{1}{T}$. This rate is called the Nyquist rate. At the Nyquist rate, which is the highest rate, and under ideal filtering, there will be no ISI.

In practice, an ideal filter is not physically realizable. In addition, if the receiver detector sampling is not performed at the exact zero crossing time, ISI will occur.

Fig. 2.8-a shows a band-limited pulse having zeros periodically spaced in time at points labeled $\pm T, \pm 2T$, etc. Assuming the information is contained in the pulse amplitude, then a sequence of pulses each of which has a peak at the periodic zeros of the other pulses can be transmitted. When such a pulse passes through a frequency selective fading channel, the received pulse shown in Fig. 2.8-b will have zero crossings that are no longer periodically spaced. Thus, the sequence of the transmitted pulses would be smeared into one another and the

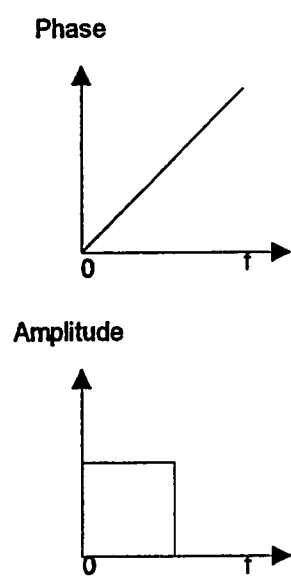


Fig 2.7 Ideal filter

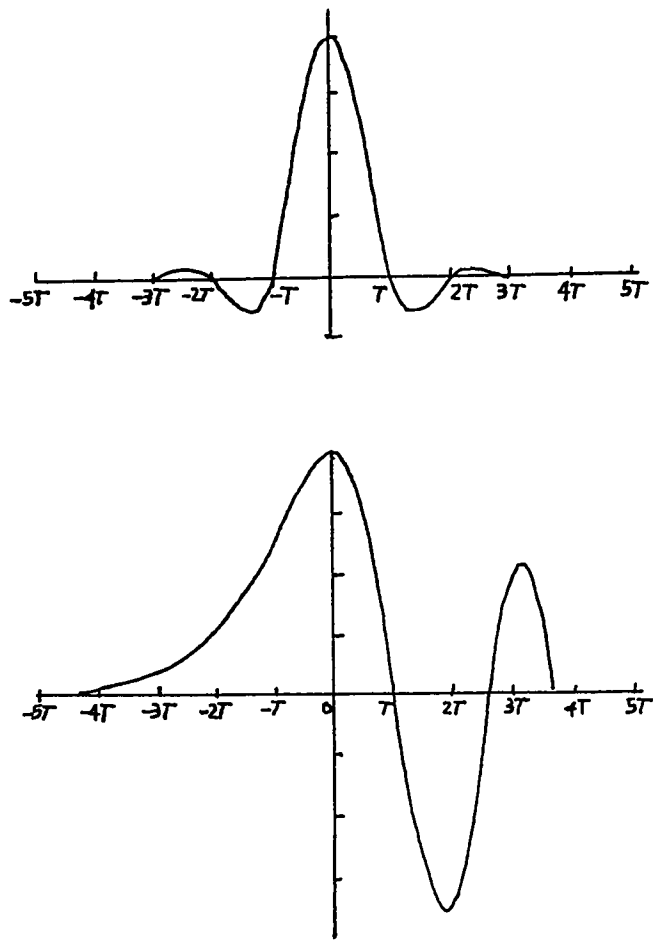


Fig 2.8 Effect of channel distortion
(a) Channel input
(b) Channel output

peaks of the pulses would no longer be distinguishable. This phenomenon is called intersymbol interference (ISI). The effect of ISI can be alleviated by employing channel equalization techniques.

Channel Equalization

In mobile radio channels, the multipath phenomenon leads to excessive ISI. The communication system performance can be enhanced by using equalization techniques. The aim of equalization is to reverse the effect of the channel. The fading phenomenon is time-varying and hence, the equalizing process has to be adaptive. In most digital communication systems, multilevel modulation schemes are employed resulting in two sources of distortion: in-phase and quadrature distortions [Proakis 1989].

The channel can degrade the performance of the system by introducing ISI and by attenuating the transmitted waveforms in a frequency-selective manner. This gives rise to two types of equalizing techniques which are frequency-domain equalizers and time-domain equalizers.

In frequency-domain equalizers, amplitude correction is introduced to restore equality in the spectral density of the signal. This can be done by slope equalizers or by notch equalizers. In the slope equalizer, two points in the power spectrum

are estimated while the notch equalizer has a transfer function which is the inverse of the channel.

ISI is a time-domain effect. Hence, the design of efficient equalizing techniques has to be made in the time domain [Al-Semari 1992]. Time domain equalizers are known to be an efficient way in reducing the effect of ISI. They consist basically of delay elements with tap gains. Different types of equalizers (transversal, fractionally spaced or decision feedback) result from different types of connections [Proakis 1989].

The simplest type of equalizers is the transversal equalizer. It consists of a certain number of delay elements connected in cascade and each weighted by a certain gain. The delay per tap \bar{T} is a design choice. When $\bar{T} = T$, the symbol duration, the equalizer is termed a synchronous equalizer. When $\bar{T} = T/m$, m an integer, it is called a fractionally spaced equalizer. Advantages and disadvantages of both types are discussed in [Proakis 1989].

One of the best features of the tapped-delay line model is the relative ease with which it can be modified. This modification is necessary to compensate either for time-varying channel characteristics, or for lack of complete knowledge about such characteristics. Clearly, if the tap gains are changed, then the transfer function of the equalizer changes accordingly. The question is how to make these

changes in a proper way, since it might be quite difficult to measure the channel characteristics accurately. The answer is to use an adaptive technique to let the equalizer know that it is compensating properly. If the channel is continuously time-varying slowly, then the equalizer will continuously adapt.

One way to implement the adaptive version of the equalizer is to vary the tap gains so as to minimize the mean square error (MSE) between the actual equalizer output and the ideal output. This is called the minimum mean square error (MMSE) criterion. In reality, unless a training sequence is used, the receiver does not know the ideal output. However, under certain conditions, the ideal output can be assumed to be known. In the digital case, the ideal output would be the error-free digital waveform input to the transmitter. If the channel does not introduce too much noise and distortion, then it can be said that the decisions are “almost” always correct and hence can be taken as the ideal output for equalizing purposes. There are other approaches to training the equalizer without knowing the transmitted sequence (blind equalization) which are discussed in [Proakis 1989].

The MMSE Criterion

In high speed modems, the tap gains are usually updated using the least mean squares (LMS) criterion. Let $d(i)$, $y(i)$ and $z(i)$ represent the transmitted, received

and equalized symbols, respectively. Then, when the number of taps is infinite,

$$z(i) = \sum_{k=-\infty}^{\infty} c(k)y(i-k) \quad (2.22)$$

where $c(k)$ is the tap gain. However, an equalizer with an infinite number of taps is physically unrealizable. Moreover, in multipath fading channels, the multipath spread is only over few symbols and hence the number of taps can be truncated to N . Thus,

$$z(i) = \sum_{k=0}^{N-1} c(k)y(i-k). \quad (2.23)$$

The error between the transmitted and equalized symbols is

$$e(i) = d(i) - \sum_{k=0}^{N-1} c(k)y(i-k). \quad (2.24)$$

The mean square error value is

$$\epsilon = E[(d(i) - z(i))^2]. \quad (2.25)$$

The MMSE criterion is based on minimizing this quantity. It can be shown that this can be achieved by letting

$$\bar{c}(i+1) = \bar{c}(i) + \alpha E[e(i)\bar{Y}]. \quad (2.26)$$

There are other criteria for updating the taps like the zero-forcing algorithm but the MMSE is more efficient and hence it is used in this thesis.

What is left is to find the expectation of $e(i)\bar{Y}$. The least mean squares (LMS) criterion can be used leading to the use of an unbiased estimator which is the

product $e(i)\bar{Y}$. Hence, the tap coefficients can be updated by

$$\bar{c}(i+1) = \bar{c}(i) + \alpha e(i)\bar{Y}. \quad (2.27)$$

When $d(i)$, $y(i)$ and $z(i)$ are complex-valued sequences which is the case in both $\pi/4$ -shifted-DQPSK and 16-QAM systems, the error is defined as the square of the difference between the transmitted in-phase component and the equalized in-phase component plus the square of the difference between the transmitted quadrature and the equalized quadrature component. Similarly, the LMS criterion will lead to

$$c_k(i+1) = c_k(i) + \alpha e(i)y^*(i-k) \quad (2.28)$$

where $*$ denotes the complex conjugate and c_k is the k -th tap gain. A typical linear adaptive equalizer based on the LMS criterion is shown in Fig. 2.9.

2.4.3 Power Amplifier Nonlinearity

The high-frequency, large output power amplifiers used in mobile communication exhibit two nonlinear distortion effects [Abulma'atti 1984]

1. a nonlinear input-output power characteristic (amplitude modulation to amplitude modulation or AM/AM conversion), and,
2. a nonlinear output phase-input power characteristic (amplitude modulation to phase modulation or AM/PM conversion).

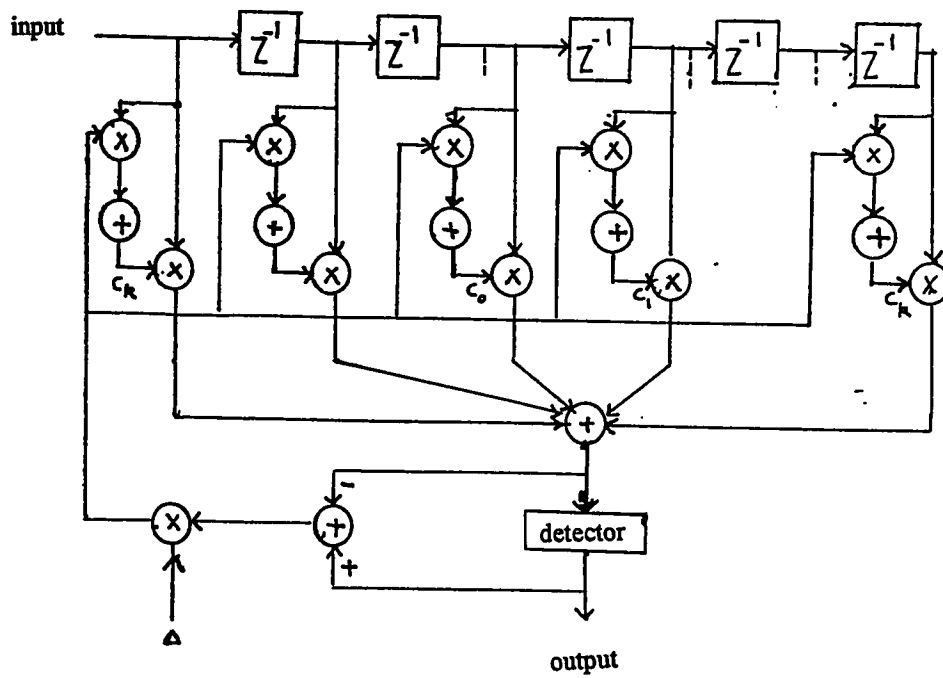


Fig 2.9 Linear adaptive equalizer based on the LMS criterion (Proakis 1989)

The power amplifier is generally described by two transfer characteristics. One expresses the input/output power relationship and the other expresses the output phase shift versus input power (see Fig. 2.10). For low input levels, the output power is essentially a linear function of the input power. As the input drive increases, the output power increases nonlinearly until a point is reached at which any additional input level increase results in a no change in the output power. This point of maximum output power is called the saturation point. The higher the backoff from this saturation point, the closer the operating point to the linear region.

Power sources are limited at subscriber radio units. Hence, the amplifiers need to be power-efficient. The use of amplifiers operating near saturation is desired to achieve high power efficiency but it results in a nonlinear distortion to the input signal if it has a non-constant envelope. Although linearization and compensation techniques can be used to minimize this effect, most of these techniques are not suitable for low-cost and small-size integrated-circuit implementations [Ariyavistakul 1990].

A quadrature model that takes into account the AM/AM and AM/PM distortion effects is usually used. This model is suitable for simulation purposes because it preserves the quadrature characteristic of the signal after it passes through the

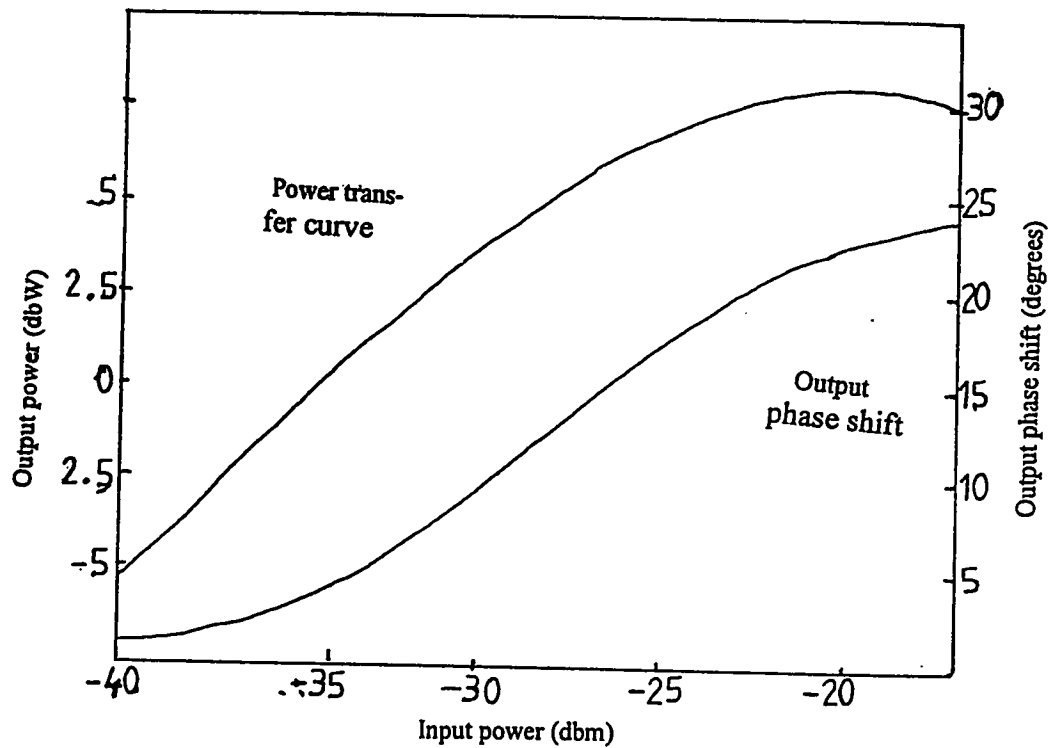


Fig 2.10 Characteristic of an Intelsat IV TWT , Hughes 261-H (Hill 1983)

nonlinear amplifier. It deals with the in-phase and the quadrature components separately.

Let the input signal to the power amplifier be represented by

$$v_i(t) = r(t) \cos[w_c t + \phi(t)] \quad (2.29)$$

where $r(t)$ is the signal envelope and $\phi(t)$ is a phase function. The power amplifier output will be [Abul-ma'ati 1984]

$$v_o(t) = z_c(r) \cos[w_c t + \phi(t)] - z_s(r) \sin[w_c t + \phi(t)] \quad (2.30)$$

where $z_c(r) = g(r) \cos f(r)$ and $z_s(r) = g(r) \sin f(r)$

$$v_o(t) = g[r(t)] \cos\{w_c t + f[r(t)] + \phi(t)\} \quad (2.31)$$

where

$$g[r(t)] = \sqrt{[z_c\{r(t)\}]^2 + [z_s\{r(t)\}]^2} \quad (2.32)$$

and

$$f[r(t)] = \tan^{-1} \left\{ \frac{z_s[r(t)]}{z_c[r(t)]} \right\}. \quad (2.33)$$

Here, $g[r(t)]$ and $f[r(t)]$ are the AM/AM and AM/PM distortions, respectively.

The quadrature model can be used to assess the performance of communication systems by computer simulation. The quadrature components $z_c[r(t)]$ and $z_s[r(t)]$ are obtained by conversion of the measured power and phase characteristics of an actual power amplifier into quadrature components using equation (2.30). Samples

of the quadrature curves which provide sufficient resolution can be stored and used to determine quadrature output values for a range of input values by means of interpolation. Another way which was shown in [Ghorban 1986] is to use a four-parameter formula to represent the AM/AM distortion $g(r)$ and the AM/PM distortion $f(r)$. These formulas are given by [Ghorban 1986]

$$g(r) = \frac{x_1 r^{x_2}}{1 + x_3 r^{x_2}} + x_4 r \quad (2.34)$$

$$f(r) = \frac{y_1 r^{y_2}}{1 + y_3 r^{y_2}} + y_4 r \quad (2.35)$$

The parameters $x_1, x_2, x_3, x_4, y_1, y_2, y_3$ and y_4 are obtained from the measurable input-power output-power and output phase shift characteristics by curve-fitting techniques. Fig. 2.11 shows both the output-power and phase shift as a function of the input voltage where the four-parameter formulas show good agreement with the measured data. In this thesis, the four-parameter formulas will be used to represent both the AM/AM and the AM/PM distortions. The systems performance will be evaluated with the back-off from saturation as a parameter.

2.5 Summary

In this chapter, the digital communication schemes are briefly discussed and compared with analog ones. The communication channel issue is discussed. Different channel models are presented with emphasis on the frequency selective fading

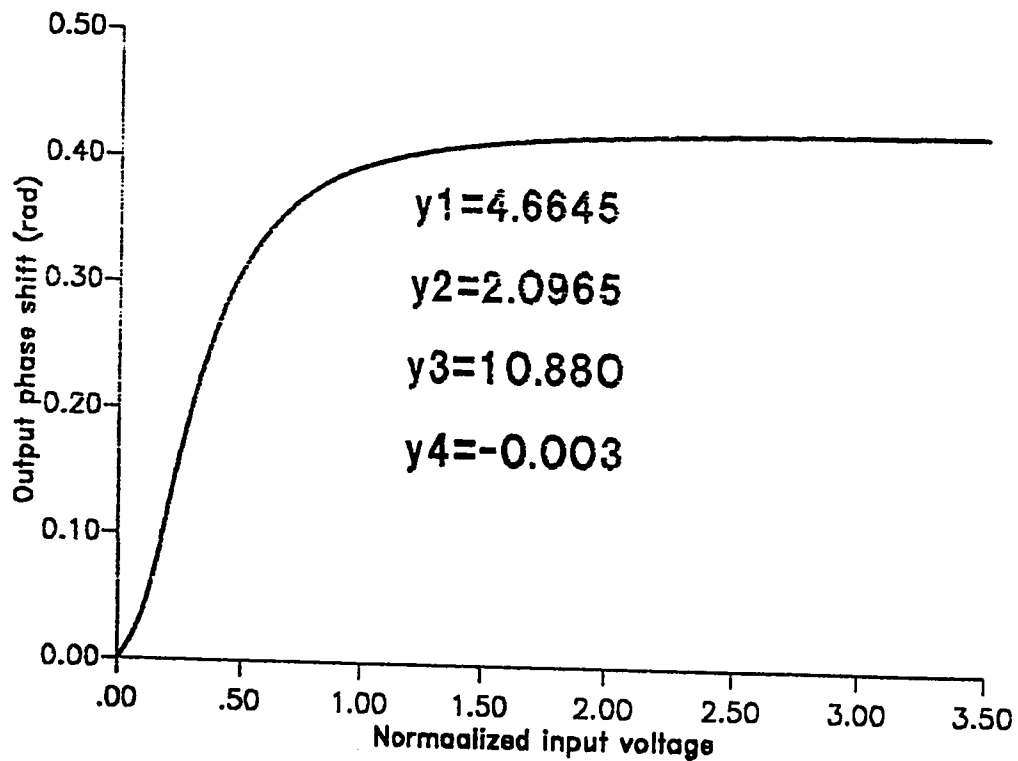
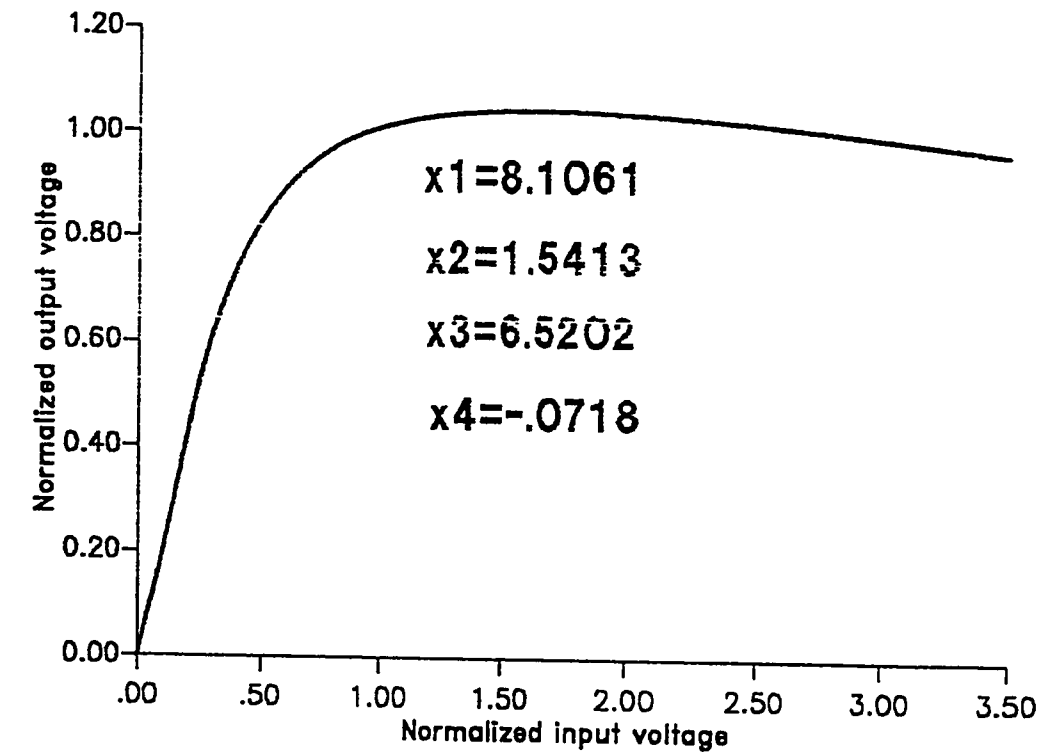


Fig 2.11 Non-linear distortion (Ghorban 1986)

channel model which is usually used in mobile communication. Transmission impairments like the additive white Gaussian noise (AWGN), the intersymbol interference (ISI) and nonlinear amplification by power amplifiers are reviewed. Also, linear adaptive equalization based on the LMS criterion which is used to alleviate the ISI effect is discussed. In the coming chapter, the three systems under investigation; GMSK, $\pi/4$ -shifted-DQPSK and the 16 QAM are discussed.

CHAPTER THREE

ANALYSIS OF $\pi/4$ -DQPSK, GMSK AND QAM SYSTEMS

3.1 Introduction

There is a variety of communication systems in which the carrier is modulated in a certain way according to the transmitted data. The modulation is usually made by keying the amplitude, the phase or the frequency of the carrier. In mobile communication, the used system has to be bandwidth-efficient due to the limited spectrum. Power amplifiers are also used at subscriber unit introducing non-linearities in both the amplitude and phase of the amplified signal if it does not have a constant envelope [Abulma'atti 1984]. Two systems employing constant envelope signals are already in use for commercial mobile communications. These are the Gaussian minimum shift keying (GMSK) [Hirade 1986, Varshney 1991] and the $\pi/4$ -shifted-differential quaternary phase shift keying ($\pi/4$ -DQPSK) [Dapuis 1979, Rappaport 1991]. In order to provide higher transmission rates, multilevel systems are proposed. One of these systems is the quadrature amplitude modulation (QAM) [Daido 1987]. The 16 QAM proposed for mobile communication is investigated here. The multilevel systems performance is known to degrade in the presence of non-linearity [Aghvami 1984].

In this chapter, the three aforementioned systems are described. They are described in a way that permits the evaluation of their performance with computer simulation.

3.2 Phase Shift Keying

Phase shift keying (PSK) was developed initially for the space program applications because of their bandwidth efficiency. PSK is now widely used for both military and commercial communication systems. The general analytic expression for PSK is given by

$$S_i(t) = \sqrt{\frac{2E}{T}} \cos[\omega_0 t + \phi_i(t)] \quad 0 \leq t \leq T \quad i = 1, 2, \dots, M. \quad (3.1)$$

For binary PSK (BPSK), M is 2. The parameter E is the symbol energy, T is the symbol time duration. In BPSK, the modulating data signal shifts the phase of the waveform, $S_i(t)$, to one of two states, either zero or $\pi(180^\circ)$.

QPSK Signaling

Fig. 3.1 shows the splitting of a typical pulse stream for QPSK modulation into in-phase stream $d_I(t)$ and quadrature stream $d_Q(t)$. If the original data stream is $d_k(t) = d_0, d_1, d_2, \dots$, then

$$d_I(t) = d_0, d_2, d_4, \dots, \text{ (even bits)}$$

$$d_Q(t) = d_1, d_3, d_5, \dots, \text{ (odd bits)}$$

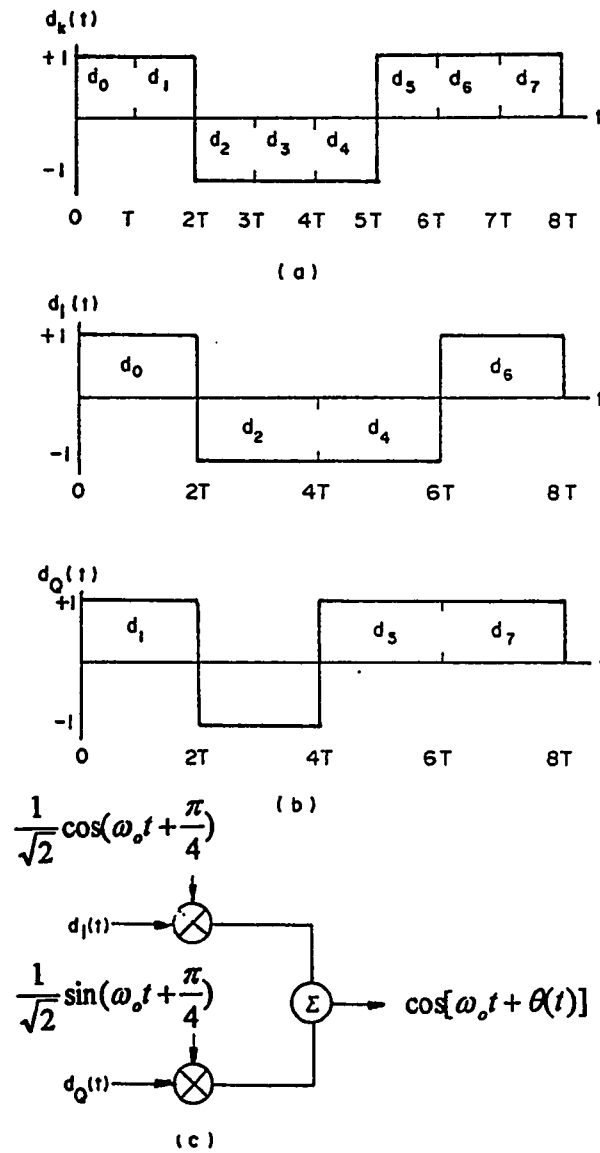


Fig 3.1 QPSK modulation (Sclar 1988)

Both $d_I(t)$ and $d_Q(t)$ have half the bit rate of $d_k(t)$. A QPSK waveform can be realized by amplitude modulating the in-phase and quadrature data streams onto the cosine and sine functions of a carrier wave as follows

$$s(t) = \frac{1}{\sqrt{2}}d_I(t) \cos\left(\omega_0 t + \frac{\pi}{4}\right) + \frac{1}{\sqrt{2}}d_Q(t) \sin\left(\omega_0 t + \frac{\pi}{4}\right). \quad (3.2)$$

Here $\frac{\pi}{4}$ can be replaced by any other value without affecting the system performance.

The signal $s(t)$ can also be written as

$$s(t) = \cos[2\pi f_0 t + \theta(t)].$$

The QPSK modulator is shown in Fig. 3.1-c. The $d_I(t)$ modulates the cosine function with the amplitude of ± 1 . This produces a BPSK waveform since the cosine phase changes by 0 or π . Similarly, the $d_Q(t)$ produces another BPSK waveform that is orthogonal to the cosine function. The summation of these two orthogonal components of the carrier produces the QPSK signal. The four different combinations of $d_I(t)$ and $d_Q(t)$ gives $\theta(t)$ four different values which are: $\theta(t) = 0, \pm 90, 180$. The resulting signal vectors or the signal constellation is shown in Fig. 3.2 [Sclar 1988].

Offset QPSK (OQPSK)

In standard QPSK, due to coincident alignments of $d_I(t)$ and $d_Q(t)$, the carrier phase can change only once every $2T$. The carrier phase can change by ± 90 or 180 degrees between different intervals. In OQPSK, the pulse streams $d_I(t)$ and $d_Q(t)$ are staggered and thus do not change states simultaneously. Thus, the possibility of the carrier phase to change by 180 degrees is eliminated resulting in a smoother phase transmission and hence lower sidelobes. Because $\cos(\omega_0 t + \pi/4)$ and $\sin(\omega_0 t + \pi/4)$ are orthogonal, the two BPSK signals can be detected separately [Sclar 1988].

$\pi/4$ -Shifted-DQPSK

The proposed U.S. digital cellular system will use a TDMA channel access method and a digital modulation scheme [Lin 1991]. Essentially, the proposed system uses the existing 30-KHz channel structure and replaces the analog FM modulation with a digital modulation having a gross bit rate of 48.6 kb/s. Each channel will be shared in a TDMA fashion. It is required to have a modulation with spectral efficiency of 1.62 bits/s/Hz in order to achieve a bit rate of 48.6 kbps in a 30 KHz channel.

While these requirements can be met by conventional filtered four-phase modu-

lation schemes such as QPSK and OQPSK, symmetric differential phase exchange keying ($\pi/4$ -shifted-QPSK) has some advantages for the mobile channel. The $\pi/4$ -shifted-QPSK signal constellation can be viewed as the superposition of two QPSK signal constellations shifted by $\pi/4$ relative to each other, resulting in eight phases. Symbol phases are alternatively selected from one of the QPSK constellations and then the other and, as a result, successive symbols have a relative phase difference that is one of four angles, $\pm\pi/4$ or $\pm3\pi/4$. Fig. 3.3 shows the $\pi/4$ -shifted-QPSK signal constellation.

A feature of this modulation is that it can be detected using coherent detector, a differential detector or a discriminator followed by an integrate and dump filter. Both differential and discriminator detection provides an advantage since both can be performed by low-complexity receiver structures. Another advantage of $\pi/4$ -shifted-QPSK is that unlike QPSK, the transitions in the signal constellation do not pass through the origin. As a result $\pi/4$ -shifted-QPSK has a better output characteristic. The proposed U.S. digital cellular system will use the $\pi/4$ -shifted-OQPSK.

The $\pi/4$ -shifted-DQPSK modulation scheme is essentially $\pi/4$ -shifted-QPSK with differential encoding of the symbol phases. While the differential encoding protects against the loss of data due to channel phase slips, it also results in

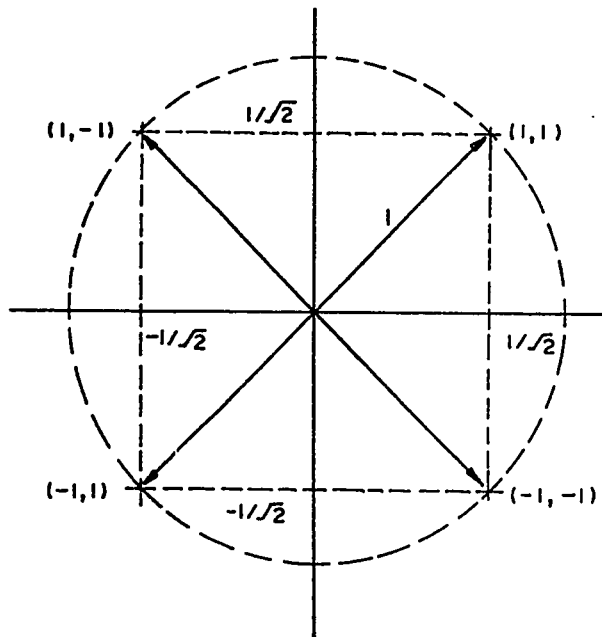


Fig 3.2 Signal space for QPSK & OQPSK

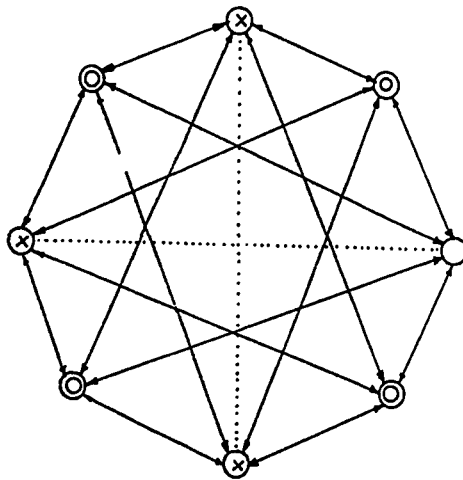


Fig 3.3 Signal space for $\pi/4$ -shifted-QPSK (Fung 1993)

a loss of a pair of symbols when an error occurs. $\pi/4$ -shifted-DQPSK can be produced by either differentially encoding the source bits and mapping them onto absolute phase angles of a $\pi/4$ -shifted-QPSK signal constellation or, alternatively, by directly mapping the pairs of input bits onto the relative phases ($\pm\pi/4, \pm3\pi/4$). This second technique is used in the simulation in this thesis. The phase of the transmitted signal is incremented by $\Delta\theta$ according to the incoming dibits. If the incoming dibits is $b_{1k}b_{2k}$, then $\Delta\theta_k$ can be determined from the following table

$b_{1k}(MSB)$	$b_{2k}(LSB)$	$\Delta\theta_k$
0	0	$\pi/4$
1	0	$3\pi/4$
1	1	$-3\pi/4$
0	1	$-\pi/4$

Table 3.1

At the receiver, the phase of the incoming signal is determined and compared with the previous decision to find $\Delta\hat{\theta}_k$ and according to which a decision about \hat{b}_{1k} and \hat{b}_{2k} is made. The system performance is evaluated under AWGN, Rayleigh fading and under frequency selective fading.

3.3 Gaussian Minimum Shift Keying

Frequency shift keying (FSK) is usually implemented as orthogonal signaling where each tone (sinusoid) in the signal set cannot interfere with another tone.

Any pair of adjacent tones must have a frequency separation of a multiple of $1/T$ hertz where T is the symbol duration, in order for the signal set to be orthogonal.

The FSK tone can be analytically described by

$$S_i(t) = \cos(2\pi f_i t) \text{rect}(t/T) \quad (3.3)$$

where

$$\text{rect}(t/T) = \begin{cases} 1 & \text{for } -T/2 \leq t \leq T/2 \\ 0 & \text{elsewhere} \end{cases} \quad (3.4)$$

The Fourier transform of $S_i(t)$ is

$$S(f) = T \text{sinc} (f - f_i)T \quad (3.5)$$

The spectrum of each of the possible two signals is shown in Fig. 3.4.

In order to prevent interference between the two tones during detection, the peak of the spectrum of one of the tones must coincide with one of the zero crossings of the spectrum of the other tone. The frequency difference between the center of the spectral main lobe and the first zero crossing represents the minimum required spacing. Thus the minimum tone spacing for noncoherent FSK signaling is $1/T$ Hz. However, for coherent detection, the minimum spacing is made only $1/2T$ Hz which is known as minimum shift keying (MSK) [Sclar 1988].

Thus, minimum shift keying (MSK) is a binary digital FM with modulation index $(T * (f_2 - f_1))$ of 0.5. The MSK has the following good properties: constant

envelope, relatively narrow bandwidth and coherent detection capability. It can be shown that MSK is a type of continuous phase FSK (CPFSK) when keying is between two frequencies separated by half the data bit rate [Peebles 1991]. These radian frequencies are $\omega_1 = \omega_0 - \Delta\omega$ and $\omega_2 = \omega_0 + \Delta\omega$, where $2\Delta\omega$ is the frequency deviation according to the digital data in a polar NRZ format with ± 1 amplitude.

Thus

$$\Delta\omega = \frac{\omega_b}{4} = \frac{\pi}{2T_b}$$

where T_b is the duration of a typical data bit and $\omega_b = 2\pi/T_b$.

In a typical CPFSK signaling, the phase information is not fully utilized and only used to provide synchronization of the receiver to the transmitter through the local oscillator's phase. In MSK, however, the phase information can be used in a more efficient way resulting in a better noise performance than the conventional CPFSK system [de Buda 1972].

3.3.1 CPFSK Signal Decomposition

Let $d(t)$ represent a polar-NRZ waveform representing a binary data source. Bits are assumed to occur independently and with equal probability. Let d_k represent the amplitudes which is $+1$ for a data "1" and -1 for a "0" in the bit interval indexed by k where $k = \dots, -1, 0, 1, 2, \dots$. These definitions are illustrated in Fig.

3.5-a.

The frequency of the CPFSK waveform in the k -th interval will be $\omega_0 + \Delta\omega = \omega_0 + (\pi/2T_b)$ if $d_k = 1$ and $\omega_0 - \Delta\omega = \omega_0 - (\pi/2T_b)$ if $d_k = -1$. Thus

$$S_{CPFSK}(t) = A \cos[\omega_0 t + \theta(t)] \quad (3.6)$$

$$= A \cos \left[\omega_0 t + \theta_k + \frac{d_k \pi t}{2T_b} \right], K T_b \leq t \leq (k+1) T_b \quad (3.7)$$

If we think of $\theta(t)$ as the phase due to data modulation at the constant frequency $d_k \pi / 2T_b$, then θ_k represents the phase at $t = 0$. The information bits d_k can change from one interval to another which means that θ_k can be different for different intervals. The phase history of $\theta(t)$ is usually illustrated by a trellis diagram as shown in Fig. 3.5-b. The phase difference, $\theta(t) - \theta_0$, is plotted so that the function is zero at $t = 0$. In the *zero*-th interval, if $d_0 = 1$, frequency is larger than $\omega_0 = \pi/2T_b$, so phase increases linearly (dashed line) by $\Delta\omega T_b = \pi/2$ to arrive at the point marked by a . If $d_0 = -1$, the solid line leads to point b .

This phase history is useful in decomposing $S_{CPFSK}(t)$ in a form useful for generation of MSK signals. Noticing that $\theta_k - \theta_0 = 0$ or π and that $d_k = \pm 1$ we have

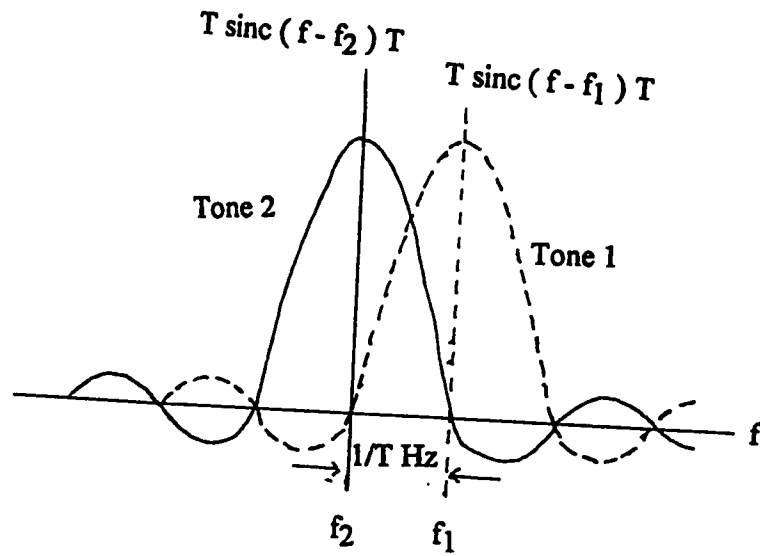
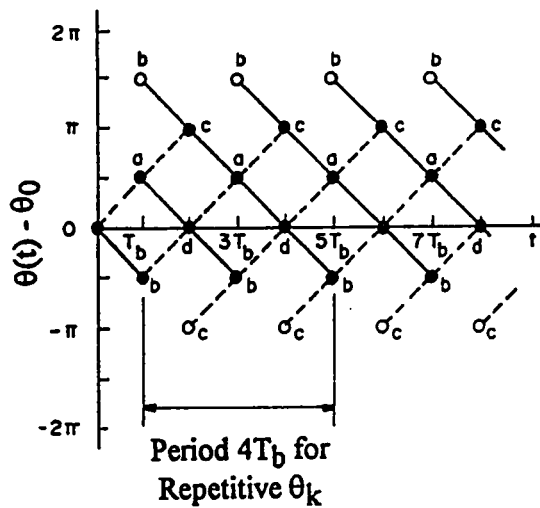
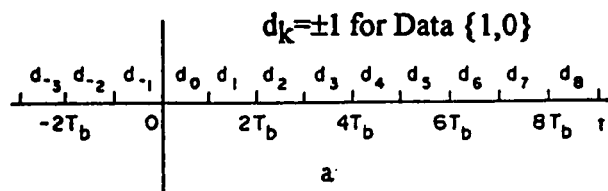


Fig 3.4 Minimum tone spacing for non coherently detected orthogonal FSK signalling (Sclar 1988)



Node at Interval Start	d_k	$\theta_k - \theta_0$ for Value of k shown								
		1	2	3	4	5	6	7	8	9
a	+1	0		π		0		π		0
	-1	π		0		π		0		π
b	+1	π		0		π		0		π
	-1	0		π		0		π		0
c	+1		0		π		0		π	
	-1		0		π		0		π	
d	+1		π		0		π		0	
	-1		π		0		π		0	

b

Fig 3.5 (a) Data interval definition in CPFSK
(b) Trellis and table to describe Phase history of CPFSK waveform

123

$$S_{CPFSK}(t) = A \cos \left(\omega_0 t + \theta_k - \theta_0 + d_k \frac{\pi t}{2T_b} \right) \quad (3.8)$$

$$\begin{aligned} &= A \cos \left(\theta_k - \theta_0 + d_k \frac{\pi t}{2T_b} \right) \cos(\omega_0 t + \theta_0) \\ &\quad - A \sin \left(\theta_k - \theta_0 + d_k \frac{\pi t}{2T_b} \right) \sin(\omega_0 t + \theta_0) \end{aligned} \quad (3.9)$$

$$\begin{aligned} &= A \cos(\theta_k - \theta_0) \cos \left(\frac{\pi t}{2T_b} \right) \cos(\omega_0 t + \theta_0) \\ &\quad - A d_k \cos(\theta_k - \theta_0) \sin \left(\frac{\pi t}{2T_b} \right) \sin(\omega_0 t + \theta_0) \end{aligned} \quad (3.10)$$

$$= S_I(t) A \cos(\omega_0 t + \theta_0) - S_Q(t) A \sin(\omega_0 t + \theta_0). \quad (3.11)$$

where

$$S_I(t) \equiv \cos(\theta_k - \theta_0) \cos \left(\frac{\pi t}{2T_b} \right) \quad (3.12)$$

$$S_Q(t) \equiv d_k \cos(\theta_k - \theta_0) \sin \left(\frac{\pi t}{2T_b} \right) \quad (3.13)$$

where $S_I(t)$ and $S_Q(t)$ are the in-phase and quadrature signal components, respectively. Looking at the table in Fig. 3.5-b, we can see that $\theta_k - \theta_0$ does not change sign at nodes *c* and *d*. This means that $\cos(\theta_k - \theta_0)$ does not change sign at nodes corresponding to kT_b , k even. However, at nodes *a* and *b* (at kT_b , k odd) changes in $\theta_k - \theta_0$ can occur. All these points show that the sign of $\cos(\theta_k - \theta_0)$ in equation (3.10) can change only at the zero crossings of $\cos(\pi t/2T_b)$.

Let us next extend the examination to $d_k \cos(\theta_k - \theta_0)$. The quantity d_k can change at any interval. Thus $d_k \cos(\theta_k - \theta_0)$ can change at kT_b , k even which is now

the zero crossings of $\sin(\pi t/2T_b)$ in equation (3.11). Turning to nodes a and b , we find that $d_k \cos(\theta_k - \theta_0)$ does not change sign. These points show that $d_k \cos(\theta_k - \theta_0)$ in equation (3.13) changes sign only at the zero crossings of $\sin(\pi t/2T_b)$ [Peebles 1991].

The previous analysis has shown that the factors $S_I(t)$ and $S_Q(t)$ multiplying the quadrature carriers in A are constant in sign over successive intervals of duration $2T_b$. The $2T_b$ intervals of $S_Q(t)$ are delayed one bit duration T_b relative to those of $S_I(t)$ because of the relative timing of $\cos(\pi t/2T_b)$ and $\sin(\pi t/2T_b)$. This timing is similar to this in offset QPSK. The signs of $S_I(t)$ and $S_Q(t)$ are related to the original data sequence d_k . Thus they can be taken as analogous to the modulating data waveform in OQPSK. However, the waveforms of duration $2T_b$ in MSK are half-cycles of a sinusoid at frequency $\Delta\omega/2\pi = 1/4T_b$, while they are rectangular in OQPSK.

3.3.2 MSK Systems

Figure 3.6 shows a typical MSK modulator that uses the analogy of equation (3.9). The input data stream $d(t)$ with bit rate $1/T_b$ is split into two data streams, $d_I(t)$ and $d_Q(t)$ each with symbol rate of $1/2T_b$. This modulator is called parallel modulator because of the use of parallel data streams and two quadrature carriers.

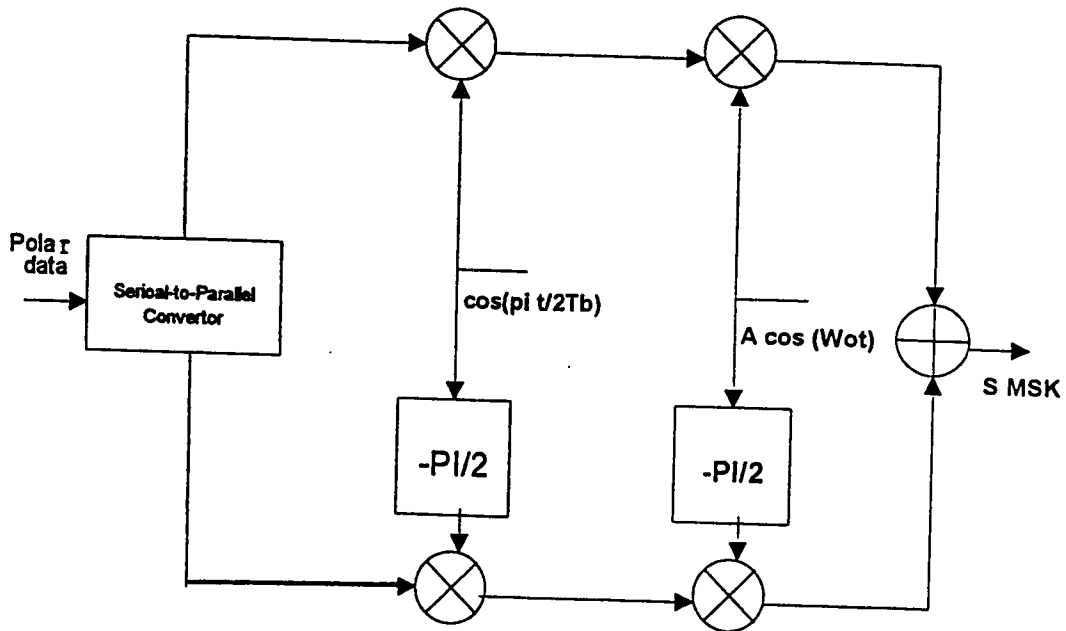


Fig 3.6 MSK parallel type demodulator (Peebles 1987)

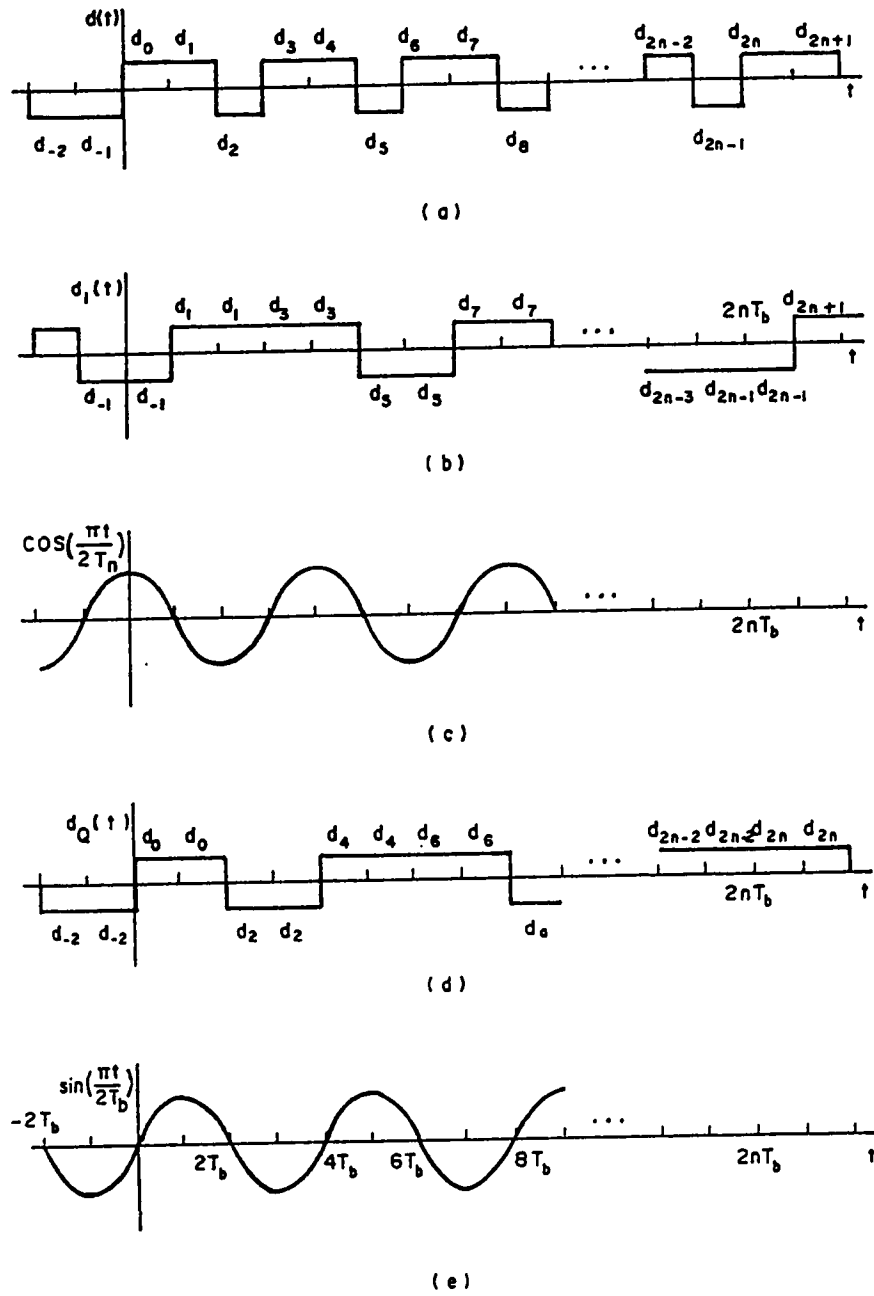


Fig 3.7 Timing diagram for MSK parallel type modulator (Peebles 1987)

The timing diagrams for the MSK modulator are shown in Fig. 3.7.

The MSK receiver is quite similar to the OQPSK since there is only a slight difference between the two systems in the involved carriers. This is shown in Fig. 3.8. It can be seen that the integrators are timed with the symbols of duration $2T_b$ in each path. A sample is taken at the end of each interval to decide about the transmitted bit. The decision is in favor of $+1$ if $D_i > 0$ and in favor of -1 otherwise [Peebles 1991].

Power Spectrum of MSK:

The power spectral density $G(f)$ for QPSK and OQPSK is given by [Sclar 1988]

$$G(f) = 2PT \left(\frac{\sin 2\pi fT}{2\pi fT} \right)^2 \quad (3.14)$$

where P is the average power in the modulated waveform. For MSK, $G(f)$ is given by [Sclar 1988]

$$G(f) = \frac{16PT}{\pi^2} \left(\frac{\cos 2\pi fT}{1 - 16f^2T^2} \right). \quad (3.15)$$

The normalized power spectral density ($P = 1$) for the well-known binary phase shift keying (BPSK), the quaternary PSK (QPSK), the offset QPSK (OQPSK) and MSK is shown in Fig. 3.9. It can be seen that BPSK requires more bandwidth than the others for a given level of spectral density. It is also clear that MSK has lower sidelobes than QPSK or OQPSK. This is a consequence of multiplying the data

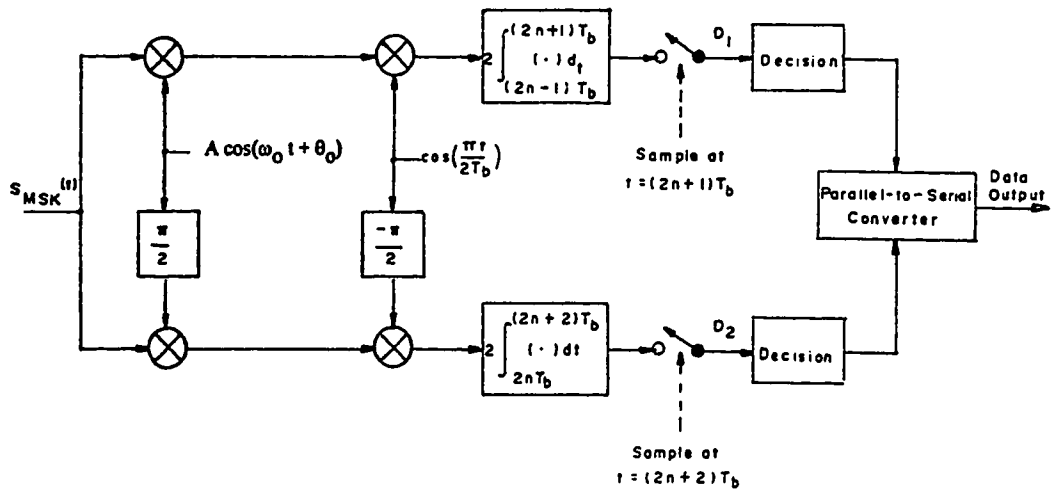


Fig 3.8 Receiver for MSK (Peebles 1987)

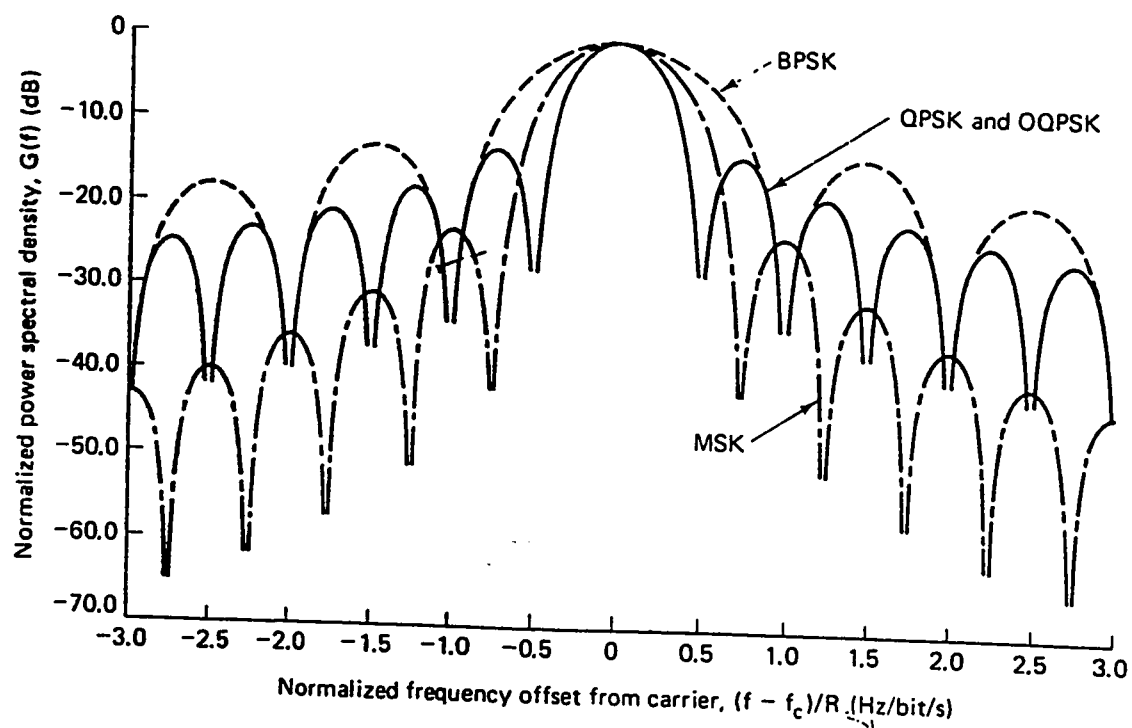


Fig 3.9 Normalised PSD for BPSK, QPSK, OQPSK, and MSK (Sclar 1988)

stream with a sinusoid, yielding more gradual phase transitions. The more gradual the transition, the faster the spectral tails drop to zero. MSK is spectrally more efficient than QPSK or OQPSK. However, MSK has a wider mainlobe than QPSK and OQPSK. Therefore, MSK may not be the preferred method for narrowband links. By filtering the MSK, the mainlobe may be decreased to the required level but this is achieved at the expense of a higher bit error rate (BER).

3.3.3 Gaussian Minimum Shift Keying (GMSK)

It is known that voice transmission in many VHF and UHF mobile radio telephone systems has usually been made by using a single-channel-per-carrier (SCPC) analog FM transmission techniques [Garber 1989]. However, in order to provide secure voice and high-speed data transmission by the use of large-scale integrated (LSI) transceivers, digital mobile radio techniques are replacing analog ones.

From the mobile radio use viewpoint, the out-of-band radiation in the adjacent channel should be generally suppressed 60–80 *dB* below that in the desired channel. Fig. 3.10 shows the fractional out-of-band power for both the MSK and the OQPSK systems. So as to satisfy this severe requirement, it is necessary to manipulate the RF output signal spectrum. Baseband filtering with frequency

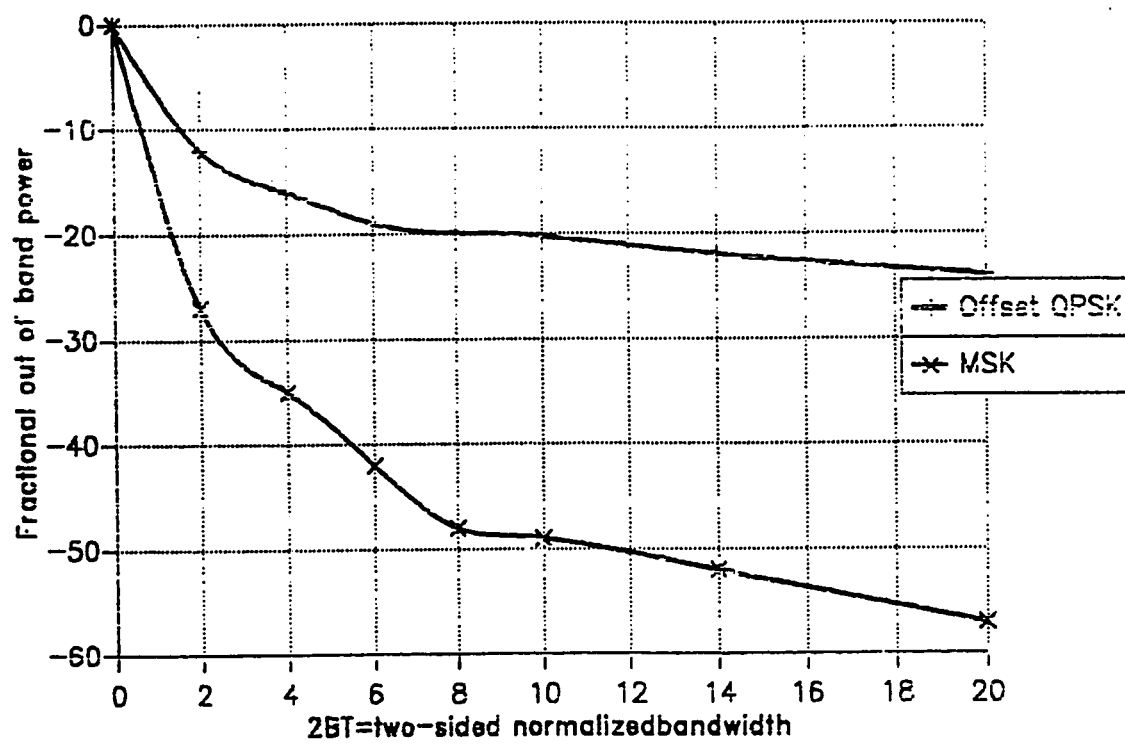


Fig 3.10 Fractional out-of-band power (Peebles 1987)

up conversion is suggested by [Hirade 1981]. The signal is filtered by a Gaussian filter and then the frequency of the carrier is changed according to the signal (FM modulation).

Gaussian Filters

Let the filter transfer function be $H(f)$. Within the bandwidth of the filter, $H(f)$ may be expressed as

$$H(f) = |H(f)|e^{j\theta(f)} \quad (3.16)$$

where $|H(f)|$ is the amplitude response characteristic and $\theta(f)$ is the phase response characteristic. The envelope delay characteristic is given by

$$\tau(f) = -\frac{1}{2\pi} \frac{d\theta(f)}{df}. \quad (3.17)$$

The filter is ideal "nondistorting" when $|H(f)|$ and $\tau(f)$ are constant for all $|f| \leq B$ where B is the bandwidth of the transmitted signal. If $|H(f)|$ is not constant, then the signal is distorted in amplitude while if $\tau(f)$ is not constant, the signal is distorted in delay.

Gaussian filters are characterized by the property that the group delay is maximally flat at the origin of the s plane. [Baher 1992]. The step response of Gaussian (Bessel) filters exhibits extremely low overshoot, typically less than 1% and both the impulse response and magnitude response tend toward Gaussian as the filter

order is increased. It should be noted that the maximally flat group delay property of continuous Gaussian filters is not generally preserved by ordinary transforming techniques, e.g. from continuous to digital conversion of signals.

Gaussian filters have the transfer function of the form

$$H(s) = \frac{d_0}{B_n(s)} \quad (3.18)$$

where $B_n(s)$ is the n -th order Bessel polynomial and d_0 is a normalizing constant of the form

$$d_0 = \frac{(2n)!}{2^n n!}. \quad (3.19)$$

The Bessel polynomials result from truncating a continued fraction expansion representation of the unit delay e^{-s} and satisfying the recursion relation

$$B_n(s) = (2n - 1)B_{n-1}(s) + s^2 B_{n-2}(s) \quad (3.20)$$

with initial conditions $B_0(s) = 1$, $B_1(s) = s + 1$. $B_n(s)$ can be put in the form

$$B_n(s) = \sum_{k=0}^n d_k s^k \quad (3.21)$$

where

$$d_k = \frac{(2n - k)!}{2^{n-k} k! (n - k)!} \quad k = 0, 1, \dots, n. \quad (3.22)$$

The log magnitude, phase and group delay response of a 10-th order Gaussian filter are shown in Fig. 3.11. The asymptotic cutoff frequency is 1000π rad/sec

or 500 Hz. For comparison, Buterworth lowpass filter characteristics are shown in Fig. 3.12 [Baher 1992].

Properties of GMSK

The GMSK is discussed in [Hirade] and many of its properties are investigated. The used system is an FM system preceded by a Gaussian lowpass filter.

Output Power Spectrum:

The output power spectrum of the GMSK signal versus the normalized frequency difference from the carrier center frequency $(f - f_c)T$ is plotted in Fig. 3.13. The 3 dB down bandwidth of the premodulation Gaussian LPF (B_bT) is used as a parameter. The effective variable parameter B_bT can be selected by the system designer considering overall spectrum efficiency of the system.

Fig. 3.14 shows the ratio of the out-of-band radiation power in the adjacent channel to the total power in the desired channel where the normalized channel spacing f_sT is taken as the abscissa and both channels are assumed to have the ideal rectangular bandpass characteristics with $B_iT = 1$, where B_iT is the normalized bandwidth of the predetection rectangular bandpass filter (BPF).

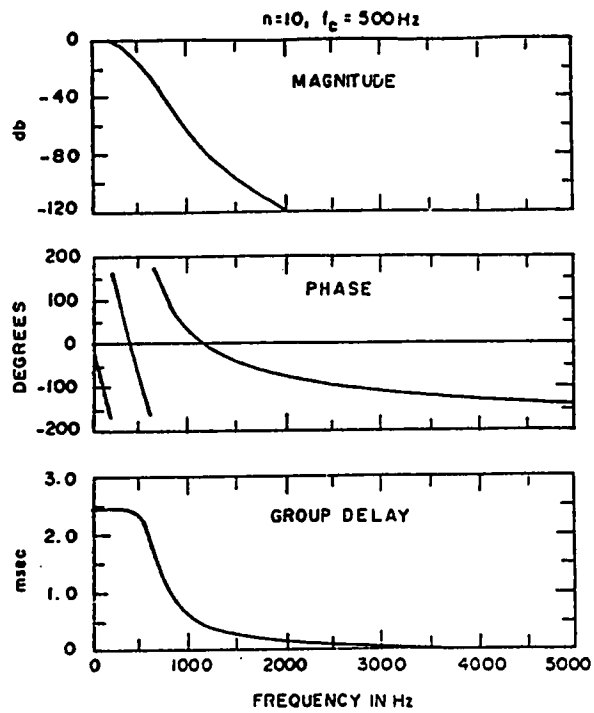


Fig 3.11 Gaussian filter characteristics (Baher 1992)

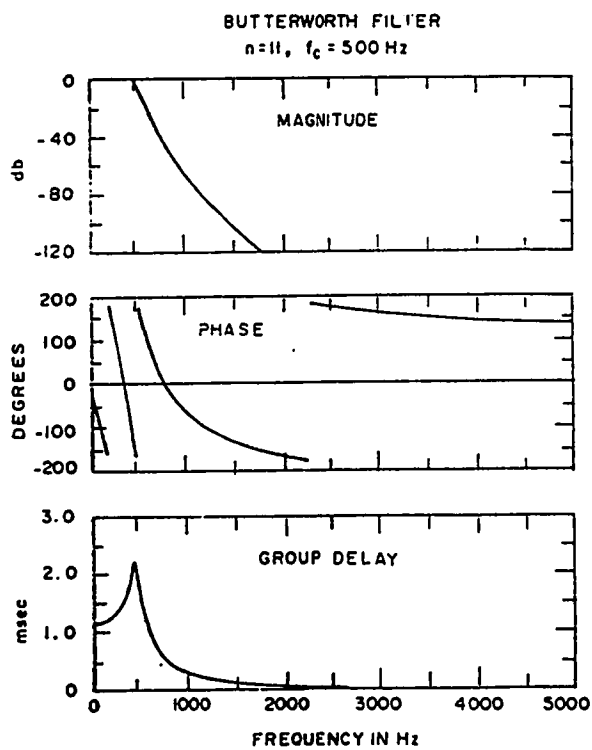


Fig 3.12 Butterworth filter characteristics (Baher 1992)

Let the channel spacing $f_s = 25$ KHz and $f_b = 1/T = 16$ Kbits/s. This corresponds to $f_s T = 1.5$. From Fig. 3.14, it has been found in [Hirade] that $B_b T = 0.28$ can be adopted as the digital modulation for conventional VHF and UHF SCPC mobile radio communications without carrier frequency drift where the ratio of out-of-band radiation power in the adjacent channel to the total power in the desired channel is less than -60 dB. However, if there is a certain amount of carrier frequency drift, a lower value for $B_b T$ is needed.

BER Performance of the GMSK:

Let us consider the theoretical BER of GMSK using coherent detection in the presence of additive white Gaussian noise (AWGN). Since the GMSK is a certain kind of binary digital modulation, its BER performance can be approximated by

$$P_e = \frac{1}{2} \operatorname{erfc} \left(\frac{d_{\min}}{2\sqrt{N_0}} \right) \quad (3.23)$$

where N_0 is the power spectrum density of the AWGN and $\operatorname{erfc}(x)$ is the complementary error function given by

$$\operatorname{erfc}(x) = \frac{2}{\sqrt{\pi}} \int_x^{\infty} \exp(-u^2) du. \quad (3.24)$$

Furthermore, d_{\min} is the minimum value of the signal distance d between mark and space in Hilbert space observed during the time interval from t_1 to t_2 where d

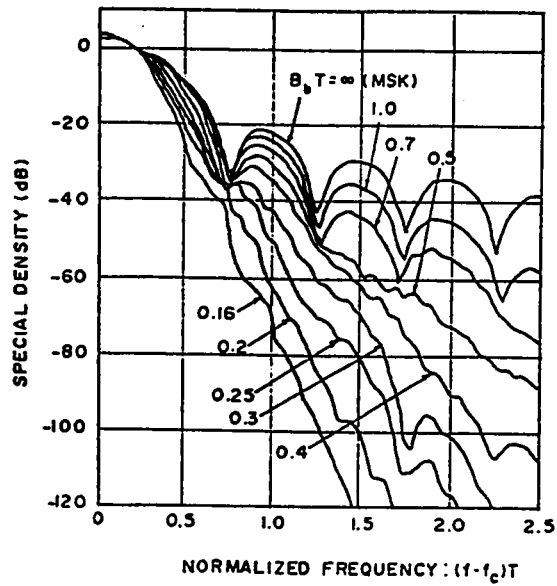


Fig 3.13 Power spectra of GMSK (Hirade 1981)

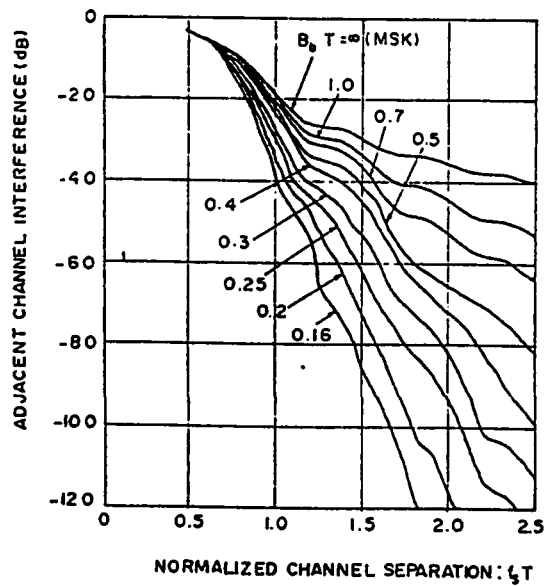


Fig 3.14 Adjacent channel interference of GMSK

is given by

$$d^2 = \frac{1}{2} \int_{t_1}^{t_2} |u_m(t) - u_s(t)|^2 dt \quad (3.25)$$

where $u_m(t)$ and $u_s(t)$ are the complex signal waveforms corresponding to the mark and space transmissions, respectively.

Fig. 3.15 shows d_{\min} of the GMSK signal versus B_bT where E_b denotes the signal energy per bit given by

$$E_b = \frac{1}{2} \int_0^T |u_m(t)|^2 dt = \frac{1}{2} \int_0^T |u_s(t)|^2 dt. \quad (3.26)$$

Predetection Filter:

Fig. 3.16 shows the degradation in the signal to noise ratio E_b/N_0 as a function of the normalized predetection filter bandwidth B_iT for different values of B_bT . The filter type is also Gaussian. It is clear from the figure that $B_iT = 0.63$ is nearly optimum.

Hirade evaluated the performance of the GMSK system which is a binary FM signal under AWGN and Rayleigh fading. In this thesis, we will implement the parallel type MSK shown in Fig 3.6. To implement the GMSK system, two Gaussian LFPs are inserted after the serial-to-parallel converter with a normalized bandwidth $B_bT = 0.125$ as shown in Fig. 3.17. The bandwidth is halved since the symbol duration is twice that of the original bits. The new proposed system

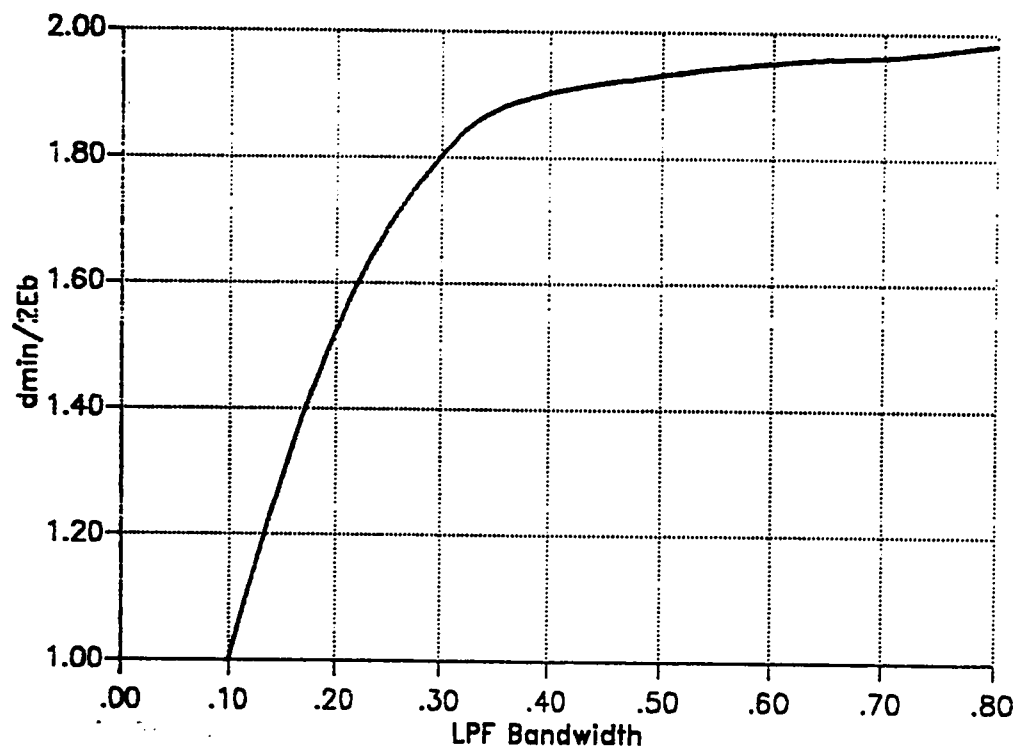


Fig 3.15 normalized minimum signal distance of GMSK (Hirade 1981)

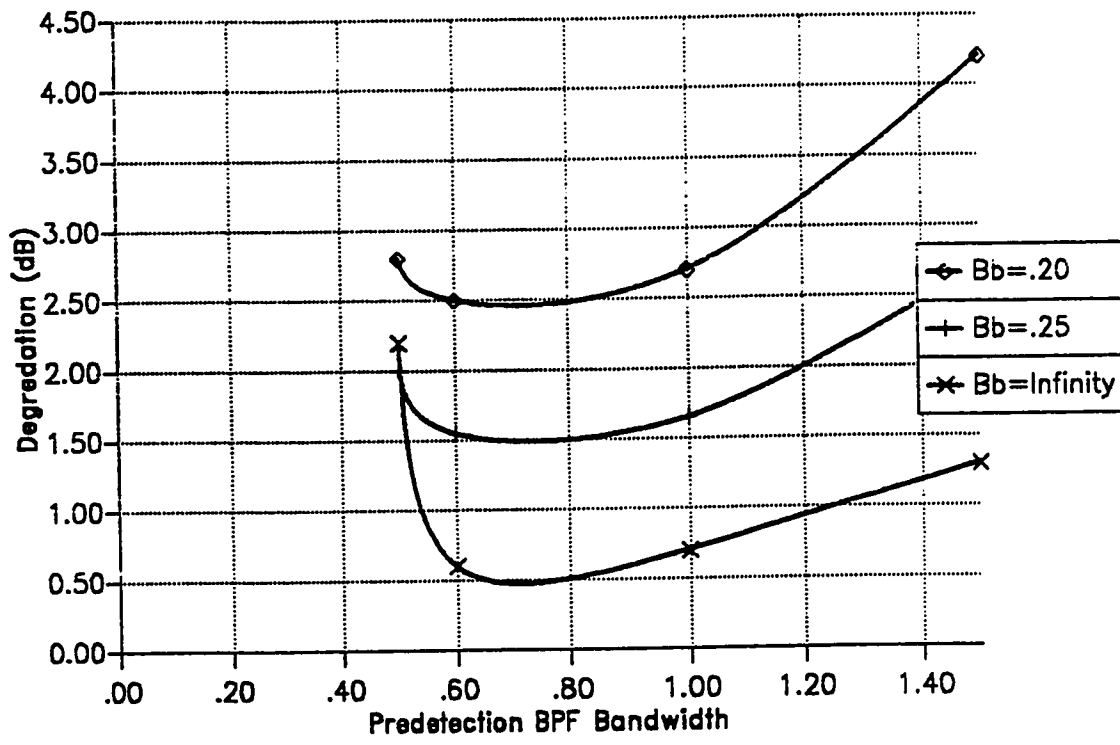


Fig 3.16 Degradation of required E_b/N_0 for obtaining BER of 10^{-3} (Hirade 1981)

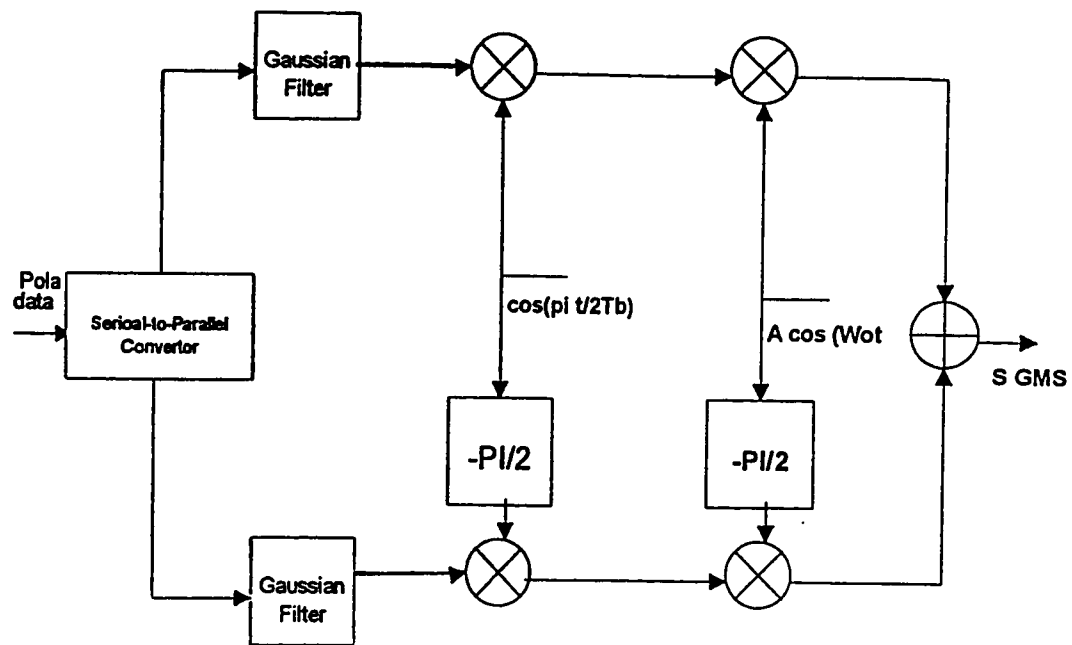


Fig 3.17 GMSK parallel type modulator

power spectral density will be evaluated and compared with the Hirade system. Also, the system performance will be investigated under different channels.

The GMSK system has been adopted as the modulation standard for the pan-European digital cellular network GSM, which was recently installed in 1991.

3.4 Quadrature Amplitude Modulation (QAM)

Coherent M -ary phase shift keying (MPSK) is known to have an efficient bandwidth utilizing. An alphabet with M symbols is used instead of using a binary alphabet with 1 bit of information per channel symbol period. This permits the transmission of $K = \log_2 M$ bits during each symbol period. The use of M -ary symbols allows a k -fold increase in the data rate within the same bandwidth. Thus, when operating with the same data rate, the use of M -ary PSK reduces the required bandwidth by a factor k [Sclar 1988].

From equation (3.2), it can be seen that QPSK modulation consists of two independent streams. One stream modulates the cosine function while the other stream modulates the sine function. The resultant waveform is called a double-sideband suppressed-carrier (DSB-SC) wave, because the RF bandwidth is twice the baseband bandwidth and there is no isolated carrier term. Quadrature am-

plitude modulation (QAM) can be considered a logical extension of QPSK. QAM consists of two independently amplitude-modulated carriers in quadrature. Each block of k bits (k is even) is split into two $(k/2)$ -bit blocks which are used to modulate the cosine and sine functions. At the receiver, each of the two signals is detected independently. QAM can also be viewed as a combination of amplitude shift keying (ASK) and phase shift keying (PSK). Thus, it is sometimes called amplitude phase keying (APK). Also, it can be viewed as amplitude shift keying in two dimensions and hence it is sometimes called quadrature amplitude shift keying (QASK) [Haykin 1988].

There is a great demand for mobile systems that can provide high-rate data communication. This requires modulation techniques with higher spectral efficiency. QAM schemes are considered good candidates. However, multi-level QAM modulation schemes are not constant envelope systems and hence their performance is expected to degrade significantly when operating in a non-linear environment. In this thesis, the effect of non-linear amplifiers having both AM/AM and AM/PM distortions on QAM systems will be investigated.

Fig. 3.18 shows a two-dimensional signal space and a set of 16-ary QAM signal vectors or points arranged in a rectangular constellation. Gray coding (where adjacent symbols differ only by one bit) is assumed.

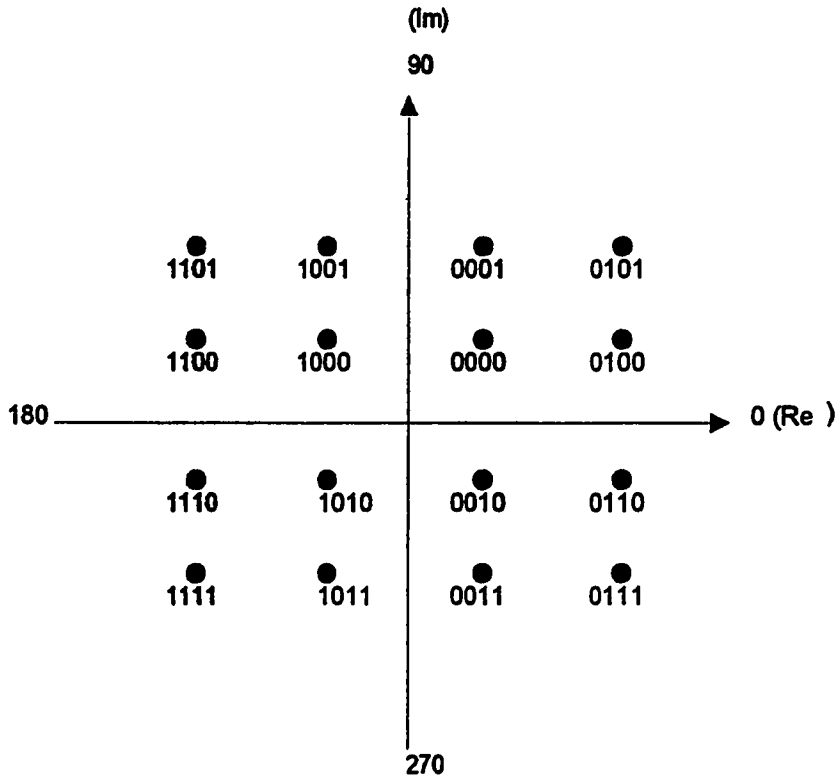


Fig 3.18 Gray encoding for 16-QAM

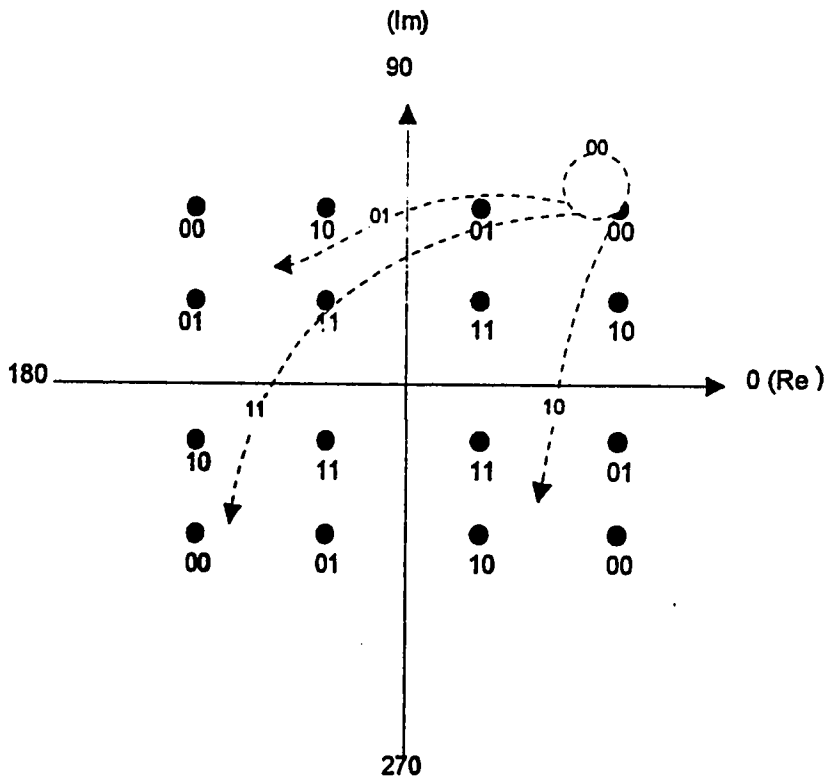


Fig 3.19 Differential encoding for 16-QAM

Fig 3.19 Table

Differential QAM (DQAM)

A common problem that usually arises at the receiver is that the receiver can recognize the pattern of the signal points but cannot distinguish between the various symmetric phase orientations of the signal set. An L -fold rotational symmetry can be defined as a signal set for which the signal set pattern remains unchanged after a rotation of $\pm I(2\pi/L)$ radians, where I and L are integers. Thus, given $M = 2^k$ signal points, the receiver cannot properly assign the k bits to each detected signal point without first resolving the L -fold ambiguity. The simplest example is BPSK. The receiver needs some absolute way of distinguishing between the two equal and opposite signal points before it can assign a binary one to one phase and a zero to the other. This ambiguity can be solved in three ways: (1) a constant reference signal of some kind can be transmitted along with the modulated data signal; (2) an acquisition signal and/or the periodic insertion of a synchronization sequence can be used in the data stream; (3) the use of a differential encoding. The first two methods have an obvious disadvantage which is the extra needed power and the extra bandwidth needed to keep the same transmission rate. The third technique, which is implemented in this thesis, has the advantage that by properly encoding and decoding the signal points, the proper bit detection takes place regardless of rotational phase ambiguities. The disadvantage is that this coding procedure slightly increases the probability of bit error over the

conventional uncoded case.

Fig. 3.19 shows the signal constellation for 16 DQAM. An easy way to implement the 16 QAM is to first differentially encode the source bits and then map them onto absolute signal points as described below.

The following procedure is taken from the V32 modem data sheets. The scrambled data stream to be transmitted is divided into groups of 4 consecutive data bits, $Q_{1_n}, Q_{2_n}, Q_{3_n}$ and Q_{4_n} where the subscript n designates the sequence number of the group. The first two bits in time Q_{1_n} and Q_{2_n} in each group are differentially encoded into Y_{1_n} and Y_{2_n} according to Table 3.2. Bits $Y_{1_n}, Y_{2_n}, Q_{3_n}$ and Q_{4_n} are then mapped into the coordinates of the signal states to be transmitted according to the signal space diagram shown in Fig. 3.20. In this thesis the performance of 16 DQAM with two different constellations will be investigated under AWGN, Rayleigh fading and frequency selective fading. Emphasis will be given to the effect of nonlinear amplification.

Star QAM(SQAM)

There are two rules for mapping a 4 bit symbol onto two dimensional space: square mapping and star mapping. 16 square QAM requires coherent detection while 16 star QAM supports differential detection. Fading is usually encountered

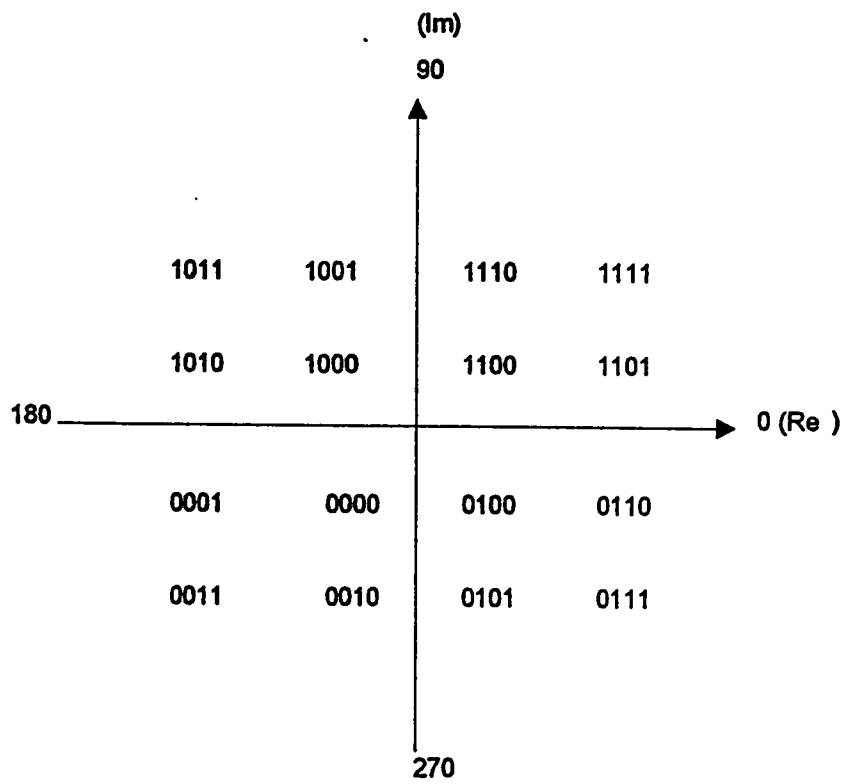


Fig 3.20 Signal constellations for signals used in the V32 modem

Differential Quadrant Coding for 4800 Bit/s

and for Nonredundant Coding at 9600 Bit/s

Input		Previous Output		Phase quadrant	Output	
Q_n^1	Q_n^2	Y_{n-1}^1	Y_{n-1}^2		Y_n^1	Y_n^2
					change	
0	0	0	0	+ 90	0	1
0	0	0	1		1	1
0	0	1	0		0	0
0	0	1	1		1	0
0	1	0	0	0	0	0
0	1	0	1		0	1
0	1	1	0		1	0
0	1	1	1		1	1
1	0	0	0	+ 80	1	1
1	0	0	1		1	0
1	0	1	0		0	1
1	0	1	1		0	0
1	1	0	0	+ 270	1	0
1	1	0	1		0	0
1	1	1	0		1	1
1	1	1	1		0	1

Table 3.2

in mobile radio channels. When fading is slow, the phase is rotated over a long number of transmitted bits. When coherent detection is employed, this phase rotation is detected and 16 square QAM outperforms 16 star QAM. However, the receiver structure can be significantly simplified by employing noncoherent detection and the phase rotation affects only the first symbol in the differential case [Adachi 1991].

The signal constellation for the 16 star QAM using Gray coding is shown in Fig. 3.21. Differential star QAM (DSQAM) performance will also be investigated. DSQAM will be implemented by a similar way as that used in DQAM. The first two bits in every four bits sequence will be differentially encoded and the resultant sequence will be mapped into absolute signal points. The effect of nonlinear amplification on both 16 SQAM and 16 DSQAM will be investigated in the following chapter.

[Chow 1992] has shown that the optimum ratio between the outer ring and the inner ring in the case of AWGN is 1.8 (see Fig. 3.22). In this thesis, the effect of nonlinear amplification on this optimum ratio will be investigated.

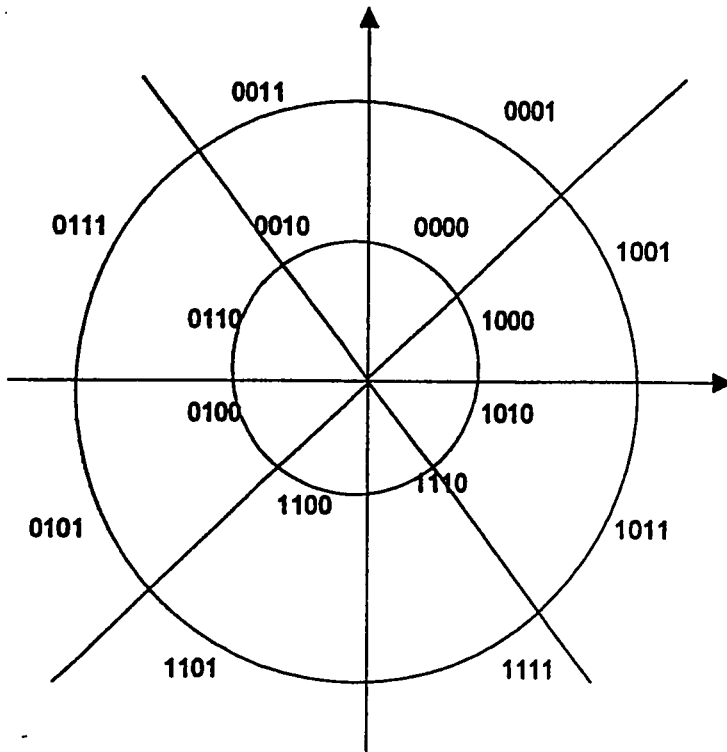


Fig 3.21 Gray coding for star 16-QAM

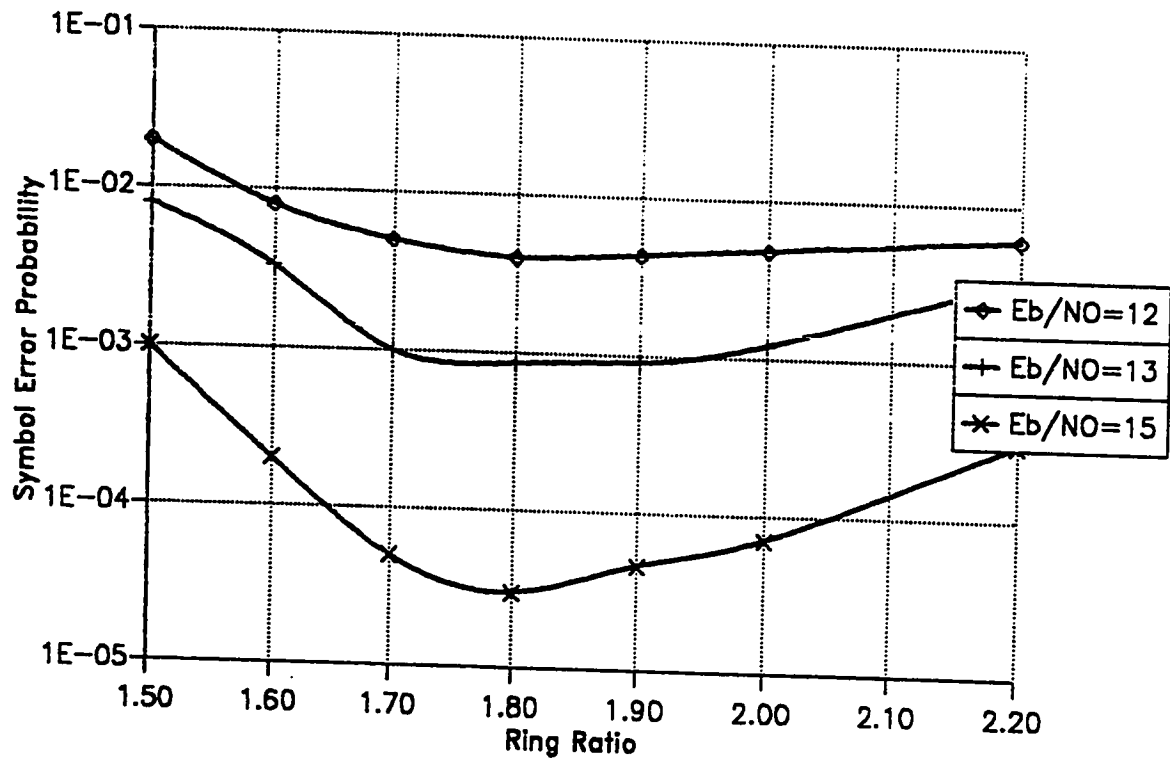


Fig 3.22 Ring ratio optimisation for Star QAM under AWGN (Adachi 1991)

3.5 Summary

In this chapter, GMSK and $\pi/4$ -DQPSK systems which are in use for mobile communication are described. The power spectrum of the GMSK and the optimum Gaussian lowpass filter bandwidth is shown with a brief description of Gaussian filters. The effect of the used Gaussian filter in reducing the out-of-band power to meet mobile communication requirements is shown. Transmission of data at high rates will require larger bandwidth which is limited in a mobile communication environment. Another alternative is to use a more spectrally-efficient modulation scheme like the QAM system. In this chapter, QAM systems are described. Two classes of proposed QAM systems according to the signal constellation are described. These are the square QAM and the star QAM. Also, it is shown how to differentially encode the data before transmission in QAM systems. The performance of the three aforementioned systems will be discussed in the next chapter.

CHAPTER FOUR

PERFORMANCE EVALUATION OF $\pi/4$ -DQPSK, GMSK AND QAM SYSTEMS UNDER DIFFERENT MOBILE CHANNEL IMPAIRMENTS

4.1 Introduction

A basic issue in the selection of the modulation system is to study the effect of noise and other different communication channel impairments on the performance of the receiver. A criterion is needed to describe the performance of different systems. In digital communication systems, the bit error rate (BER) is usually used as a measure of performance.

The main mobile channel impairments are reviewed in Chapter two. In this chapter, we evaluate each of the proposed modulation scheme presented in the preceding chapter when used in such impairments. The AWGN channel is a very simple model for the communication channel. If the transmitted signal is $s(t)$, then the received signal in one signaling interval is

$$r(t) = s(t) + n(t) \quad 0 \leq t \leq T \quad (4.1)$$

where $n(t)$ denotes the additive white Gaussian noise and T is the symbol duration.

Fluctuations in the amplitude of the received signal due to receiving the signal

via different paths in a time-varying manner (fading) result in a multiplicative distortion of the transmitted signal. Hence, the received signal will be [Proakis 1989]

$$r(t) = \alpha e^{-j\phi} s(t) + n(t) \quad 0 \leq t \leq T. \quad (4.2)$$

In ideal coherent detection, the phase shift ϕ is estimated. The fading is assumed slow enough to make this estimation without error.

Multipath mobile radio channels are usually modeled as frequency-selective fading channels. These channels are characterized by the delay spread which is the delay between the shortest and the longest paths. These channels introduce ISI and hence degrade the performance of the system as discussed in Chapter 2 [Shanmugan 1992].

The work conducted in this thesis has shown that the parallel structure of the GMSK transmitter is superior over that proposed in [Hirade 1981]. Not only is a lower out-of-band energy achieved, but also the design of the Gaussian filters is made easier. More details about this are provided later.

In this chapter, the performance of the three systems described in the preceding chapter, namely, GMSK, 16-QAM (square, star and differential) and $\pi/4$ -shifted-DPSK systems will be investigated under different channel impairments. This chapter is organized as follows. Section 4.2 deals with baseband representation

of systems. In section 4.3, the $\pi/4$ -shifted-DQPSK system's performance under different channels is investigated. Section 4.4 deals with the GMSK system. The system implementation and performance are discussed. Section 4.5 is devoted to the recently proposed 16 QAM systems. Different 16 QAM systems are investigated. This includes square QAM, Star QAM and differential QAM. Being of a non-constant envelope, the effect of non-linearity introduced by the power amplifiers is investigated. In the case of Star QAM, the effect of non-linearity on the optimum ratio between the outer and the inner rings which was reported to be 1.8 is investigated.

4.2 Baseband Representation

To use the carrier phase information, the GMSK was implemented in the pass-band domain where the carrier is included. Since this information is not needed for the $\pi/4$ -shifted-DQPSK and the QAM systems, they are implemented in the baseband domain without including the carrier. This results in a considerable reduction in the simulation process.

A bandpass signal $s(t)$ can be represented as [Hayakin]

$$s(t) = \text{Re}[\hat{s}(t)e^{j2\pi f_c t}] \quad (4.3)$$

where f_c is the carrier frequency and $Re[\cdot]$ denotes the real part. The baseband signal is a complex signal and is given by

$$\hat{s}(t) = s_I(t) + js_Q(t) \quad (4.4)$$

where $s_I(t)$ is the in-phase component and $s_Q(t)$ is the quadrature component. The quantity $\hat{s}(t)$ is termed the complex envelope of the signal [Haykin 1988].

Noise also can be represented in the same manner yielding

$$\hat{n}(t) = n_I(t) + jn_Q(t) \quad (4.5)$$

where $n_I(t)$ and $n_Q(t)$ are modeled as sample functions of independent zero-mean white Gaussian random processes. Both $n_I(t)$ and $n_Q(t)$ have a power spectral density of $N_0/2$ watts/Hz. The impulse response of the channel is given by

$$h(t) = 2\text{Re}[\hat{h}(t)e^{j2\pi f_c t}] \quad (4.6)$$

where

$$\hat{h}(t) = h_I(t) + jh_Q(t). \quad (4.7)$$

The output signal baseband representation is given by

$$\hat{x}(t) = \hat{s}(t) \otimes \hat{h}(t) + \hat{n}(t) \quad (4.8)$$

where \otimes denotes the convolution operation. Both of the QAM and the $\pi/4$ -shifted-DQPSK systems are simulated here in the baseband domain.

4.3 The $\pi/4$ -Shifted-DQPSK

This system is discussed previously in Chapter 3. In coherent reception of QPSK signals, it is assumed that a good estimate of the carrier phase is available. In real systems, the carrier phase is extracted from the received signal by performing some non-linear operation that introduces phase ambiguity. For instance, in QPSK, the received signal is raised to the fourth power in order to remove the digital modulation and the resulting fourth harmonic of the carrier frequency is filtered and divided by four in order to extract the carrier component. This yields a carrier frequency component containing an estimate of the carrier phase but with a phase ambiguity of 90 degrees [Sclar 1988].

The phase ambiguity problem can be overcome by encoding the information in phase differences between successive signal transmissions as opposed to absolute phase encoding. This is called differential QPSK (DQPSK). As an example in DQPSK, the relative phase shifts between successive intervals are 0, 90, 180 and - 270 degrees corresponding to the information bits, 00, 01, 11 and 10, respectively. In the $\pi/4$ -shifted-DQPSK the phase shifts are 45, 135, - 135 and - 45 corresponding to the information bits 00, 10, 11 and 01, respectively.

The demodulation of the DPSK is achieved by assuming an absolute phase ref-

erence. Then, the received signal is demodulated to one of the possible transmitted sequences by the known slicing process [Sclar 1988]. Following the demodulator is a phase comparator that compares the phases of the demodulated signal over two consecutive intervals in order to extract the information bits. Coherent demodulation of DQPSK which is employed in this thesis is known to result in a higher probability of error than the error derived for absolute phase encoding due to error propagation.

The BER for the DQPSK system under AWGN is given by [Proakis 1989]

$$P_b = Q(a, b) - \frac{1}{2} I_0(ab) \exp \left[-\frac{1}{2} (a^2 + b^2) \right]. \quad (4.9)$$

where $Q(a, b)$ is the Q function given by $Q(x) = \frac{1}{\sqrt{2\pi}} \int_x^\infty \exp \left(-\frac{u^2}{2} \right) du$, and $I_0(x)$ is the modified Bessel function of order zero and the parameters a and b are defined as

$$\begin{aligned} a &= \left[2\gamma_b \left(1 - \frac{1}{\sqrt{2}} \right) \right]^{1/2} \\ b &= \left[2\gamma_b \left(1 + \frac{1}{\sqrt{2}} \right) \right]^{1/2} \end{aligned} \quad (4.10)$$

where γ_b is the signal-to-noise ratio per bit.

Figure 4.1 shows the performance of the $\pi/4$ -shifted-DQPSK system under both the AWGN and the Rayleigh fading channels. The performance of the DQPSK system under AWGN was reported in [Proakis 1989] and it is with good

agreement with the simulation results obtained in this thesis. The $\pi/4$ -shifted-QPSK system performance under a Rayleigh fading channel was also reported in [Yoshiko 1987]. The simulation results have also good agreement with the reported results. These are included here so that the system performance can be compared with other systems working under AWGN or Rayleigh fading channels.

Figure 4.2 shows the performance of the $\pi/4$ -shifted-DQPSK system when the channel is assumed to be frequency-selective fading. The figure shows the performance when $u = 0.06$ and $u = 0.1$. As expected, there is an error floor in both cases due to ISI which can not be compensated for by adding extra power. We can notice that the normalized *rms* delay spread (u) effect is more significant at large E_b/N_0 values where the ISI effect is dominant. Looking at the figure, we notice that the irreducible bit error rate (IBER) is 3×10^{-3} when $u = 0.06$ while it is 7×10^{-3} when $u = .1$. Any desired probability of error can be reached by decreasing u but this will be at the expense of a lower transmission rate. Another alternative is to try to reduce the ISI effect by employing equalization.

A 5-tap transversal equalizer is used to reduce the ISI effect. The 5-tap equalizer is standard in digital microwave systems [Justin 1989]. The equalizer receives a signal (real or complex) and has five tap gains which are adapted according to the least mean square (LMS) criterion described in Chapter Two. Initially, the tap

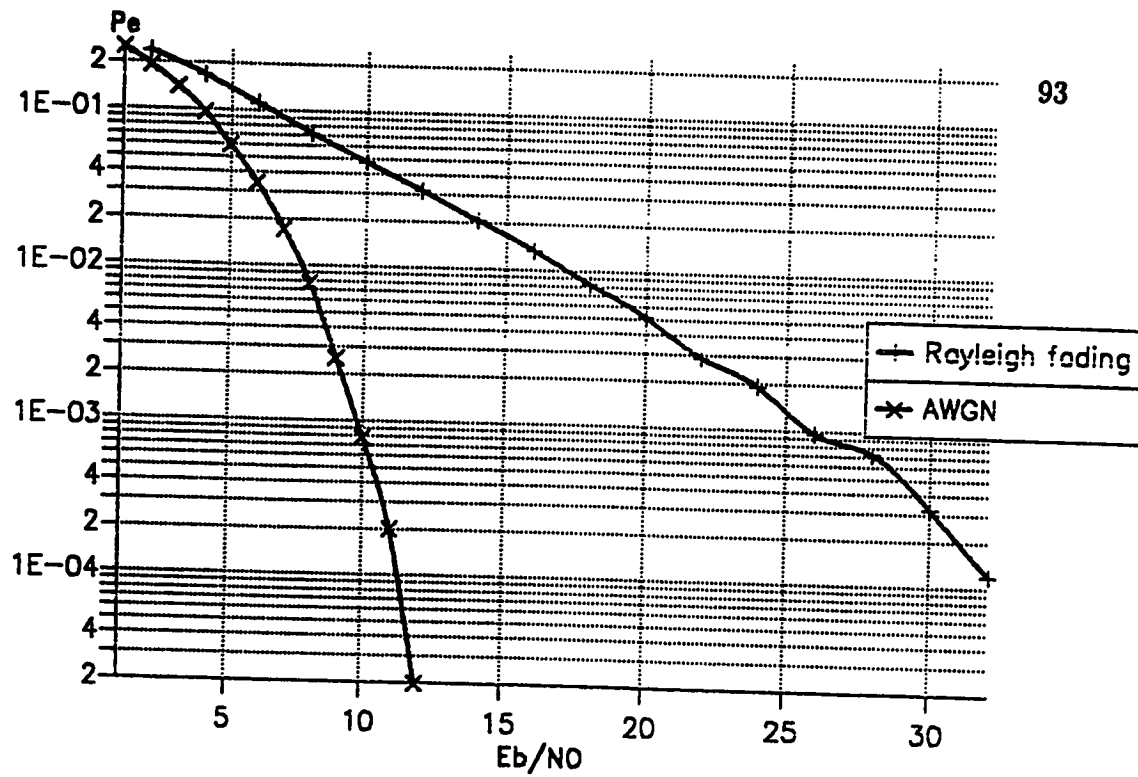


Fig 4.1 $\pi/4$ -shifted-DQPSK under AWGN & Rayleigh fading channels

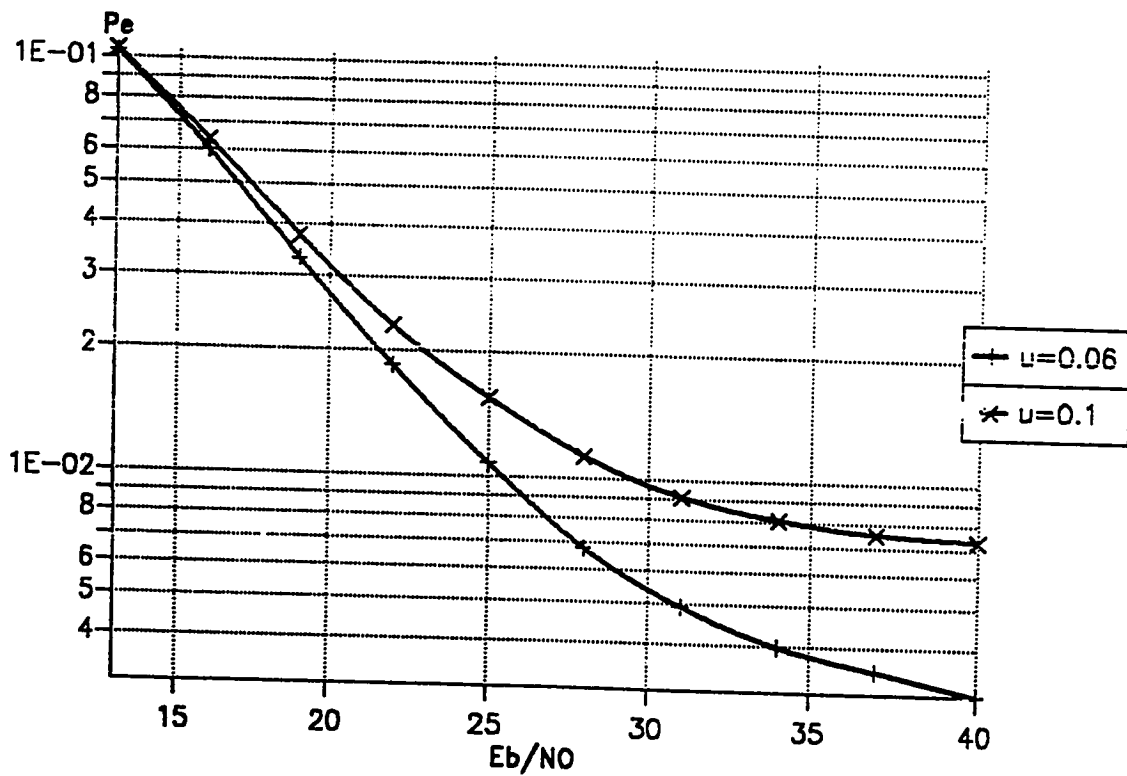


Fig 4.2 $\pi/4$ -shifted-DQPSK under frequency selective fading

gains are set to zero. The optimum tap gains are reached by training the equalizer with 10000 symbols. The step size was chosen to be 0.05 which satisfies the upper bound for the choice of the step size [Proakis 1989].

The effect of equalizing the channel by the aforementioned 5-tap linear equalizer is shown in Fig. 4.3. The unequalized performance is shown for comparison. The used normalized *rms* delay spread (u) is equal to 0.1 which is a high value and hence the IBER is expected to be high too. Looking at the figure we see that the IBER dropped from 7×10^{-3} to 2×10^{-4} when equalization is employed. A BER of 10^{-3} can be tolerated in mobile communication [Lee 1989]. It can be noticed also that when equalization is used, the error rate curve decreases linearly until $E_b/N_0 \simeq 17$ dB. After this point, the curve goes toward the IBER smoothly. The equalizer is unable to cancel the effect of the ISI completely because the ISI characteristics is not deterministic but rather it is changing in a random manner.

4.4 The GMSK System

As discussed in the preceding chapter, the GMSK differs from the well-known MSK in the introduction of a base-band Gaussian filter at the transmitter side and a pass-band Gaussian filter at the receiver side as shown in Fig. 4.4. The GMSK system shown in Fig. 4.4 is the standard used in the GSM and originally

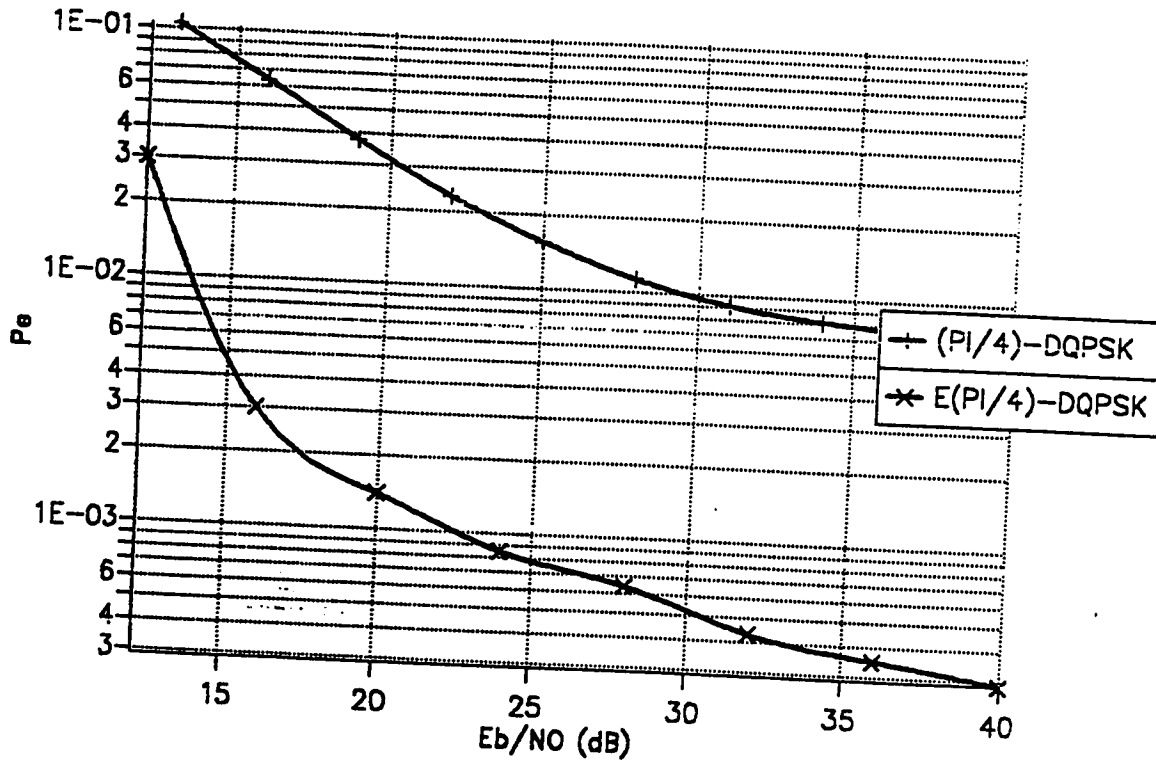


Fig 4.3 Equalized performance of $\pi/4$ -shifted-DQPSK

proposed by [Hirade 1981].

In this thesis, the parallel type MSK modulator discussed earlier is used. This parallel type modulator is used with two Gaussian filters inserted in each branch of the modulator as shown in Fig. 4.5. Since the data is split into the in-phase and the quadrature branches resulting in symbols with half the bit rate ($T/2$) and since the optimum normalized filter bandwidth (B_0T) found by Hirade was 0.25, the inserted Gaussian filters are with a 0.125 normalized bandwidth. Both power spectral densities (PSD) of the filtered series and parallel types MSK system are shown in Fig. 4.6. It is assumed that the center frequency is 100 kHz and the transmission rate is 16 kbps. From Fig. 4.6, it is quite clear that the parallel type modulator is spectrally more efficient, especially at the edge of the band. The proposed parallel type offers additional 15 dB attenuation for the out-of-band energy over that offered by the series type.

To reduce the effect of the additive white Gaussian noise (AWGN), another Gaussian filter is inserted at the front end of the receiver. By reducing the filter bandwidth, less noise will pass but also the received signal will be partially suppressed. The optimum value for the normalized bandwidth (B_iT), where B_i is the receiving filter bandwidth, was found in [Hirade 1981] to be 0.63 and this value is used in this thesis.

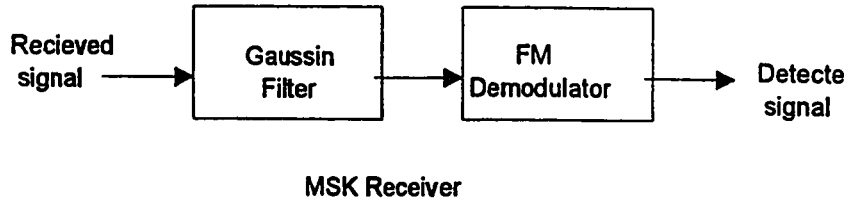
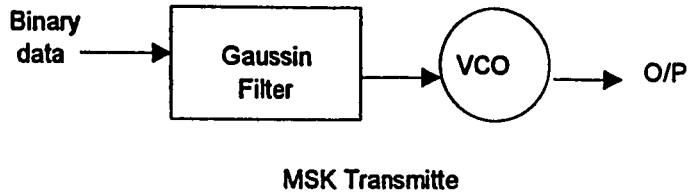


Fig 4.4 Conventional GMSK system (Hirade 1981)

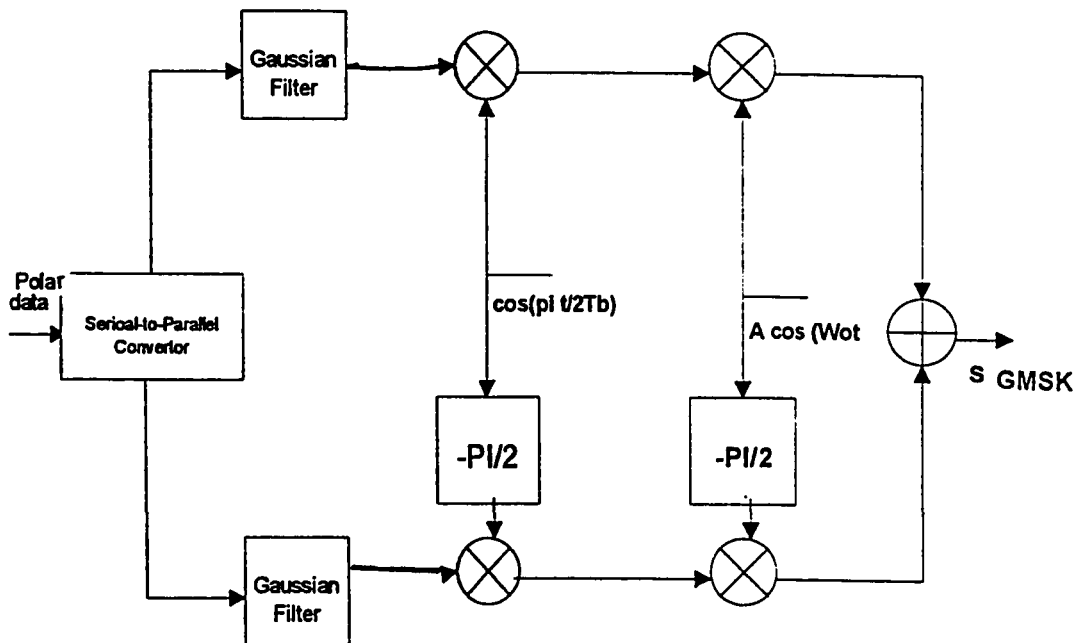


Fig 4.5 New proposed transmitter structure for the GMSK system

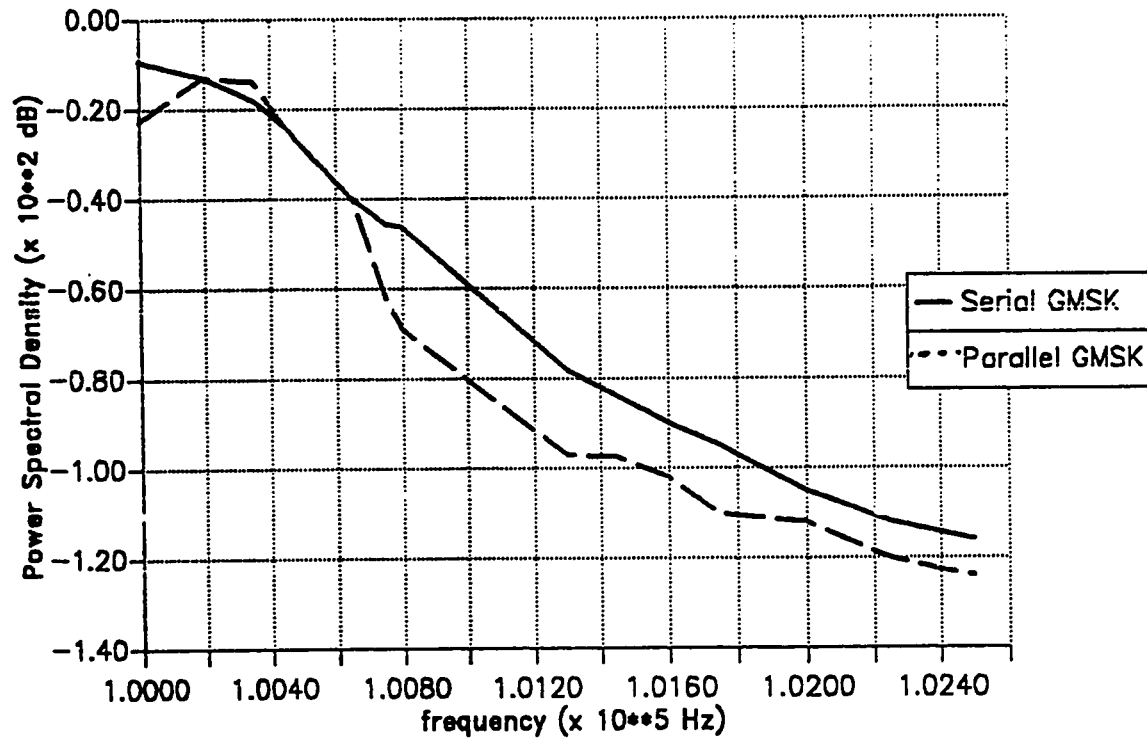


Fig 4.6 PSD of the GSM system

When the parallel type demodulator mentioned earlier in Section 3.3.3 is used to demodulate the MSK signal, the MSK system performance will be equal to that of the BPSK which is

$$P_B = Q\left(\sqrt{\frac{2E_b}{N_0}}\right) \quad (4.11)$$

where E_b is the signal energy per binary symbol and $Q(x)$ is the Q function given in section 4.3.

The MSK can be coherently detected as an FSK signal over an observation interval of one symbol duration (T). Fig. 4.7 shows a filtered binary signal that is used to modulate a carrier and the demodulated signal when the channel is noise-free. A phase-locked loop (PLL) is designed and used in the demodulation process. The system performance is found to be inferior to the BPSK system by 3 dB which is expected as reported in [Sclar 1988]. This is because information provided in the phase is not utilized. This information can be used to achieve an additional 3 dB by combining processing every two symbol periods in each of the in-phase and quadrature-phase components [de Buda 1972]. Thus, the demodulation will be performed using the parallel type demodulator.

The system is simulated using Transient System Level Analysis (TESLA). The simulated test system has the following parameters. The carrier frequency and bit-rate are $f_c = 1\text{MHz}$ and $R_b = 16\text{ kb/S}$, respectively. The normalized

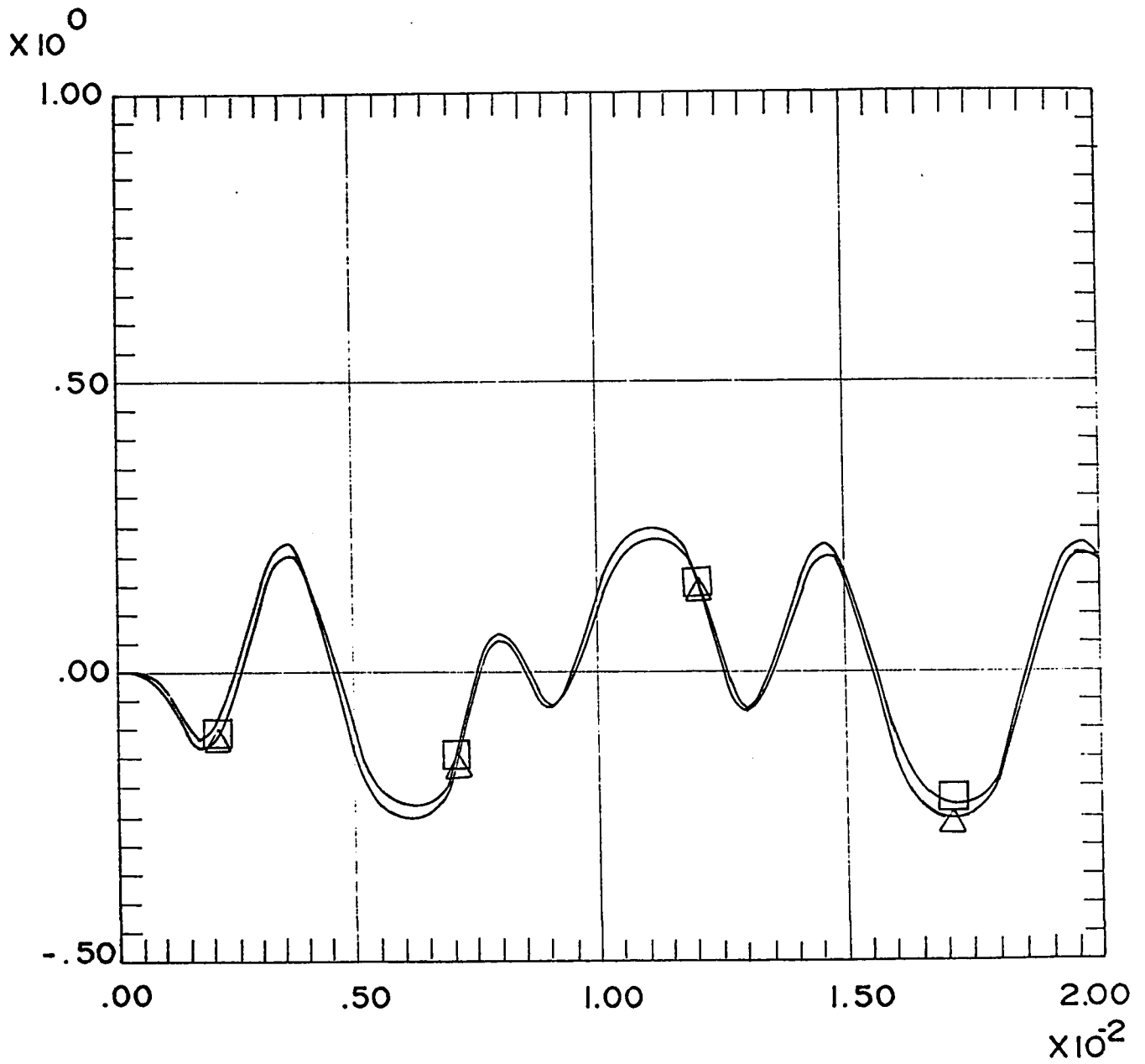


Fig 4.7 The GSM signal demodulated as an FM signal (noise free)

□ modulating signal
△ demodulated signal

premodulation Gaussian low-pass filter bandwidth is set at 0.125 agreeing with whatever reported in literature [Hirade 1981]. The frequency deviation of the RF signal is set equal to $\Delta f_d = 8$ kHz, which corresponds to the MSK condition for the 16 k bits/S transmission. The normalized predetection Gaussian band-pass filter bandwidth is equal to 0.63 which is the optimum value found in [Hirade 1981]. A pseudo-noise (PN) pulse sequence with a repetition period of $N = (2^{20} - 1)$ bits is generated by a 20-stage feedback shift register (FSR) and is used as a test pattern signal. The bandpass filtered output is demodulated using the parallel type demodulator described in the previous chapter and a decision is made. This decision is fed into the error-rate counter for the BER measurement.

GMSK System Performance

The GMSK system performance in AWGN channels can be approximated by [Hirade 1981]

$$P_e(\gamma) = \frac{1}{2} \operatorname{erfc}(\sqrt{\alpha\gamma}) \quad (4.12)$$

where

$$\alpha \simeq \begin{cases} .68 & \text{for GMSK} \\ .85 & \text{for MSK} \end{cases} \quad (4.13)$$

and γ is the received signal bit energy-to-noise-ratio (E_b/N_0).

When a quasi-stationary slow fading model is assumed, the BER performance is given by [Hirade 1981]

$$P_e(\Gamma) = \int_0^{\infty} P_e(\gamma)P(\gamma)d\gamma \quad (4.14)$$

where Γ is the average E_b/N_0 and $P(\gamma)$ is the probability density function (pdf) of γ given by

$$P(\gamma) = \frac{1}{\Gamma} \exp\left(-\frac{\gamma}{\Gamma}\right). \quad (4.15)$$

Substitution of $p(\gamma)$ from equation (4.15) into equation (4.14) yields

$$p_e(\Gamma) \simeq \frac{1}{2} \left(1 - \sqrt{\frac{\alpha\Gamma}{1 + \alpha\Gamma}}\right) \simeq \frac{1}{4\alpha\Gamma} \quad (4.16)$$

where α is the same constant as given in (4.13). It should be noted that this approximation is valid for high signal to noise ratios.

To check the validity of the simulated system, the system performance is tested under AWGN and Rayleigh fading channels. The results indicated in Fig. 4.8 show good agreement with those reported in [Hirade 1981]. We can notice that a SNR of 26 dB is needed to achieve a 10^{-3} BER in the Rayleigh fading channel while it is only 8 dB in the AWGN channel. In Hirade's paper, these two figures are 25 dB and 8.5 dB for the Rayleigh and AWGN channels respectively. That is to say Rayleigh fading has degraded the performance at this BER by nearly 18 dB. From Figs. 4.1 and 4.8, we can conclude that both GMSK and $\pi/4$ -shifted-DQPSK have the same performance when operated under AWGN or Rayleigh fading conditions.

GMSK Performance under Frequency Selective Fading

Time division multiple access (TDMA) is more preferred to frequency division multiple access (FDMA) in the mobile environment because only one carrier frequency is used at a time and hence no inter-modulation products are generated. Also, in contrast to the FDMA, the TDMA system does not need complex frequency synthesizers. Thus mobile units in TDMA require simpler hardware and hence are more economical [Lee 1989]. However, TDMA systems require high transmission rates causing intersymbol interference (ISI) in the multipath fading channel environment. Thus, the received signal is distorted according to the transmission rate which is termed frequency-selective fading. As discussed in Chapter 2, a common parameter to characterize such channels is the normalized root-mean square (*rms*) delay spread which will be denoted by the symbol u . Here, the normalization is to the symbol rate $1/T$ where T is the symbol duration. In the frequency domain, the coherence bandwidth of the channel is defined as the reciprocal of the multipath delay spread of the channel. When the transmission bandwidth is larger than the coherence bandwidth of the channel, frequency-selective fading occurs.

Figure 4.9 shows the probability of error performance for both the MSK and the GMSK systems for $u = 0.1, 0.2$ and 0.3 . We notice that the BER increases

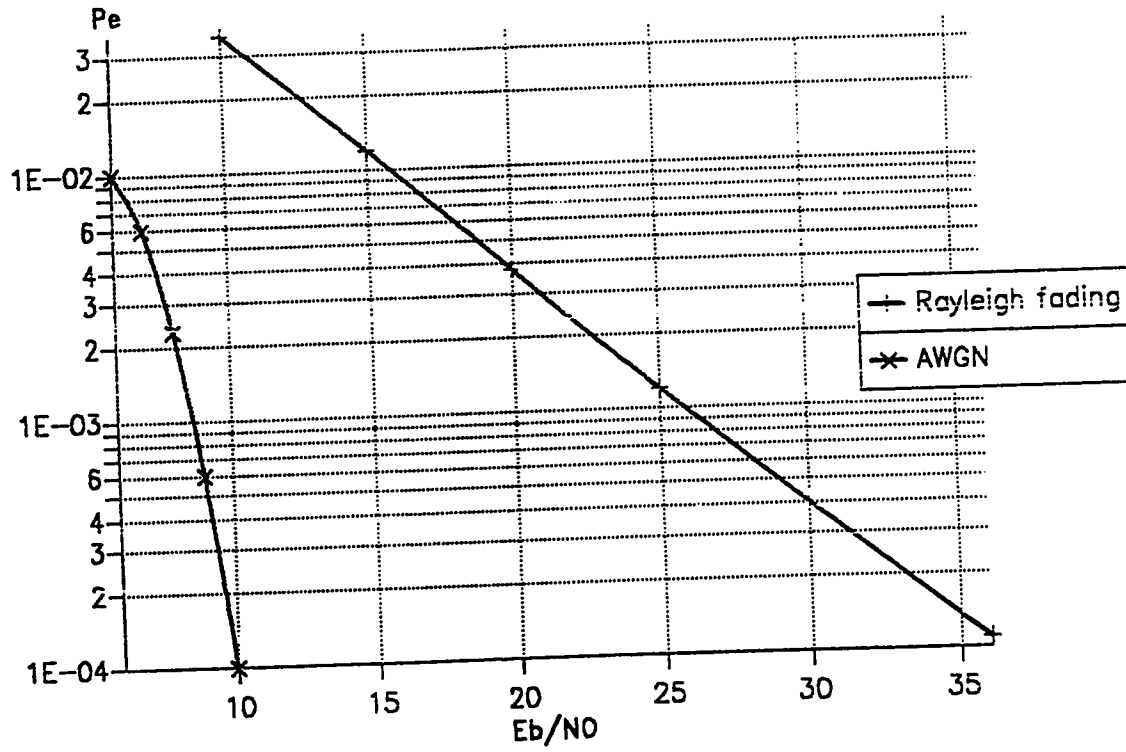


Fig 4.8 GMSK under AWGN & Rayleigh fading channels

as u increases which is expected. It is known that the MSK system outperforms the GMSK in terms of BER when the communication channel is assumed to be AWGN or a non-selective fading channel. However, we notice that the GMSK system has a lower BER than the MSK system when the channel is assumed to be a frequency-selective fading channel. This is a surprising result but might be explained in the following manner. The GMSK system transmission bandwidth is less than that of the MSK system and hence it is expected to suffer less from the limited coherence bandwidth.

For the case of $u = 0.2$, we notice that there is a slight difference between the MSK and the GMSK system for very low values of E_b/N_0 and then both curves decrease linearly until $E_b/N_0 \sim 14$ dB and then the curves reach to what is called the irreducible bit error rate (IBER) at about 23 dB with the GMSK having a lower IBER ($25 * 10^{-2}$) than the MSK system ($3 * 10^{-2}$). This is explained as follows. The two dominant factors contributing to decision errors in the frequency-selective fading environment are the AWGN and the ISI. For small values of E_b/N_0 , the effect of the additive white Gaussian noise is the dominant compared to the distortions caused by the ISI. Thus, as the value of E_b/N_0 is increased, the BER is decreased until the distortions caused by ISI become dominant. When the ISI effect is dominant, increasing E_b/N_0 even to infinity (noise-free case) will not result in an error-free transmission but rather the system BER will reach to what

is called the IBER. Taking the case of $u = 0.1$ as an example, we notice that the IBER of GMSK is 8×10^{-3} which is slightly higher than the $\pi/4$ -shifted-DQPSK performance (7×10^{-3}).

It is clear that the frequency-selective fading channel imposes a limit on the transmission rate in order to achieve a certain BER. For the case of $u = 0.1$ the IBER for the MSK is about 9×10^{-3} which agrees with what is reported in [Justin 1989] [10^{-2}] while it is about 8×10^{-3} for the GMSK. When $u = 0.2$, the IBER is about 3×10^{-2} for the MSK and about 2.5×10^{-2} for the GMSK. The value of u can be determined according to the desired BER. Since the *rms* delay spread is a channel characteristic, what is left to be changed is the transmission rate.

It is quite obvious from Fig. 4.9 that none of the systems has a reasonably acceptable performance. It has been found that in case of frequency selective fading channels, the use of adaptive equalization is inevitable [Justin 1989].

The aforementioned 5-tap linear equalizer is used here to alleviate the ISI effect. Fig. 4.10 shows the performance of the equalized GMSK when u is set to 0.1. The unequalized performance is shown for comparison. We notice that the irreducible error rate has dropped from 8×10^{-3} to 2×10^{-4} by means of equalization. The irreducible error is due to the fact that the channel is changing in a random manner and hence the equalizer tap gains are always changing.

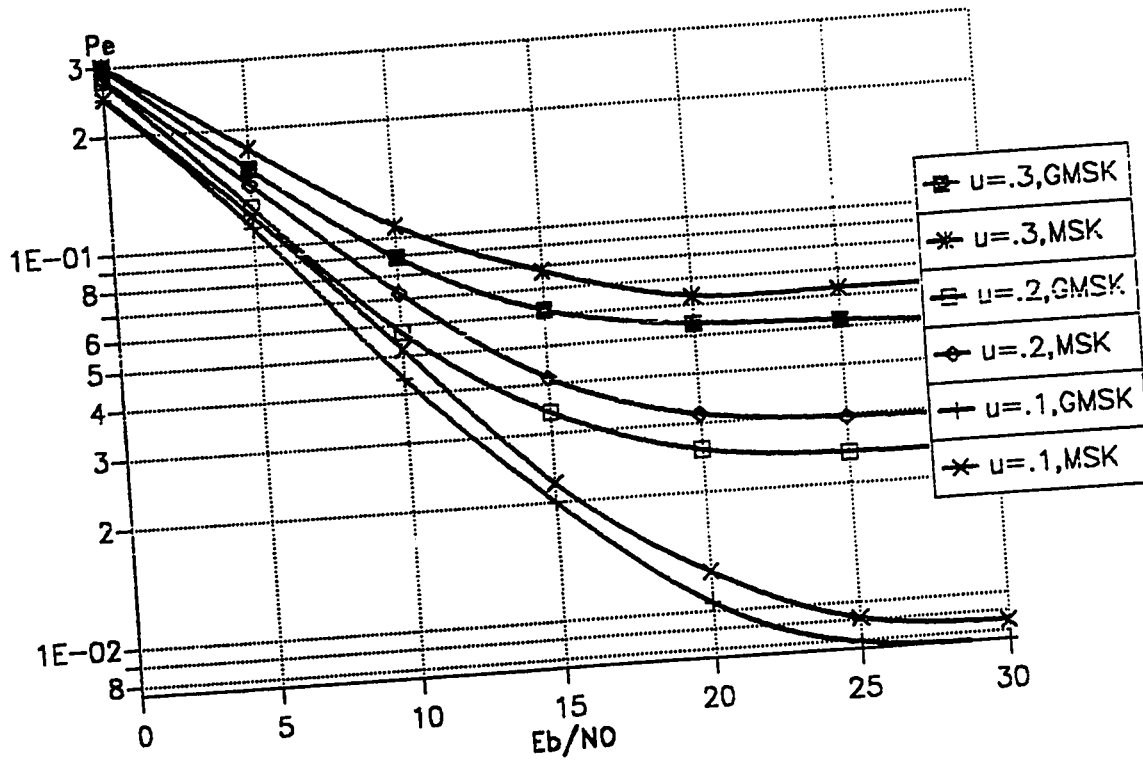


Fig 4.9 GMSK&MSK under frequency selective fading

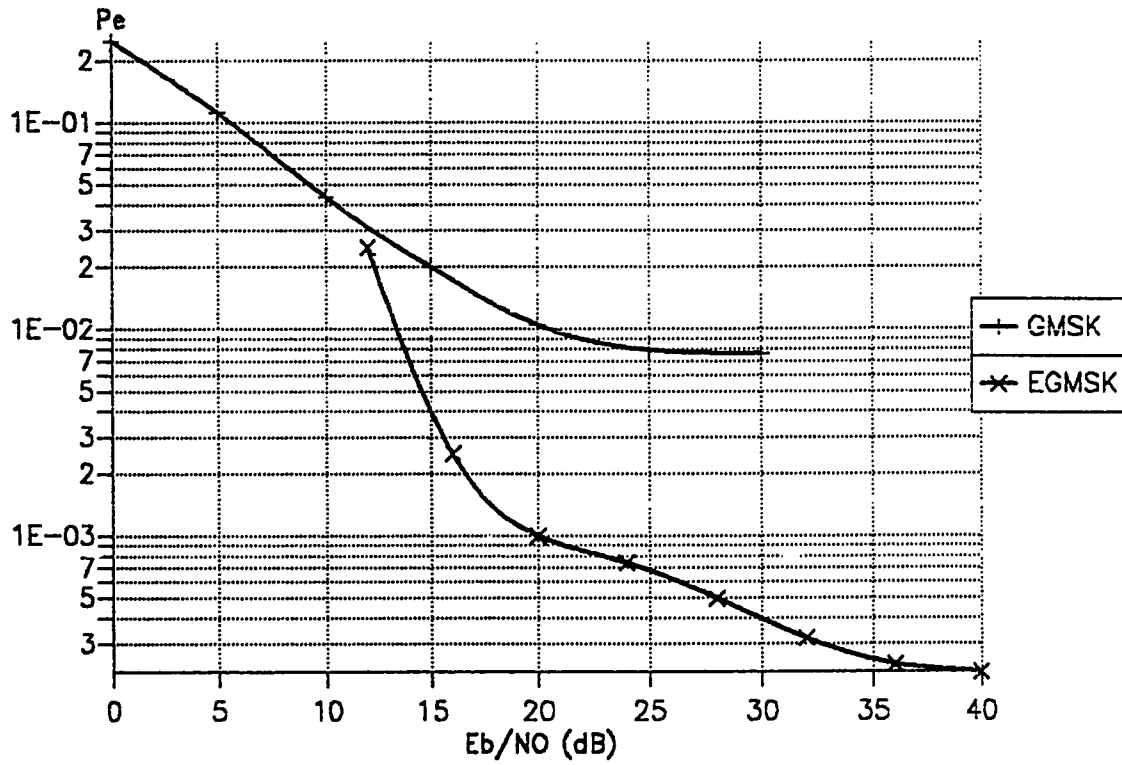


Fig 4.10 Equalized performance of GMSK

It is to be noted that the *rms* delay spread u can be controlled by the system designer through the bit rate. It might appear that u should be made as small as possible in order to lower the BER. However, reducing u will result in lowering the transmission rate and hence reducing the communication efficiency. Choosing the proper value for u is the designer task which is a compromise between the required BER and the transmission rate.

4.5 QAM Systems

QAM systems can be viewed as a combination of amplitude shift keying (ASK) and phase shift keying (PSK) systems. An attractive feature of these systems is their being spectrally efficient and hence requiring less bandwidth which is a desirable feature in mobile communication systems [Lee 1989].

The simulation system under consideration is shown in Fig. 4.11. The data source generates data in a random manner using a pseudo-noise (PN) generator. The modulator puts the data in a format suitable for transmission via the communication channel. The modulator combines every four bits in one symbol and a vector is chosen for transmission according to the signal constellation which is shown previously for both the square QAM and the star QAM (SQAM) in Figures

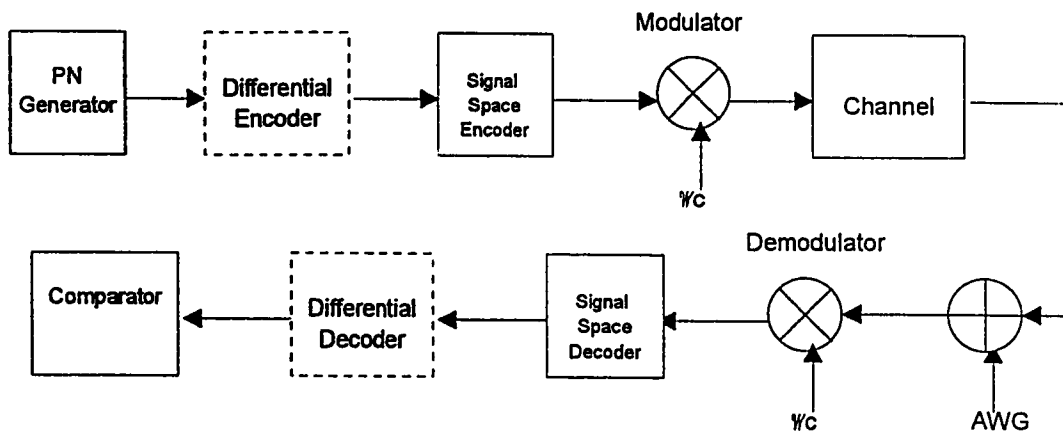


Fig 4.11 Typical communication system

3.18 and 3.21, respectively. The channel affects the transmitted vector as described before.

The demodulation process is the opposite to that of modulation. Let the transmitted vector be denoted by \bar{s}_i and the received vector denoted by \bar{r} . According to the maximum likelihood receiver, the demodulator, after receiving \bar{r} , calculates the distance $d(\bar{r}, \bar{s}_i) = \|\bar{r} - \bar{s}_i\|$ for the whole possibly transmitted vectors. A decision is made in favor of \bar{s}_i that gives the minimum distance. The procedure is termed the slicing process. Received bits and transmitted bits are compared to calculate the BER [Sclar 1988].

Note that, since we use base-band representation in the simulation process, both modulators and demodulators are omitted and the pass-band channel is replaced by its base-band equivalent.

Noise Performance of QAM Systems

The probability of error for the M -ary QAM system under *AWGN* channel is equal to [Proakis 1989]

$$P_M = 1 - (1 - P_{\sqrt{M}})^2 \quad (4.17)$$

where

$$P_{\sqrt{M}} = \left(1 - \frac{1}{\sqrt{M}}\right) \operatorname{erfc} \left[\left(\frac{3}{M-1} \frac{1}{2} \gamma_{dv} \right)^{1/2} \right] \quad (4.18)$$

in which γ_{dv} is the average signal-to-noise ratio SNR per symbol.

There are different types of QAM systems which are discussed previously in Chapter 3. These include square QAM which will be denoted simply QAM, differential square QAM (DQAM), star QAM (SQAM) and differential star QAM (DSQAM). The ratio between the outer ring and the inner ring in the SQAM system has an optimum value of 1.8 and the system will be denoted optimum star QAM (OSQAM) [Adachi]. Fig 4.12 shows the performance of QAM, DQAM, SQAM, DSQAM and OSQAM under an additive white Gaussian noise (AWGN) channel. The performance of the QAM system is compared with the one reported in [Proakis 1989] and shows good agreement. To get a BER of 10^{-3} , 11.5 dB is needed in the simulation and about 11.8 dB in Proakis. As expected, the performance of the SQAM is worse than the QAM but it has the advantage of simpler receiver structure [Adachi]. At 12 dB, for example, the BER for QAM is 3×10^{-4} while it is 4×10^{-3} for SQAM. Also, we notice that the differential systems are worse than conventional systems due to error propagation. We notice that the BER for the DQAM at 12 dB is 5×10^{-4} while it is 3×10^{-4} for QAM. However, by the differential encoding of transmitted data, the phase ambiguity at the receiver can be resolved.

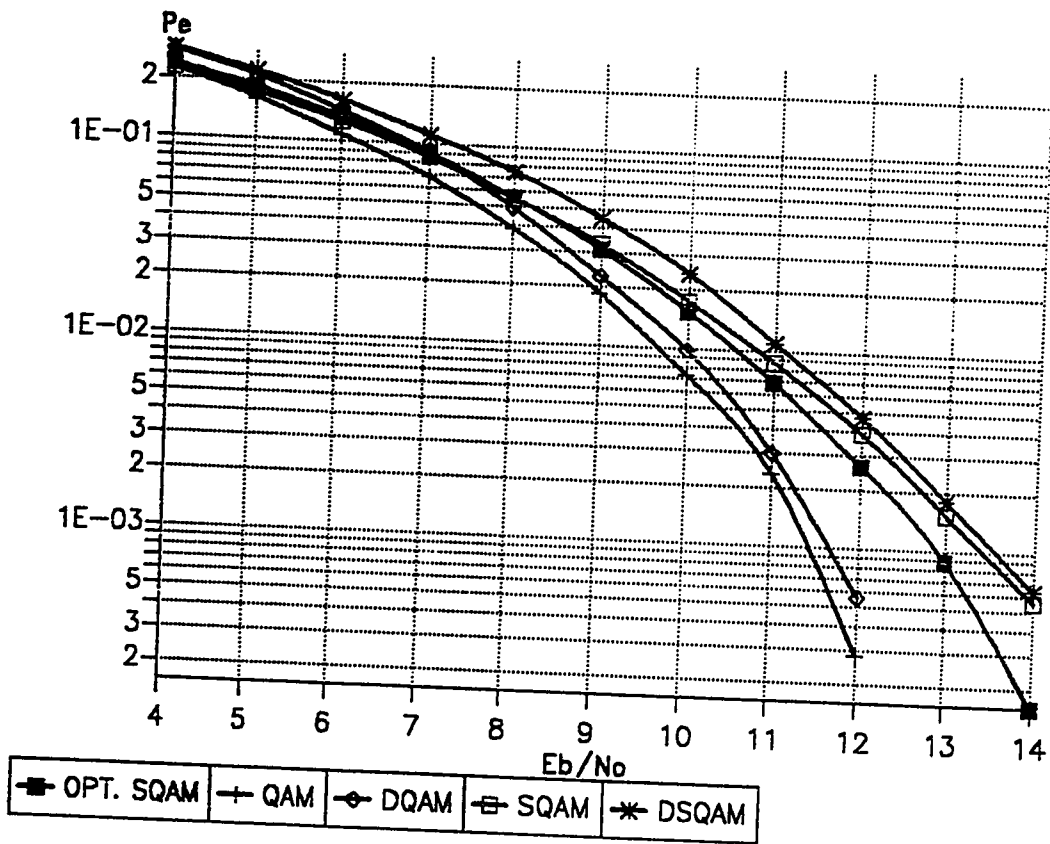


Fig 4.12 Different 16-QAM systems under AWGN

A major obstacle of QAM systems is that the transmitted signal does not have a constant envelope. When such a signal passes through a non-linear amplifier that has both AM/AM and AM/PM distortions, the system performance is degraded. The four-parameter formula which was discussed earlier in Section 2.4.3 is used to model both the magnitude non-linearity (AM/AM) and the phase non-linearity (AM/PM). A common parameter to measure the performance of systems amplified by such non-linear amplifiers is the backoff from saturation as mentioned in Section 2.4.3. When the backoff is large, the system will be in the linear region and when the backoff is small, the system will be operating in the non-linear region and considerable degradation in the system performance is expected [Ghorban 1986].

Figure 4.13 shows the performance of the QAM, DQAM, SQAM and DSQAM systems in the form of BER versus backoff from the saturation point and with E_b/N_0 as a parameter. Fig. 4.14 shows the performance of the aforementioned systems in the form of BER versus E_b/N_0 with the backoff from saturation as a parameter. Looking at these figures we can see that at a certain E_b/N_0 , the bit error rate (BER) decreases almost linearly when the backoff from saturation is increased. We also notice that at a certain backoff from saturation, the difference in performance between the differential and conventional systems is apparent only at high values of E_b/N_0 . Table 4.1 shows the required E_b/N_0 to achieve a BER of 10^{-3} for different backoff values.

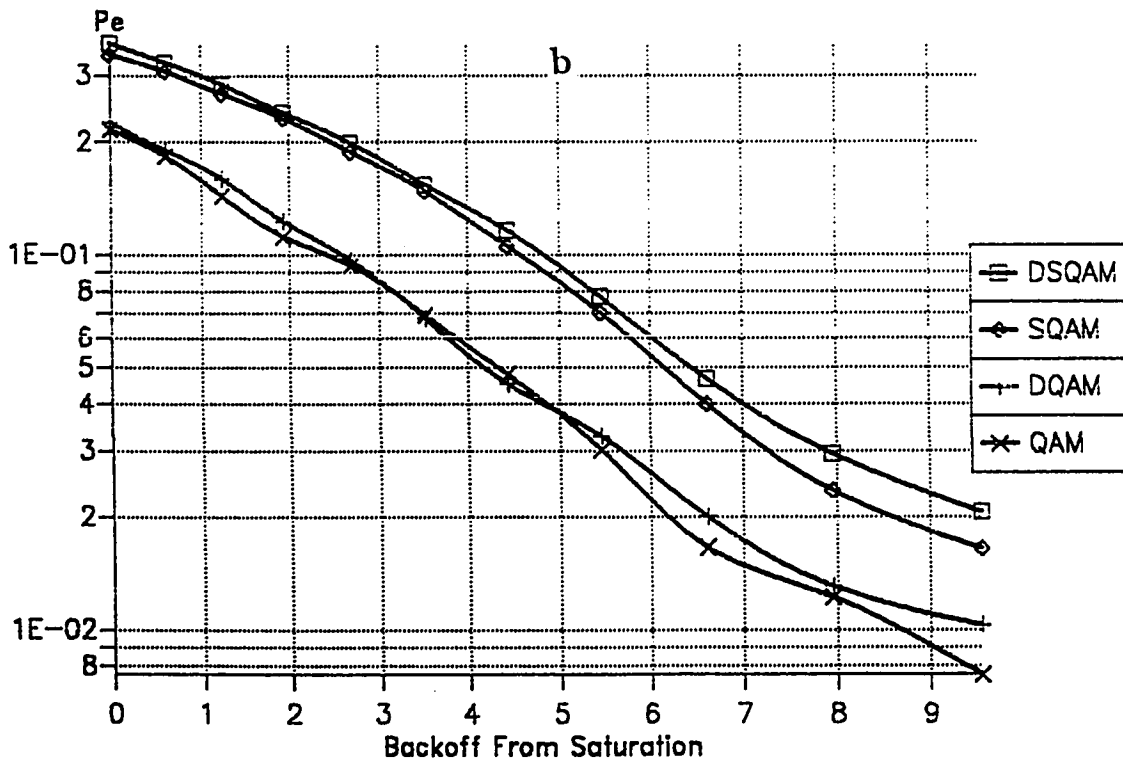
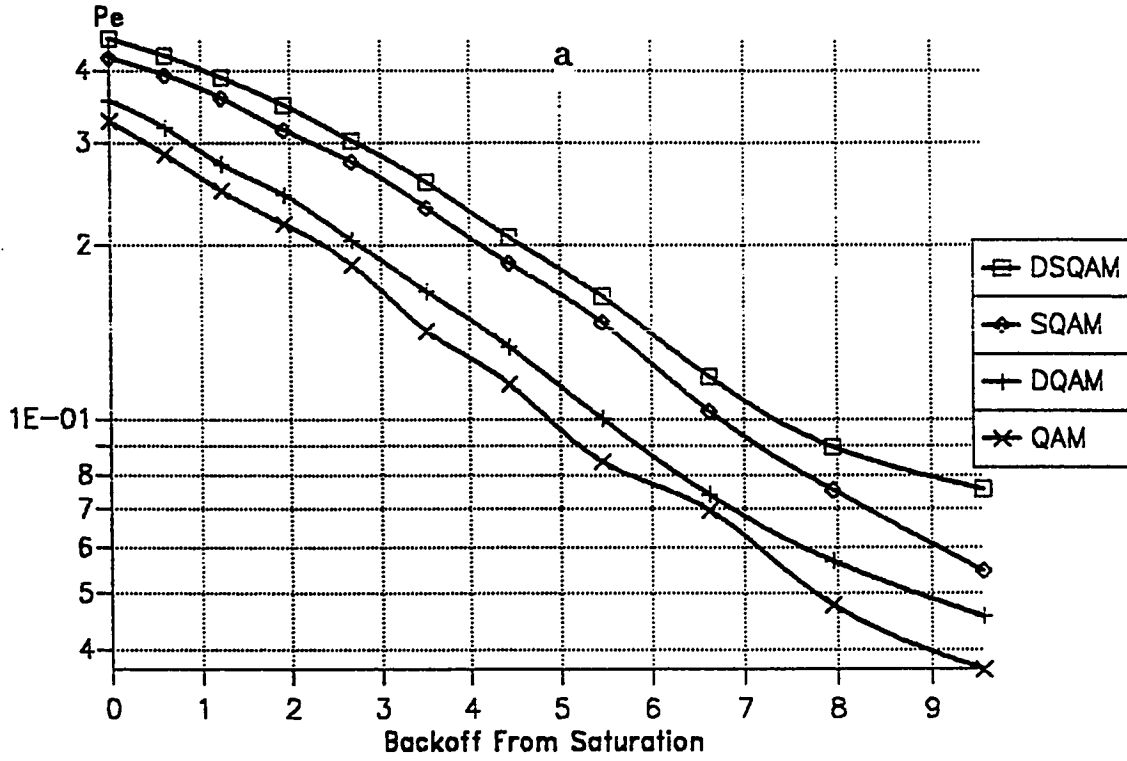


Fig 4.13 Non linearly amplified 16-QAM under AWGN
 a) SNR= 8 dB
 b) SNR= 10 dB

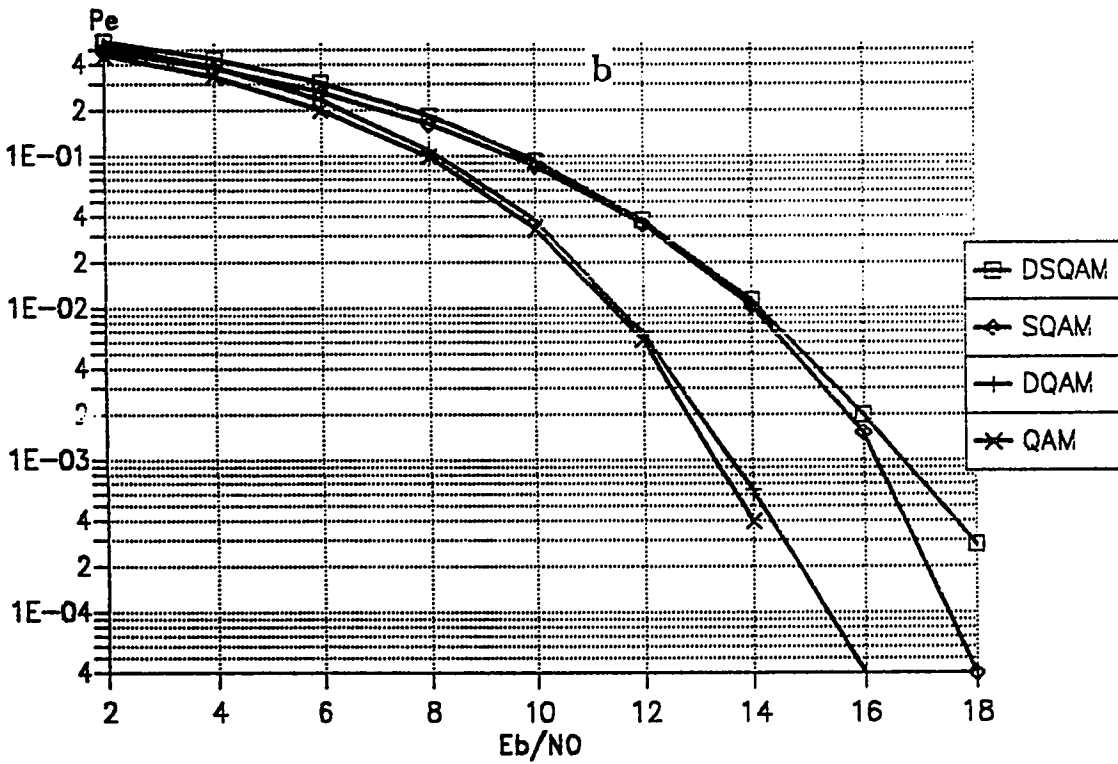
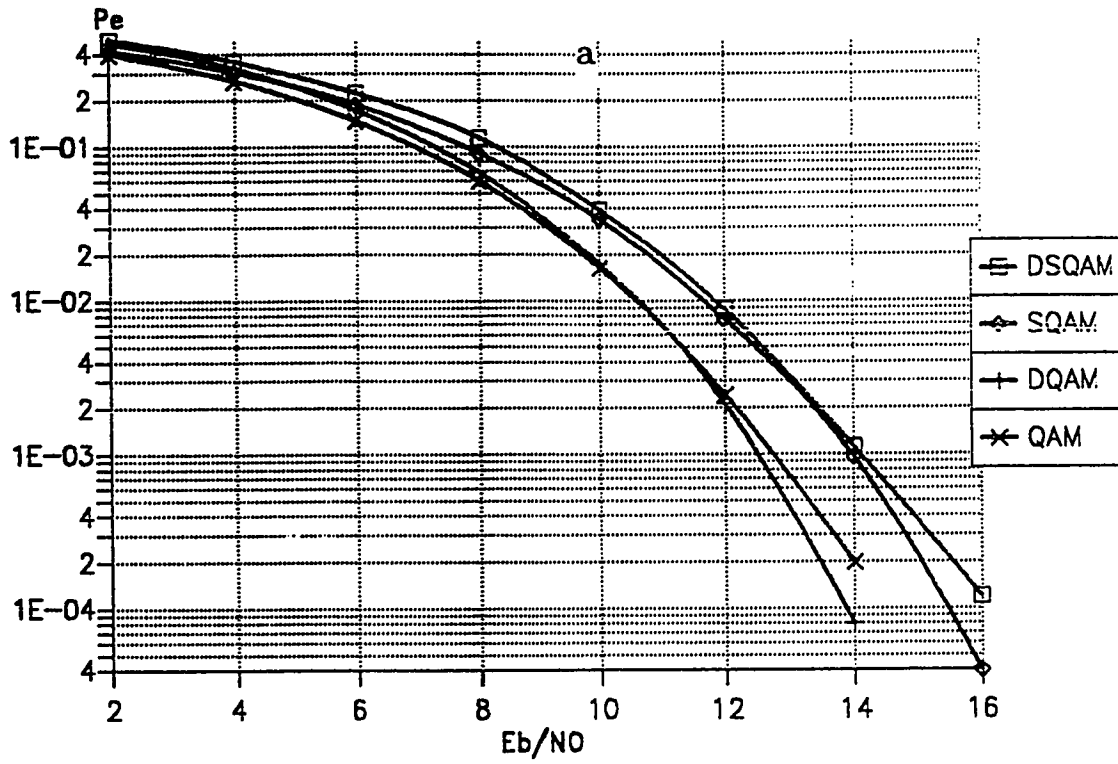


Fig 4.14 Non-linearly amplified 16-QAM under AWGN
 a) backoff=7 dB
 b) Backoff=5 dB

Saturation backoff	System				E_b/N_0
	QAM	DQAM	SQAM	DSQAM	
2	14.9	15.1	18.1	18.3	
5	13.3	13.5	16.2	16.75	
7	12.4	12.6	14.1	14.4	
9	11.6	11.7	13.3	13.5	

Table 4.1 Different E_b/N_0 values to achieve a BER of 10^{-3} for different saturation backoff values

With reference to Fig. 4.8, we can see that the required value of E_b/N_0 for GMSK system to achieve the 10^{-3} is about 8 dB. Note that what is required for different QAM systems with a variety of nonlinearities (as in Table 4.1) ranges from 11.6 dB (for QAM - Sat. Backoff = 9) to 18.3 dB (for DSQAM - Sat. Backoff = 2). In other words, as far as nonlinearities are concerned, GMSK is superior to QAM systems by 3.6 - 10.3 dB. Note that system nonlinearities are known to the system designer and therefore, a prediction of the performance can be obtained with a great deal of accuracy.

Optimum SQAM Ring Ratio with Nonlinearities

As mentioned earlier, the optimum value for the ratio between the outer ring and the inner ring in the case of SQAM is found to be consistent at 1.8. Fig. 4.15 shows the performance of the SQAM as a function of the ratio between the outer and the inner ring and with the backoff from saturation as a parameter. We notice

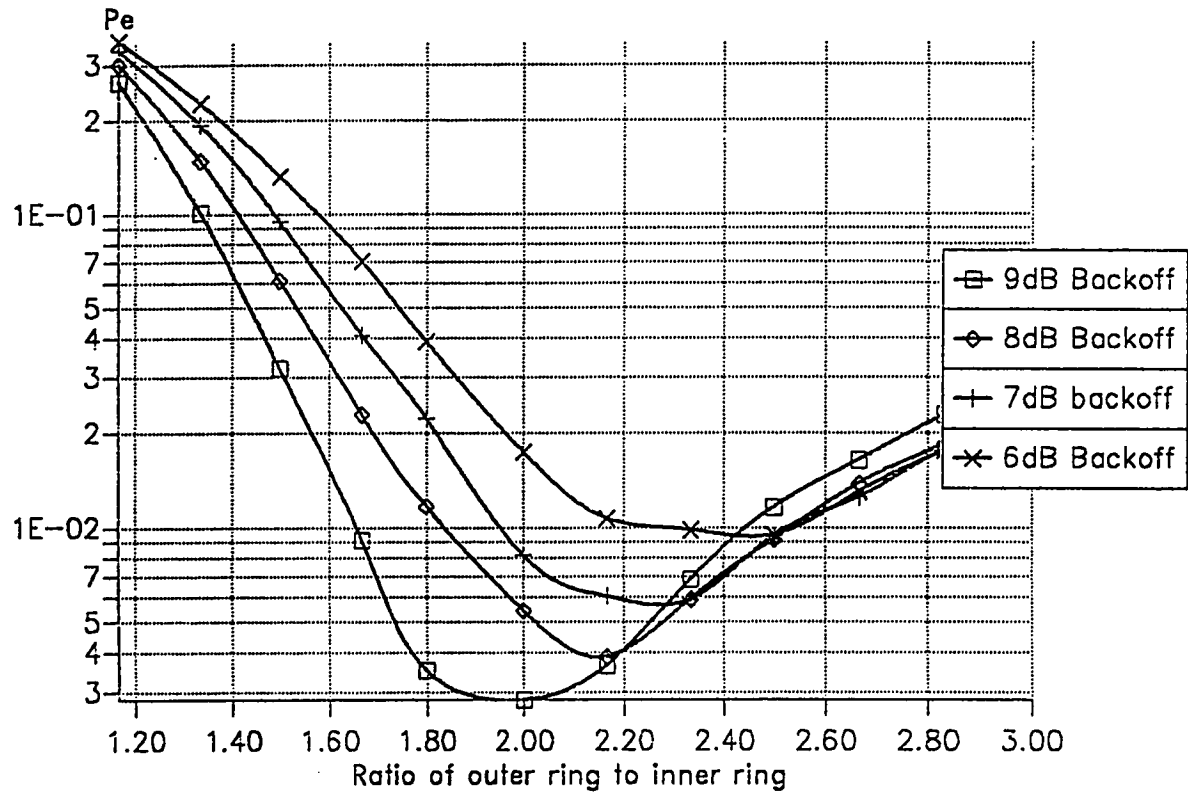


Fig 4.15 Non-linearly amplified Star 16-QAM at different backoffs

that as the backoff from saturation is decreased, the optimum ratio value increases. Fig. 4.16 shows the SQAM performance at a certain backoff for different E_b/N_0 values. We notice that there is a different optimum ratio at different backoff values. For example, when the backoff is 8 dB, the optimum ratio value is 2.1. Table 4.2 shows the optimum ratios for different saturation backoff values. Looking at such a table, the system designer can choose the optimum ratio when the backoff value is known.

Saturation backoff (dB)	Optimum ratio
4	2.61
5	2.47
6	2.35
7	2.25
8	2.13
9	2.00

Table 4.2 Optimum ratio for different saturation backoff values.

QAM under Rayleigh Fading

Also, the effect of non-linear amplification on the four aforementioned systems when the channel is assumed to be a Rayleigh fading channel is investigated. Figs. 4.17 and 4.18 show the performance as a function of E_b/N_0 for two different backoff values. We notice that the performance of the differential system is much more affected than conventional ones. This is expected since coherent demodulation was employed.

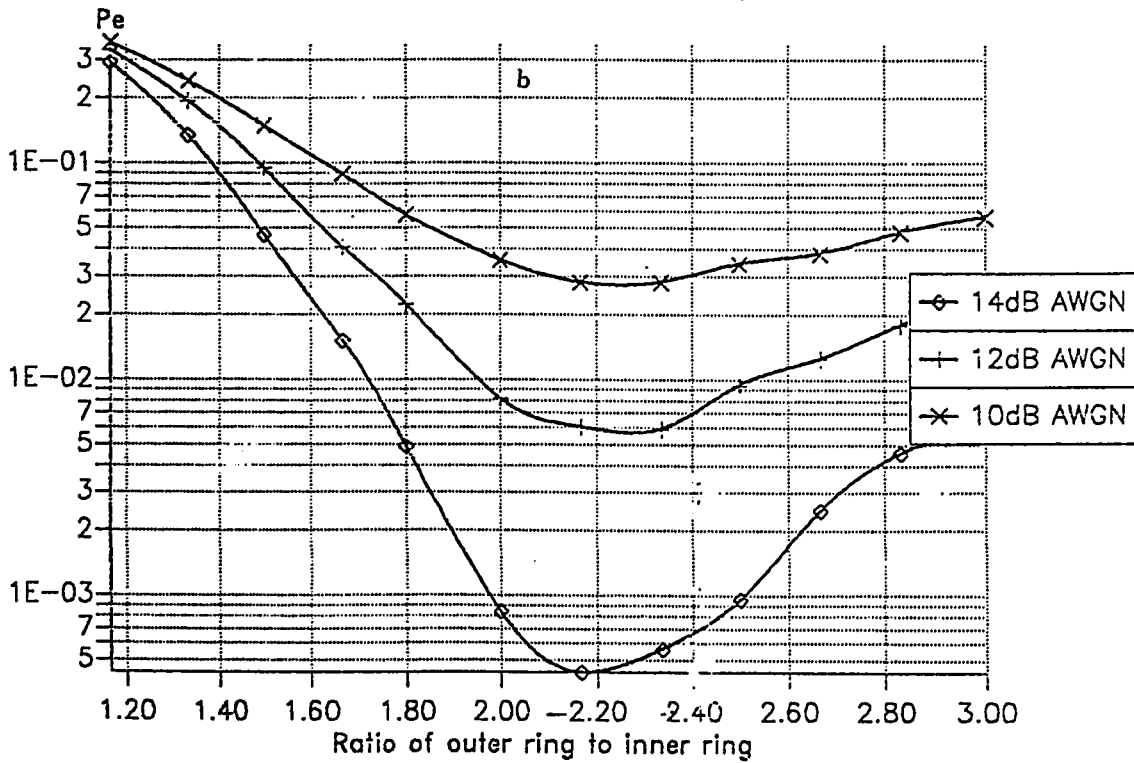
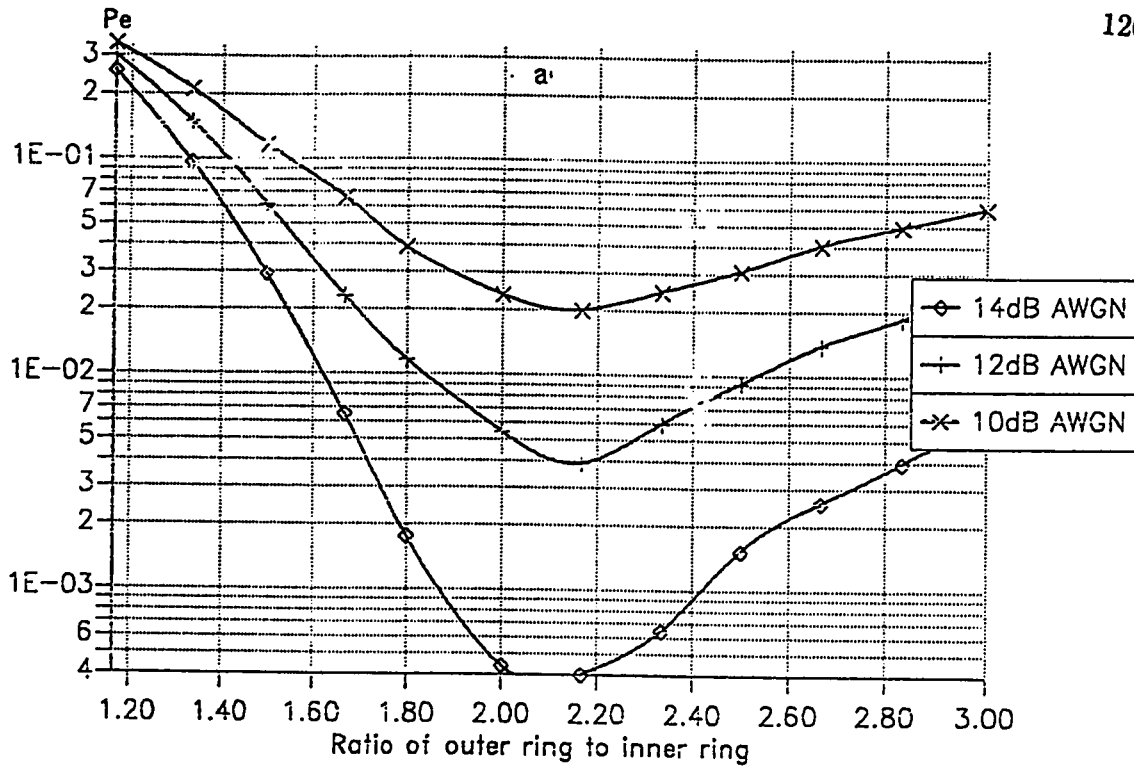


Fig 4.16 Non-linearly amplified Star 16-QAM at a fixed backoff
 a) backoff = 8 dB
 b) backoff = 7 dB

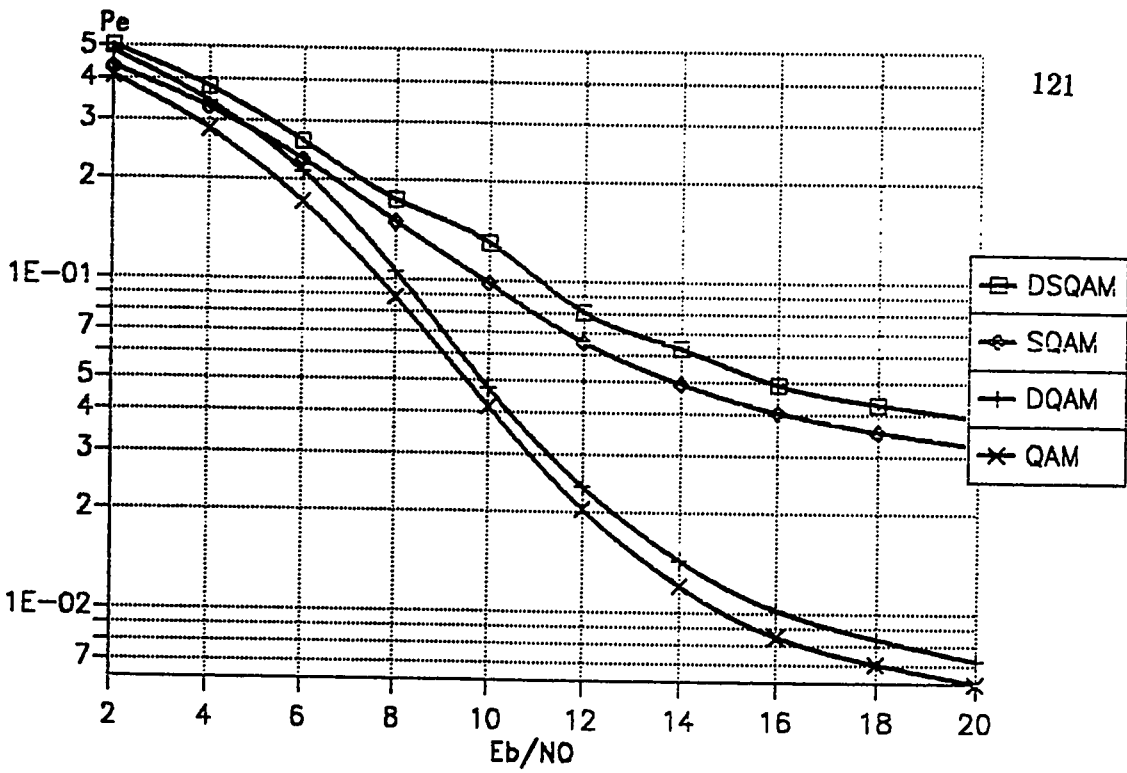


Fig 4.17 16-QAM under Rayleigh fading(backoff=7dB)

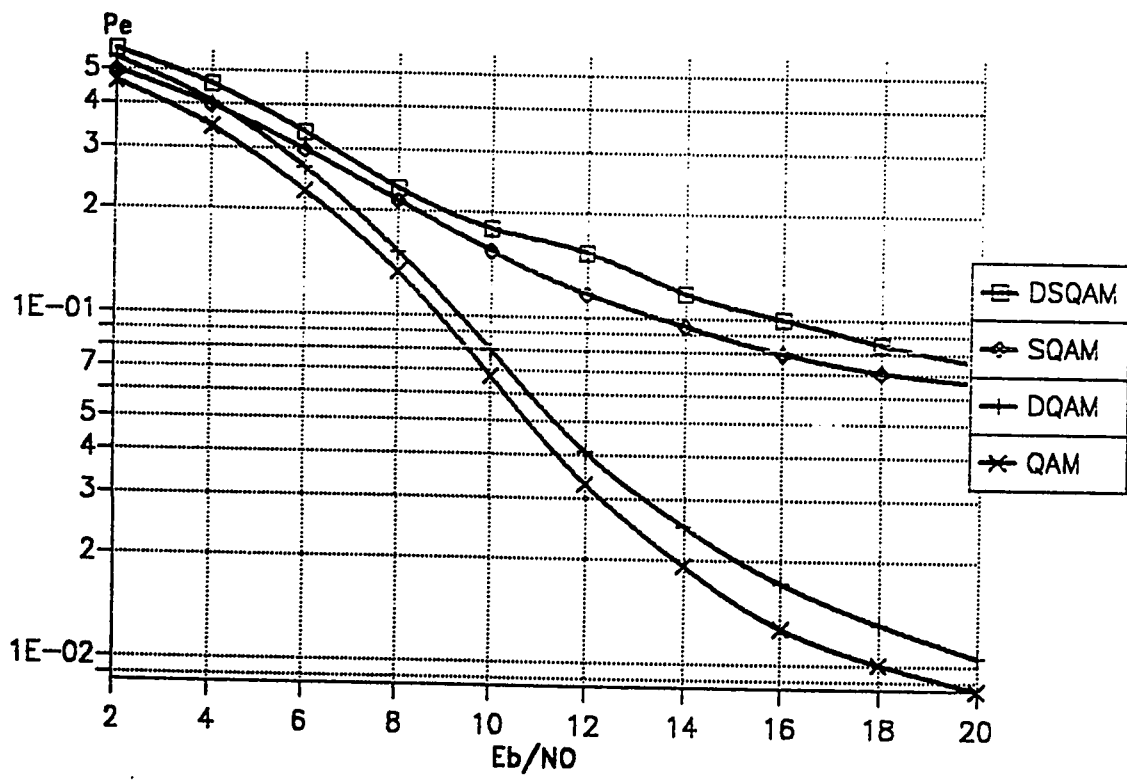


Fig 4.18 16-QAM under Rayleigh fading(backoff=5dB)

Let us take the case for which the backoff is 7 dB (Fig. 4.17). as an example. We see that there is a difference of about 2 dB between conventional and differential QAM at large E_b/N_0 values. We notice also that when $E_b/N_0 = 20$ dB, the BER for the SQAM system is 3×10^{-2} while it is 6×10^{-3} for the QAM system. This suggests using some performance enhancing techniques like equalization or diversity reception in order to achieve lower acceptable BER values.

QAM Under Frequency Selective Fading

What is left to be investigated is the performance of the QAM systems under frequency-selective fading. The normalized *rms* delay spread (u) is the dominant factor in determining the distortion level in a frequency-selective fading channel. Figs. 4.19 and 4.20 show the performance of the four QAM types (QAM, DQAM, SQAM, DSQAM) under a frequency-selective channel for two different values of the normalized *rms* delay spread (u) of 0.06 and 0.1, respectively. As noticed in the GMSK system, the bit error rate (BER) decreases linearly for small values of E_b/N_0 where the additive white Gaussian (AWGN) is the dominant distortion cause. However, for large E_b/N_0 values, the ISI caused by the channel is dominant and hence increasing E_b/N_0 will not reduce the error but the curve will reach to what is called the irreducible error rate. We notice also that when $u = 0.06$, which is a small value, the irreducible error rate is about 9×10^{-3} for the QAM which is

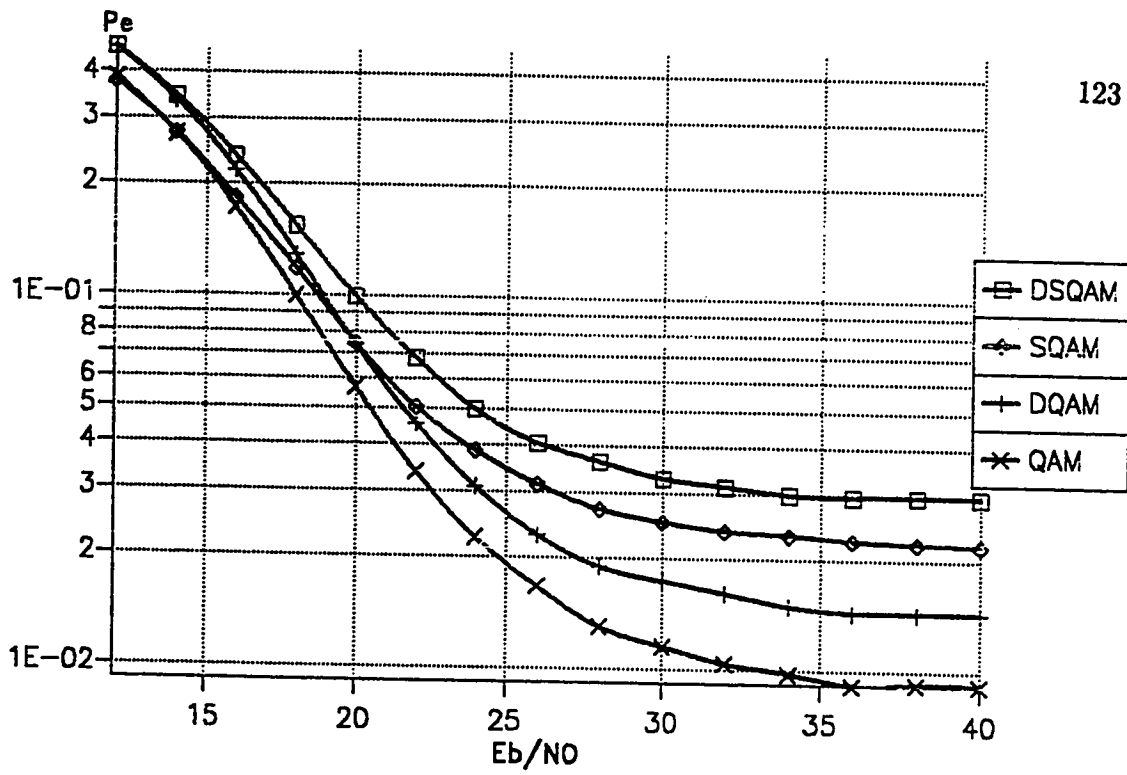


Fig 4.19 16-QAM under frequency selective fading ($u=0.06$)

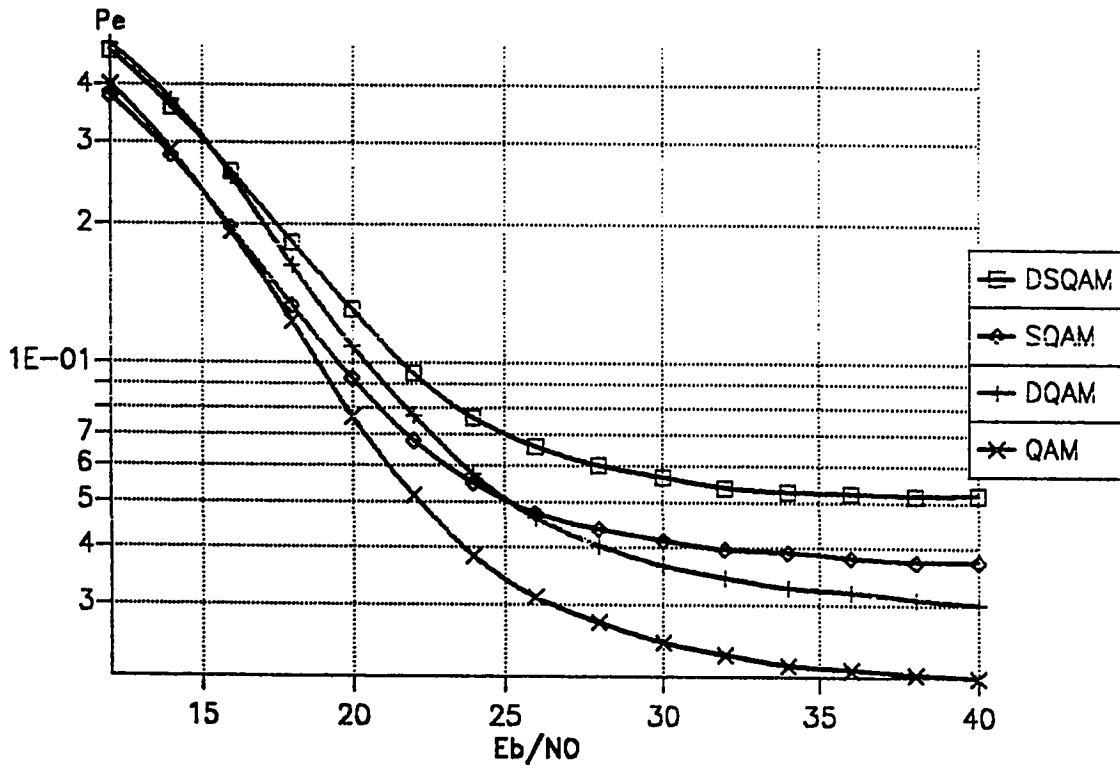


Fig 4.20 16-QAM under frequency selective fading ($u=1$)

a high value. When $u = 0.1$, the irreducible error rate reported in [Justin 1989] is 2×10^{-2} . The simulation result is so close to this figure. This mandates the need for a channel equalizer to reduce the effect of the ISI caused by the frequency-selective fading. We consider equalization later.

Fig. 4.21 shows the effect of non-linear amplification on the performance of the QAM system when operating under a frequency-selective fading channel. For the QAM with $u = 0.06$ we recall that the irreducible error rate was 9×10^{-3} . From Fig. 4.21 we see that this value becomes 10^{-2} for a 7 dB backoff and 2×10^{-2} for a 3 dB backoff. Figs. 4.22 and 4.23 show the performance of the DQAM and DSQAM, respectively operating under the same conditions. The irreducible error rate for the DSQAM is 3×10^{-2} while it is 4×10^{-2} when the signal is non-linearly amplified with a 5 dB backoff from saturation. Hence, we see that the ISI is still the dominant factor in determining the irreducible error rate.

To reduce the effect of the ISI, a linear 5-taps transversal equalizer is used for the four systems. The equalizer considered here is similar to the one described in the Section 4.3.

Figures 4.24, 4.25, 4.26 and 4.27 show the performance of the DAM, DQAM, SQAM and DSQAM, respectively, operating through a frequency-selective fading channel, amplified by a non-linear amplifier and with the aforementioned equalizer

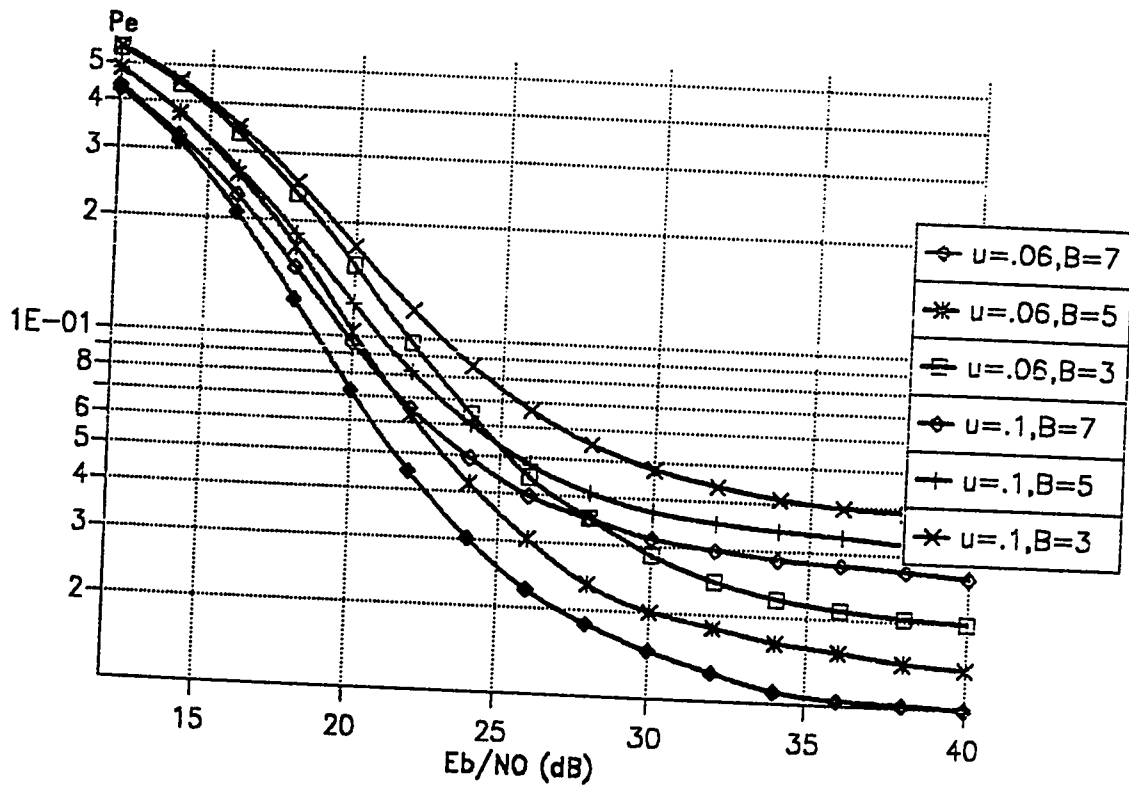


Fig 4.21 Nonlinearly amplified square 16-QAM
under frequency selective fading

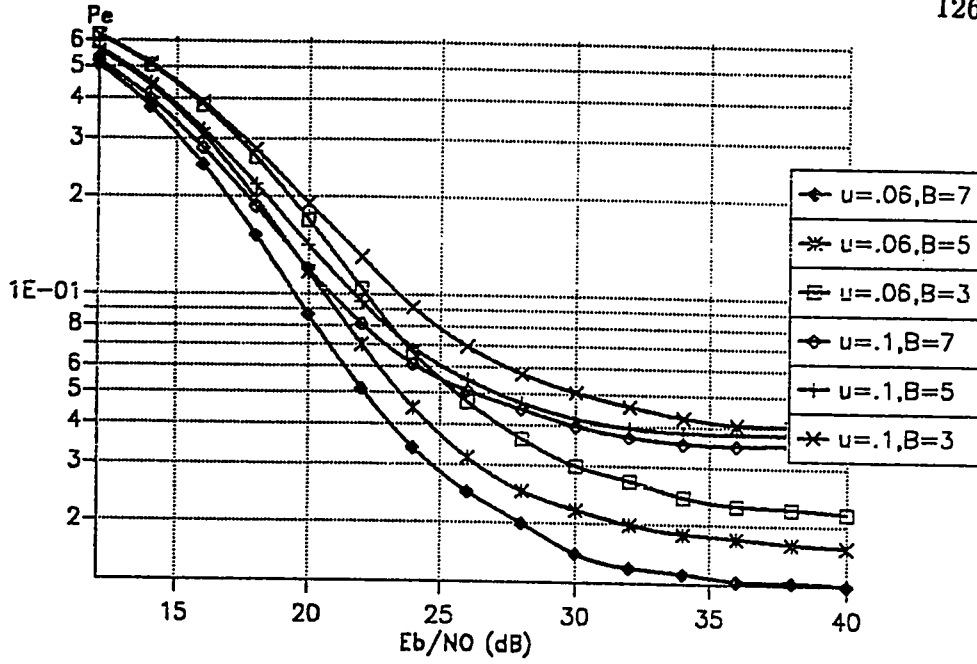


Fig 4.22 Nonlinearly amplified differential square 16-QAM under frequency selective fading

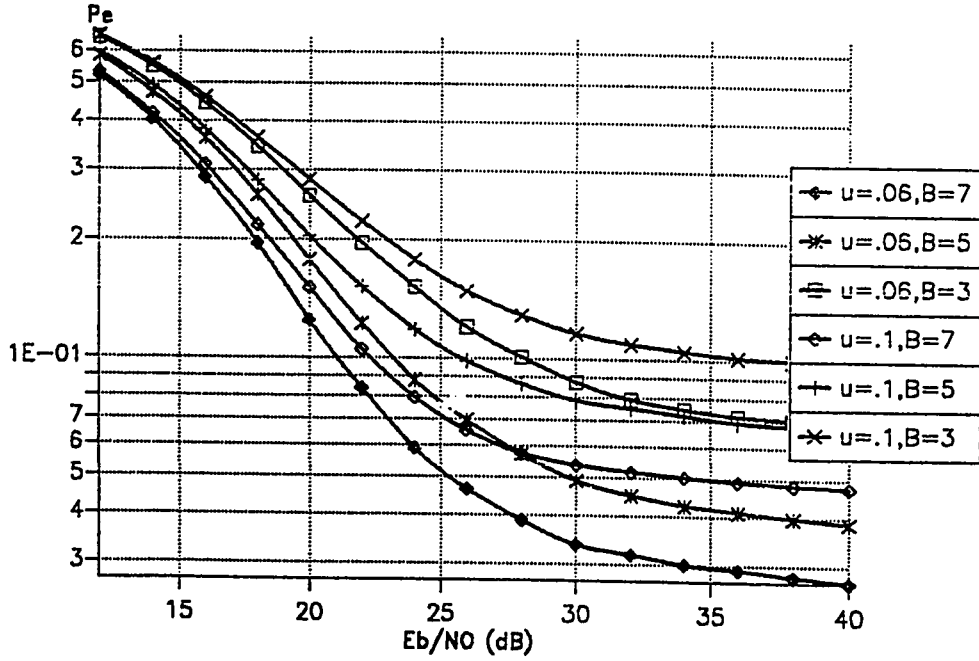


Fig 4.23 Nonlinearly amplified differential star 16-QAM under frequency selective fading

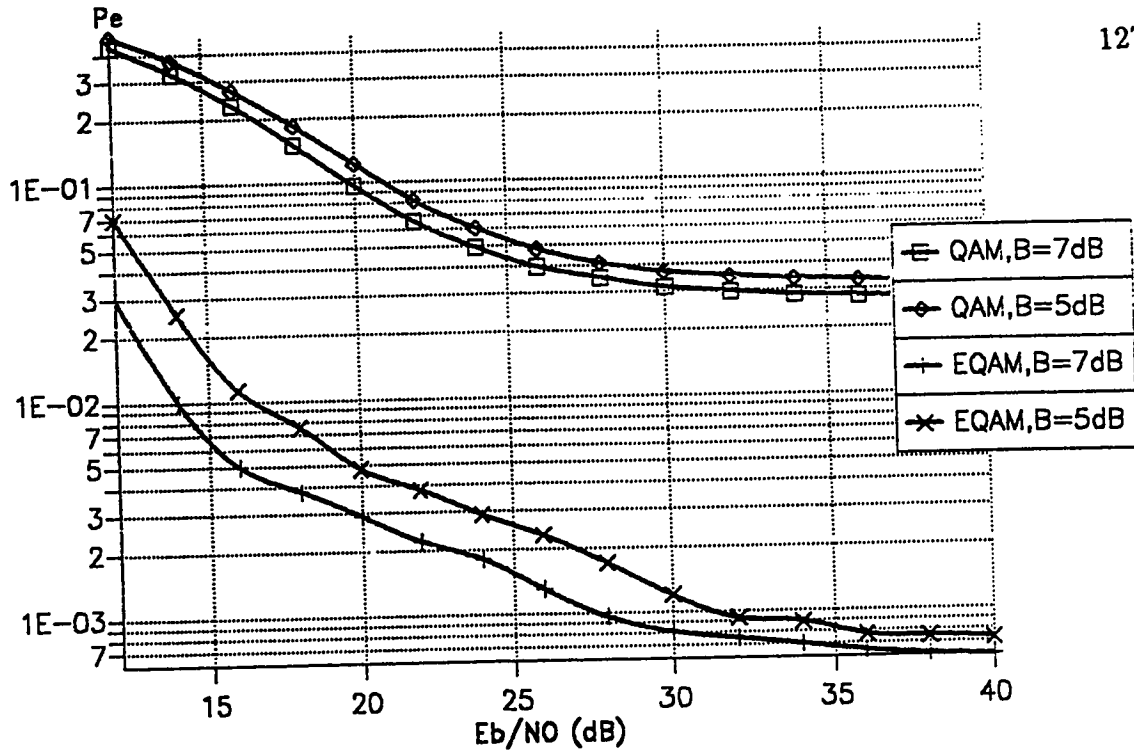


Fig 4.24 Equalized square 16-QAM (u=.1)

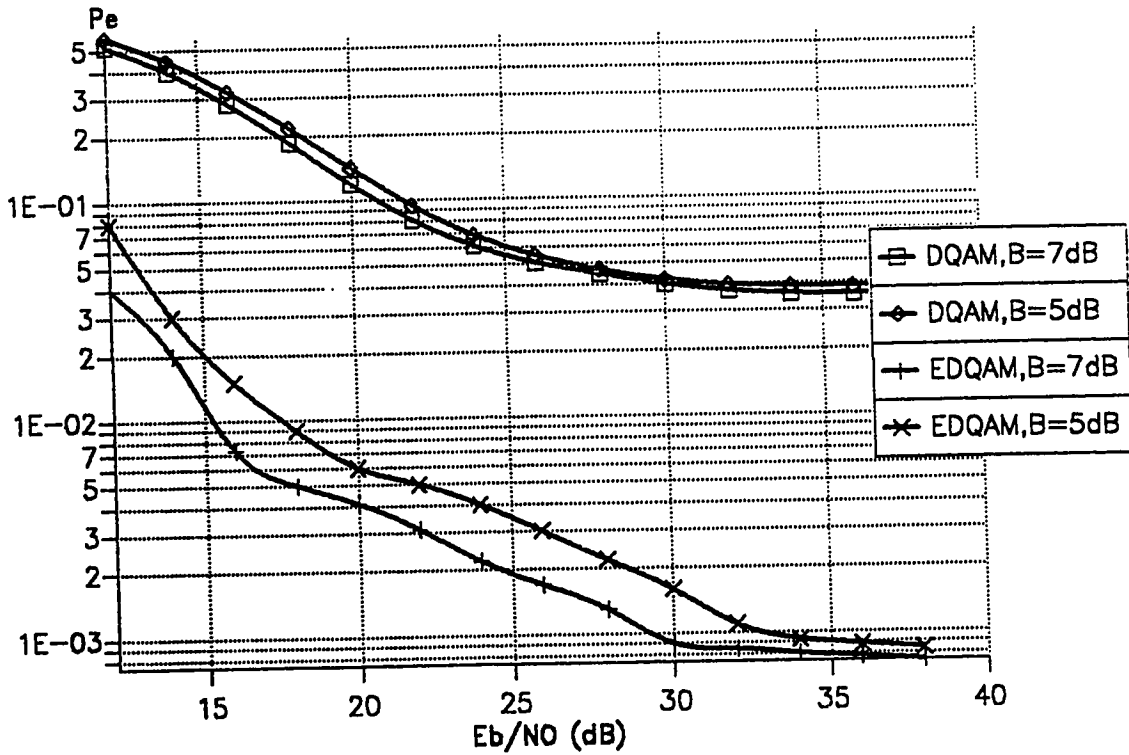


Fig 4.25 Equalized differential square 16-QAM (u=.1)

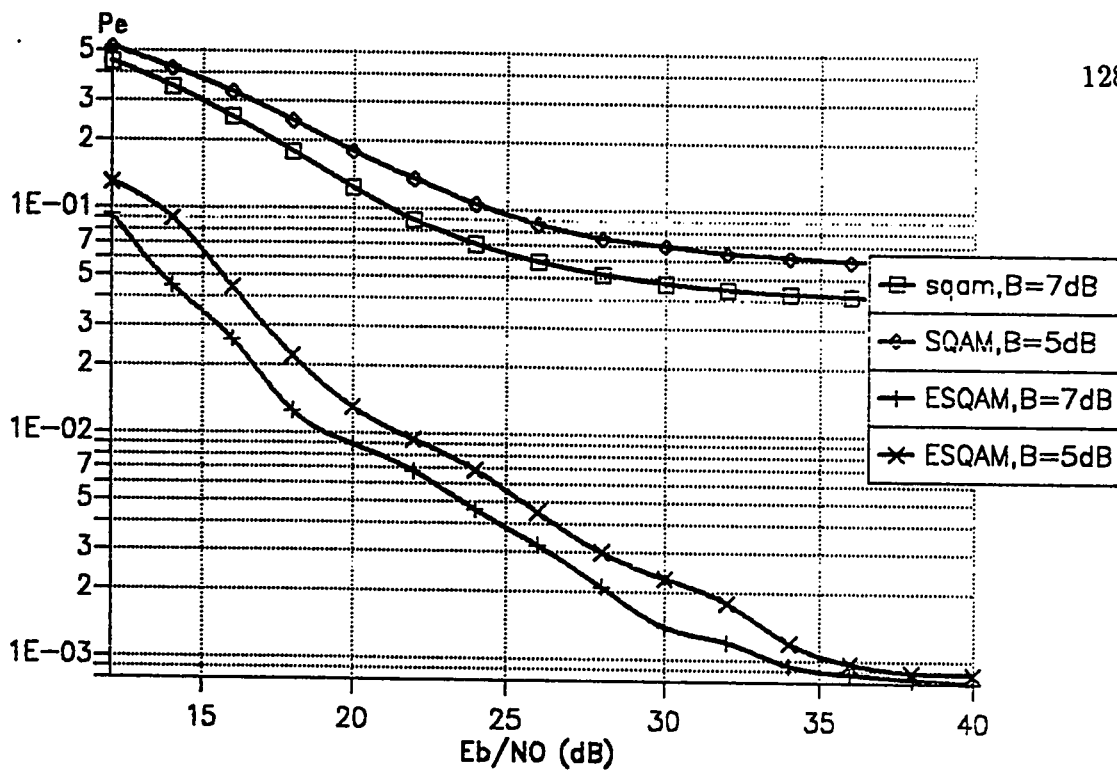


Fig 4.26 Equalized star 16-QAM (u=1)

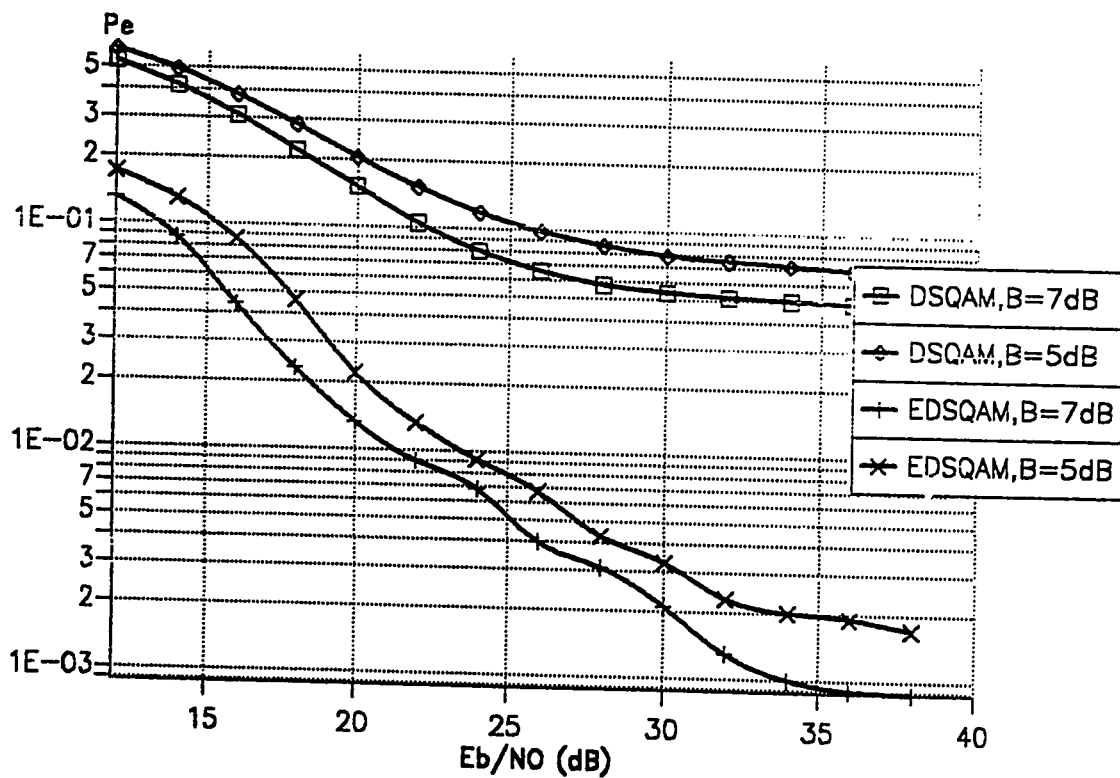


Fig 4.27 Equalized differentail star 16-QAM (u=1)

employed. The unequalized performance is also shown for comparison. Considering the QAM system, we see that at a backoff of 7 dB the irreducible error rate drops from 3×10^{-2} when no equalization is employed to 6×10^{-4} with equalization. Similarly, the figure drops considerably for the DQAM, SQAM and DSQAM systems. The performance might even be enhanced further by using more advanced equalization techniques like the decision feedback equalizer (DFE) or more accurate adaptive schemes [Haykin 1988, Proakis 1989]. Fractionally spaced equalizers adapting according to Kalman algorithm were reported to be efficient when the channel is modeled as a multipath channel but they are still limited by the fade rate. However, this will be at the expense of increasing the system complexity. We notice that there is still an irreducible error even with the equalization employed. This can be explained as follows. The channel is not deterministic but rather it is a time-varying channel and hence the ISI characteristic is not constant. When the channel is deterministic, the training sequence transmitted initially is enough to determine the induced ISI and hence can be eliminated completely. However, when the channel is random in nature, the equalization efficiency will depend on the speed of change of the channel.

4.6 Summary

The GMSK and the $\pi/4$ -shifted-DQPSK are currently used in mobile communication systems in both Europe and North America, respectively. The QAM system is being investigated because of its bandwidth efficiency for higher transmission rate. The performance of the GMSK, 16 QAM (square, star and differential) and $\pi/4$ -DQPSK systems are investigated under AWGN, Rayleigh fading and frequency-selective fading conditions. The GMSK performance under frequency-selective fading is investigated with the normalized *rms* delay spread as a parameter. We noticed that the GMSK outperforms the MSK system in terms of BER in a frequency-selective environment.

Four types of QAM are studied. These are the square QAM (QAM), differential square QAM(DQAM), star QAM(SQAM) and differential star QAM (DSQAM). The performance of these systems is investigated under the three aforementioned channels taking into consideration non-linear magnitude distortions (AM/AM) and non-linear phase shifts (AM/PM) caused by power amplifiers operating near the saturation region.

To alleviate the effect of the intersymbol interference (ISI) caused by the fre-

quency selective fading, channel equalization is employed for the three systems. The systems performance enhanced considerably but the channel effect could not be completely eliminated due to its random characteristic. The performance of the $\pi/4$ -shifted-DQPSK system is investigated under the same channels. To reduce the effect of ISI, channel equalization is employed for the three systems.

CHAPTER FIVE

CONCLUSIONS AND RECOMMENDATIONS FOR FUTURE WORK

5.1 Conclusions

The GMSK system is chosen as the modulation scheme for the GSM system installed in Europe while the $\pi/4$ -shifted-DQPSK is chosen for the North American system. Due to the need to transmit higher data rates in addition to voice, new modulation schemes with a more efficient bandwidth like the 16-QAM are being proposed. In this thesis, the performance of GMSK, $\pi/4$ -shifted-DQPSK and 16-QAM modulation schemes are investigated under AWGN, Rayleigh fading and frequency selective fading channels. Moreover, the effects of non-linearity on the QAM (non-constant envelope) systems are studied.

New implementation for the GMSK receiver structure is proposed where Gaussian filters are inserted in each branch of the parallel type modulator. The system performance is found to be comparable in terms of bit error rate (BER) with the system proposed by [Hirade 1981] in case of AWGN and Rayleigh fading channels. However, the new system is more spectrally efficient than Hirade's system. Out of band attenuation has an extra 15 dB.

Since QAM systems use signals with a non-constant envelope, their performance is known to degrade when non-linear power amplifiers are employed. It is clear from Fig. 4.24 that to reach a certain irreducible bit error rate (IBER), the power amplifier operating point has to be restricted to a certain value and only increasing the power will not result in a lower IBER. When the backoff is 7 dB, the IBER is 4×10^{-4} while it is 7×10^{-4} when the backoff is only 5 dB under frequency selective fading with equalization employed. The effect of the power amplifier's non-linearity on the optimum ring ratio in the star QAM case is investigated too. It is found that the optimum ratio is a function of the location of the operating point and there is a different optimum ratio at each operating point. Therefore, the ring ratio has to be chosen by the system designer according to the operating point. As expected, the performance of the Star QAM system is worse than conventional QAM system. However, its receiver structure is simpler.

The $\pi/4$ -shifted-DQPSK performance is investigated too. The differential encoding of data gives the receiver robustness against phase ambiguity but results in higher BER when coherent demodulation is used due to error propagation. The $\pi/4$ -shifted-DQPSK is found of a very close performance to that of the GMSK under the variety of channel impairments considered: AWGN, Rayleigh and frequency selective fading.

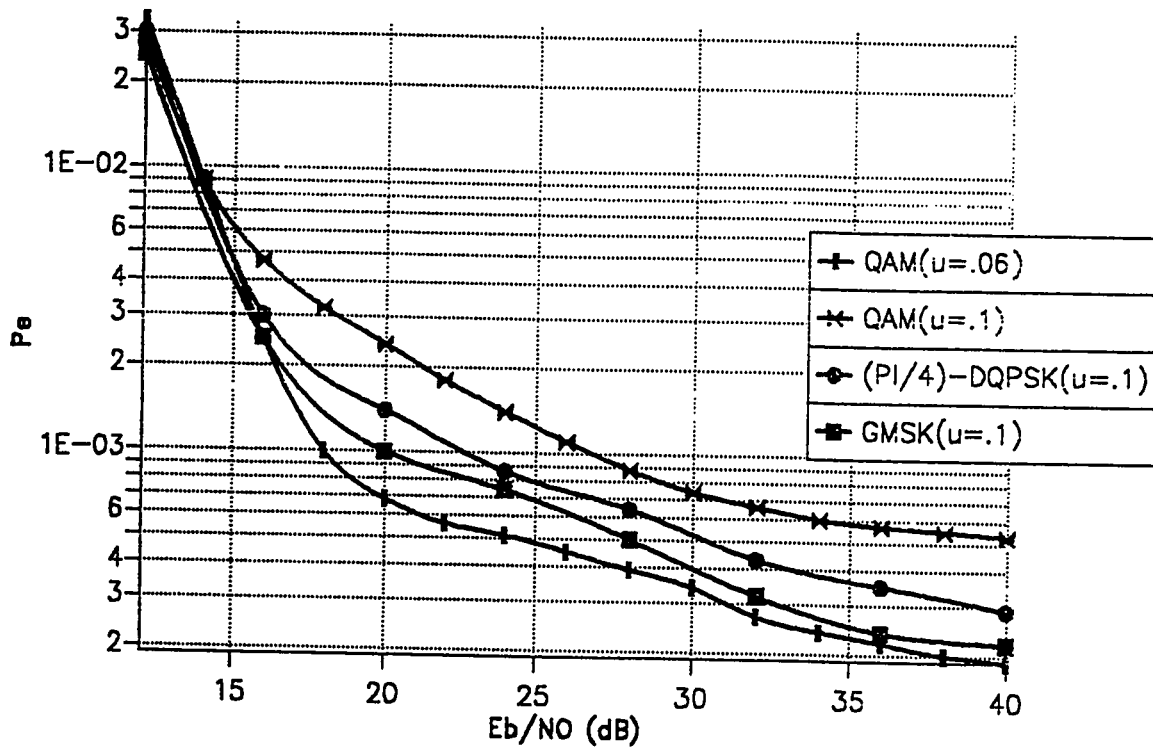


Fig 5.1 Equalized performance of the three systems

The performance of each of the three systems is investigated under frequency selective fading. It is found here that the use of equalization is inevitable if the mobile channel involves frequency selective fading for any of the systems considered. In this thesis, linear adaptive equalization is employed. Fig. 5.1 shows the performance of the three systems under a frequency selective fading channel when a 5-tap linear equalizer is used. Equalization enhances the performance from 8×10^{-3} to 2×10^{-4} in both the $\pi/4$ -shifted-DQPSK and the GMSK. We notice that the QAM system has the highest IBER (5×10^{-4}). One way to lower this IBER is to reduce the normalized *rms* delay spread by lowering the transmission rate. If we choose to keep the same rate, then an extra 3 dB should be paid to get to a BER of 10^{-3} compared to the $\pi/4$ -shifted-DQPSK system. Fig. 5.1 shows the performance of the 16-QAM system after decreasing the transmission rate ($u = .06$). We notice that IBER drops to about 2×10^{-4} . At this transmission rate, QAM performance is comparable with the other two systems but the system spectral efficiency is decreased. Lowering the *rms* delay spread from .1 to .06 means that only 20% spectral efficiency over QPSK systems is gained by introducing QAM modulation. We should not forget that the system is also vulnerable to non-linearity. In practical systems the power amplifier's operating point will be near saturation to get high power efficiency. This suggests that some linearization techniques should be employed to alleviate the effect of non-linearity.

5.2 Recommendations for Future Work

In this thesis computer simulation programs are used to evaluate the systems performance. Future work can include the following:

1. Other equalization techniques like the decision feedback equalizers and the fractionally spaced equalizers can be studied to enhance the performance further.
2. The effect of other performance enhancing techniques like diversity reception and coding can be studied.
3. New simple and efficient linearization techniques of power amplifiers can be proposed.
4. Other fading channel types like the non-Gaussian channel for the Rician fading channel effect on the systems can be studied.
5. The systems can be implemented experimentally and tested at different transmission rates.

APPENDIX A

SAMPLE PROGRAM
DIFFERENTIAL 16-QAM

```

*****
*** B ( ) :GENERATED BITS ,BB ( ) ENCODED BITS
*** Q ( ) :RCIEVED BITS ,RBB ( ) DECODED BITS
*** U ( ) : DECISION VARIABLE
*** S ( ) : SENT DATA VECTOR
*** NR : # SENT BITS
*** JV : # TAPS IN THE EQUALISER
*** MS : # POINTS BETWEEN THE ORIGION & THE SATURATION POIN
*** C1 ( ) ,C2 ( ) : TAP GAINS USED TO REPRESENT THE FREQUENCY
SELECTIVE CHANNEL
*****
PARAMETER(NN = 40,MM = 25000,JV = 5)
REAL MAG(MM),PHASE(MM).PI
INTEGER NR,B(100000),Q(100000),L(25010),BB(100000),RBB(100000

REAL R(100000),GAUS1(25000),GAUS2(25000),PB(500),N0,GGAUS1
+ (25000),GGAUS2(25000),NN0,COUNT(500),ES,ES2,MIN,XX2(20)
+ ,RALY1(25100),RALY2(25100),ALPHA(25000),RALY3(25100)
COMPLEX X(20),RR(25000),U(20),S(25010) .XX(20).CC(JV)
+ ,V(9),VC(9),ER,R1(25000),QX1
EXTERNAL FF,PSI

***DELTA IS USED IN THE EQUALISER
*****
PI=4.*ATAN(1.)
DELTA=.01
ZERO=0
NNR=NR/4
MS=30
*****

DO 238 KY= 10,12,2

***INITIALISE THE EQUALISER TAPS
*****
DO 113 KC= 1,JV
V(KC)=CMLX(ZERO,ZERO)

```



```

113 CC(KC)=CMPLX(ZERO,ZERO)
*****
C=(REAL(KY)/REAL(MS)*(.5**.5))/3.
*****
***TO GET 3,5,7 OFFSET D.B
C=.1668644216
C=.1325451
C=.1052843
*****
***16QAM SIGNAL COSTELLATION

X(11)=CMPLX(-3*C,+3*C)
X(10)=CMPLX(-3*C,+1*C)
X(9)=CMPLX(-C,+3*C)
X(8)=CMPLX(-C,C)
X(15)=CMPLX(3*C,3*C)
X(13)=CMPLX(3*C,C)
X(14)=CMPLX(C,+3*C)
X(12)=CMPLX(C,C)
X(3)=CMPLX(-3*C,-3*C)
X(1)=CMPLX(-3*C,-1*C)
X(2)=CMPLX(-C,-3*C)
X(16)=CMPLX(-C,-C)
X(7)=CMPLX(3*C,-3*C)
X(6)=CMPLX(3*C,-C)
X(5)=CMPLX(C,-3*C)
X(4)=CMPLX(C,-C)
ES1=((2**.5*C)**2.
ES2=(18**.5*C)**2.
ES3=((10**.5*C)**2.
ES=(ES1+ES2+2.*ES3)/4.
*****
***INCLUDE THE EFFECT OF THE POWER AMPLIFIER
***FF( ) IS THE MAGNITUDE NON-LINEARITY
***PSI( ) IS THE PHASE NON-LINEARITY

DO 887 KV=1,16
AMPL=CABS( X(KV))
AMPL= FF(AMPL)
PHS=ANGL( REAL( X(KV) ) , AIMAG( X(KV) ) )
PHS=PHS + PSI(AMPL)
RL=AMPL*COS(PHS)
XM=AMPL*SIN(PHS)

```

```
XX(KV)=CMPLX(RL,XIM)
887 CONTINUE
```

```
*****GENERATE A RANDOM VARIABLE BETWEEN 0 AND 1
*****CONVERT IT TO BIT
```

```
CALL RNUN(NR,R)
DO 100 I=1,NR
IF (R(I).GT.0.5)THEN
B(I)=1
ELSE
B(I)=0
ENDIF
100 CONTINUE
BB(1)=B(1)
BB(2)=B(2)
BB(3)=B(3)
BB(4)=B(4)
```

```
***** ENCOD THE DATA
DO 51 I=1,NR,4
IF(I.EQ.1 ) GOTO 51
BB(I+2)=B(I+2)
BB(I+3)=B(I+3)
```

```
*****
IF(B(I).EQ.0.AND.B(I+1).EQ.0.AND.BB(I-4).EQ.0.AND.
+ BB(I-3).EQ.0) THEN
BB(I)=0
BB(I+1)=1
ENDIF
```

```
IF(B(I).EQ.0.AND.B(I+1).EQ.0.AND.BB(I-4).EQ.0.AND.
+ BB(I-3).EQ.1) THEN
BB(I)=1
BB(I+1)=1
ENDIF
```

```
IF(B(I).EQ.0.AND.B(I+1).EQ.0.AND.BB(I-4).EQ.1.AND.
+ BB(I-3).EQ.0) THEN
BB(I)=0
BB(I+1)=0
ENDIF
```

```
IF(B(I).EQ.0.AND.B(I + 1).EQ.0.AND.BB(I-4).EQ.1.AND.  
+ BB(I-3).EQ.1) THEN  
BB(I) = 1  
BB(I + 1) = 0  
ENDIF
```

```
IF(B(I).EQ.0.AND.B(I + 1).EQ.1.AND.BB(I-4).EQ.0.AND.  
+ BB(I-3).EQ.1) THEN  
BB(I) = 0  
BB(I + 1) = 0  
ENDIF
```

```
IF(B(I).EQ.0.AND.B(I + 1).EQ.1.AND.BB(I-4).EQ.0.AND.  
+ BB(I-3).EQ.1) THEN  
BB(I) = 0  
BB(I + 1) = 1  
ENDIF
```

```
IF(B(I).EQ.0.AND.B(I + 1).EQ.1.AND.BB(I-4).EQ.1.AND.  
+ BB(I-3).EQ.0) THEN  
BB(I) = 1  
BB(I + 1) = 0  
ENDIF
```

```
IF(B(I).EQ.0.AND.B(I + 1).EQ.1.AND.BB(I-4).EQ.1.AND.  
+ BB(I-3).EQ.1) THEN  
BB(I) = 1  
BB(I + 1) = 1  
ENDIF
```

```
IF(B(I).EQ.1.AND.B(I + 1).EQ.0.AND.BB(I-4).EQ.0.AND.  
+ BB(I-3).EQ.0) THEN  
BB(I) = 1  
BB(I + 1) = 1  
ENDIF
```

```
IF(B(I).EQ.1.AND.B(I + 1).EQ.0.AND.BB(I-4).EQ.0.AND.  
+ BB(I-3).EQ.1) THEN  
BB(I) = 1  
BB(I + 1) = 0  
ENDIF
```

```
IF(B(I).EQ.1.AND.B(I + 1).EQ.0.AND.BB(I-4).EQ.1.AND.
```

```

+ BB(I-3).EQ.0) THEN
BB(I)=0
BB(I+1)=1
ENDIF

```

```

IF(B(I).EQ.1.AND.B(I+1).EQ.0.AND.BB(I-4).EQ.1.AND.
+ BB(I-3).EQ.1) THEN
BB(I)=0
BB(I+1)=0
ENDIF

```

```

IF(B(I).EQ.1.AND.B(I+1).EQ.1.AND.BB(I-4).EQ.0.AND.
+ BB(I-3).EQ.0) THEN
BB(I)=1
BB(I+1)=0
ENDIF

```

```

IF(B(I).EQ.1.AND.B(I+1).EQ.1.AND.BB(I-4).EQ.0.AND.
+ BB(I-3).EQ.1) THEN
BB(I)=0
BB(I+1)=0
ENDIF

```

```

IF(B(I).EQ.1.AND.B(I+1).EQ.1.AND.BB(I-4).EQ.1.AND.
+ BB(I-3).EQ.0) THEN
BB(I)=1
BB(I+1)=1
ENDIF

```

```

IF(B(I).EQ.1.AND.B(I+1).EQ.1.AND.BB(I-4).EQ.1.AND.
+ BB(I-3).EQ.1) THEN
BB(I)=0
BB(I+1)=1
ENDIF

```

```

51 CONTINUE

```

```

.....

```

```

*** INITIALISE THE VECTORS BY CONVERTING THEIR BINARY BIT
*** 16 REPRESENTS 0000
*** CONVERT EVERY 4 BITS TO VECTOR

```

```

K=0

```

```

DO 200 I=1, NR, 4
K=K+1
J=BB(I+3)+BB(I+2)*2+BB(I+1)*4+BB(I)*8
IF(J.EQ.0) THEN
S(K)=XX(16)
ELSE
S(K)=XX(J)
ENDIF

```

```

200 CONTINUE
*****

```

```

**NOW S(K) REPRESENTS A COMPLEX VECTOR ACCORDING TO THE DATA
**WITH NEW AMPL. AND PHASE ACCORDING TO POWER AMPL

```

```

**GENERATE GAUSSIAN RANDOM VARIABLES TO BE USED IN THE CHANNE
ISEED=25678
CALL RNNOA(NNR, RALY3)
ISEED=8743
CALL RNNOA(NNR, RALY1)
ISEED=9867
CALL RNNOA(NNR, RALY2)
DO 534 KJI=1, NNR

```

```

534 ALPHA(KJI) = ( ABS( RALY1(KJI) )**2. + ABS(RALY2(KJI) )**2. ) **.5

```

```

*GENERATE 2 INDEPENDENT GAUSS RANDOM VAR : GAUS1 AND GAUS2
ISEED=123456
NNR=NR/4
CALL RNNOA(NNR, GAUS1)
ISEED=45876
CALL RNNOA(NNR, GAUS2)

```

```

*** CALCULATE THE ENERGY/BIT
EB=ES/4.
DO 511 IZ=1, 11
N0=(ES)/(10.** (REAL(IZ)/10.))

```

```

** ADJUST THE VARIANCE OF THE NOISE
DO 19 I=1, NR/4
GGAUS1(I) = (N0/2.0) **.50 * GAUS1(I)
GGAUS2(I) = (N0/2.0) **.50 * GAUS2(I)
19 CONTINUE

```

** RR IS A COMPLEX VECTOR REPRESENTING THE RECEIVED SIGNAL

```
DO 400 I=1,NR/4
RR(I)=ALPHA(I)*S(I) + CMPLX(GGAUS1(I),GGAUS2(I))
```

```
IF( MOD(MH,300).NE.0) THEN
READ(5,12) C1(I),C2(I)
ELSE
C1(I)=C1(I-1)
C2(I)=C2(I-1)
ENDIF
```

```
IF( I.GT.3) THEN
RR(I)=RR(I) + ( C1(I)*S(I-1) + C2(I)*S(I-2) )
ELSE
RR(I)=S(I)
ENDIF
```

```
400 CONTINUE
SUM=0
DO 404 I=3,NR/4
*****EQUALIZWER
```

```
V(1)=RR(I-2)
V(2)=RR(I-1)
V(3)=RR(I)
V(4)=RR(I + 1)
V(5)=RR(I + 2)
QX1=0
DO 978 KA = 1,JV
978 QX1=QX1 + CC(KA)*V(KA)
```

** NOW WE FIND RR IS CLOSEST TO WHICH X
** L WILL REPRESENT THE CLOSEST VECTOR #

```
MIN=1E6
DO 500 KJ=1,16
U(KJ)=QX1-XX(KJ)
ZX=CABS(U(KJ))
IF(ZX.LT.MIN)THEN
```

```

MIN=ZX
L(I)=KJ
ENDIF
500 CONTINUE
*****
** CALCULAT THE ERR
IF(I.LT.10000) THEN
ER=S(I)- QX1
ELSE
ER=XX( L(I) ) - QX1
ENDIF
** UPDATE THE COFF
DO 979 KA=1,JV
REV=REAL( V(KA))
AMV=AIMAG( V(KA))*(-1)
VC(KA)=CMPLX(REV,AMV)

979 CC(KA)=CC(KA) + DELTA*ER*VC(KA)
SUM=SUM + CABS(ER)
SUM2=SUM/REAL(I)
*****

404 CONTINUE

*** NOW WE CONVERT THE VECTORS TO BITS AND STORE IT IN Q( )
K=0
DO 600 I= 1,NR,4
K=K+1
IF (L(K).EQ.16)THEN
Q(I)=0
Q(I+1)=0
Q(I+2)=0
Q(I+3)=0
ELSE

*THE VECTOR#L() REPRESENTS THE BITS SO WE CONVERT FROM DECIMA
*** TO BINARY

Q(I+3)=MOD(L(K),2)
K1=L(K)/2
Q(I+2)=MOD(K1,2)
K2=K1/2
Q(I+1)=MOD(K2,2)

```

```

K3 = K2/2
Q(I) = MOD(K3,2)
ENDIF
600 CONTINUE

```

```

*** DECODE THE RECEIVED BITS

```

```

RBB(1) = B(1)
RBB(2) = B(2)
RBB(3) = B(3)
RBB(4) = B(4)
DO 52 I = 1, NR, 4
RBB(I+2) = Q(I+2)
RBB(I+3) = Q(I+3)
IF (I.EQ.1) GOTO 52

```

```

IF(Q(I).EQ.0.AND.Q(I+1).EQ.1.AND.Q(I-4).EQ.0.AND.
+Q(I-3).EQ.0)THEN
RBB(I) = 0
RBB(I+1) = 0
ENDIF

```

```

IF(Q(I).EQ.1.AND.Q(I+1).EQ.1.AND.Q(I-4).EQ.0.AND.
+Q(I-3).EQ.1)THEN
RBB(I) = 0
RBB(I+1) = 0
ENDIF

```

```

IF(Q(I).EQ.0.AND.Q(I+1).EQ.0.AND.Q(I-4).EQ.1.AND.
+Q(I-3).EQ.0)THEN
RBB(I) = 0
RBB(I+1) = 0
ENDIF

```

```

IF(Q(I).EQ.1.AND.Q(I+1).EQ.0.AND.Q(I-4).EQ.1.AND.
+Q(I-3).EQ.1)THEN
RBB(I) = 0
RBB(I+1) = 0
ENDIF

```

```

IF(Q(I).EQ.0.AND.Q(I+1).EQ.0.AND.Q(I-4).EQ.0.AND.
+Q(I-3).EQ.0)THEN
RBB(I) = 0
RBB(I+1) = 1

```


ENDIF

```

IF(Q(I).EQ.0.AND.Q(I+1).EQ.1.AND.Q(I-4).EQ.0.AND.
+Q(I-3).EQ.1)THEN
RBB(I)=0
RBB(I+1)=1
ENDIF

```

```

IF(Q(I).EQ.1.AND.Q(I+1).EQ.0.AND.Q(I-4).EQ.1.AND.
+Q(I-3).EQ.0)THEN
RBB(I)=0
RBB(I+1)=1
ENDIF

```

```

IF(Q(I).EQ.1.AND.Q(I+1).EQ.1.AND.Q(I-4).EQ.1.AND.
+Q(I-3).EQ.1)THEN
RBB(I)=0
RBB(I+1)=1
ENDIF

```

```

IF(Q(I).EQ.1.AND.Q(I+1).EQ.1.AND.Q(I-4).EQ.0.AND.
+Q(I-3).EQ.0)THEN
RBB(I)=1
RBB(I+1)=0
ENDIF

```

```

IF(Q(I).EQ.1.AND.Q(I+1).EQ.0.AND.Q(I-4).EQ.0.AND.
+Q(I-3).EQ.1)THEN
RBB(I)=1
RBB(I+1)=0
ENDIF

```

```

IF(Q(I).EQ.0.AND.Q(I+1).EQ.1.AND.Q(I-4).EQ.1.AND.
+Q(I-3).EQ.0)THEN
RBB(I)=1
RBB(I+1)=0
ENDIF

```

```

IF(Q(I).EQ.0.AND.Q(I+1).EQ.0.AND.Q(I-4).EQ.1.AND.
+Q(I-3).EQ.1)THEN
RBB(I)=1
RBB(I+1)=0
ENDIF

```

```

IF(Q(I).EQ.1.AND.Q(I + 1).EQ.0.AND.Q(I-4).EQ.0.AND.
+Q(I-3).EQ.0)THEN
RBB(I) = 1
RBB(I + 1) = 1
ENDIF

```

```

IF(Q(I).EQ.0.AND.Q(I + 1).EQ.0.AND.Q(I-4).EQ.0.AND.
+Q(I-3).EQ.1)THEN
RBB(I) = 1
RBB(I + 1) = 1
ENDIF

```

```

IF(Q(I).EQ.1.AND.Q(I + 1).EQ.1.AND.Q(I-4).EQ.1.AND.
+Q(I-3).EQ.0)THEN
RBB(I) = 1
RBB(I + 1) = 1
ENDIF

```

```

IF(Q(I).EQ.0.AND.Q(I + 1).EQ.1.AND.Q(I-4).EQ.1.AND.
+Q(I-3).EQ.1)THEN
RBB(I) = 1
RBB(I + 1) = 1
ENDIF

```

52 CONTINUE

```

**NOW WE COMPARE THE SENT BITS B() WITH RECIVED ONES RBB()
KKK = 0
COUNT(II) = 0
CCC = 0

```

```

** COUNT() IS THE TOTAL ERROR RATE
** CCC IS THE ERROR RATE AFTER EQUALISER TRAINING FINISH

```

```

DO 700 I = 1, NR, 4
KKK = KKK + 1
IF(B(I).NE.RBB(I).OR. B(I + 1).NE.RBB(I + 1).OR.B(I + 3).NE.
+ RBB(I + 3).OR.B(I + 2).NE.RBB(I + 2) ) THEN
COUNT(II) = COUNT(II) + 1.
IF(I.LT.4000) GOTO 700
CCC = CCC + 1.
ENDIF

```

```

700 CONTINUE
ERR = CCC/(REAL(I)/4.-1000)
*** CONVERT THE SYMBOL ERROR RATE TO BER
ERR = ERR/4.
TT = (COUNT(I))/(REAL(NR)/4.)
XXX = 20.*LOG10( (.5)**.5/(3*C))
WRITE(13,*)XXX,ERR
511 CONTINUE

```

```

238 CONTINUE

```

```

STOP
END

```

```

REAL FUNCTION FF(ZR)
REAL ZR,X1,X2,X3,X4
X1 = 8.1081
X2 = 1.5413
X3 = 6.5202
X4 = -.0718
FF = X1*(ZR**X2)/(1 + X3*ZR**X2)
FF = FF + X4*ZR
RETURN
END
REAL FUNCTION PSI(ZR)

```

```

Y1 = 4.6645
Y2 = 2.0965
Y3 = 10.88
Y4 = -.003
PSI = Y1*ZR**Y2/(1. + Y3*ZR**Y2) + Y4*ZR
RETURN
END

```

```

REAL FUNCTION ANGL(XC, YC)
PI = 4.*ATAN(1.)
ANGL = ATAN(YC/XC)

```

```

IF(XC.LT.0.AND.YC.GT.0) ANGL = ANGL + PI
IF(XC.LT.0.AND.YC.LT.0) ANGL = ANGL - PI
RETURN
END

```

SAMPEL PROGRAM
(PI/4)-DQPSK

```

*****
*** B( ) GENERATED BITS
*** RB( ) RECEIVED BITS
*** U() DECISION VARIABLE
*** S() SENT VECTOR
*** RR() RECEIVED VECTOR
*** PB() THEORETICAL BIT ERR
*** NR # BITS TO BE TRANSMITTED
*** C1( ),C2( ): TAP GAIN COEFFICIENTS TO BE USED IN THE
        FREQUENCY-SELECTIVE FADING CHANNEL
PARAMETER(NN=25100,MM=50010,JV=5)
INTEGER NR ,B(MM),RB(MM),L(NN)

REAL GAUS1(NN),GAUS2(NN),PB(500),N0,GGAUS1
+ (NN),GGAUS2(NN),NN0,COUNT(100),ES,MIN,ANGLL(10),RPHASE(NN)
+ ,RALY1(NN),RALY2(NN),ALPHA(NN).A(10).PHASE(NN),RALY3(NN)

COMPLEX X(20),RR(NN),U(20),S(NN),ER.V(JV).VC(JV),CC(JV),R1(NN)
+ ,QX1
EXTERNAL FF,PSI

DELTA IS THE SEP SIZE IN THE EQUALIZER
*****
PI=4.*ATAN(1.)
DELTA=.01
ZERO=0
NR=50000
NNR=NR/2

INITIALISE THE VECTORS BY CONVERTING THEIR BINARY BIT
16 REPRESENTS 0000

INITIALISE THE TAP GAINS IN THE EQUALIZER
*****
DO 113 KC=1,JV
V(KC)=CMPLX(ZERO,ZERO)
113 CC(KC)=CMPLX(ZERO,ZERO)
*****
C=1./(2.**.5)

THE (PI/4)-DQPSK SIGNAL CONSTELLATION

```

```

*****
X(1)=CMPLX(1.*C, + 1.*C)
X(2)=CMPLX(ZERO, + 1.)
X(3)=CMPLX(-C,C)
X(4)=CMPLX(-1.,ZERO)
X(5)=CMPLX(-1.*C,-1.*C)
X(6)=CMPLX(ZERO,-1.)
X(7)=CMPLX(C,-1.*C)
X(8)=CMPLX(1.,ZERO)

*** GENERATE A RANDOM VARIABLE BETWEEN 0 AND 1
*** CONVERT IT TO BIT

CALL RNUN(NR,B)
DO 100 I=1,NR
IF (B(I).GT.0.5)THEN
B(I)=1
ELSE
B(I)=0
ENDIF
100 CONTINUE
KP=0
DO 109 J=1,NR,2
KP=KP+1
IF( KP.NE.1) THEN

*** CHANGE THE PHASE ACCORDING TO THE DATA

IF( B(J).EQ.1.AND.B(J+1).EQ.1) PHASE(KP)=PHASE(KP-1)+PI/4.
IF( B(J).EQ.1.AND.B(J+1).EQ.0) PHASE(KP)=PHASE(KP-1)-PI/4.
IF( B(J).EQ.0.AND.B(J+1).EQ.1) PHASE(KP)=PHASE(KP-1)+3*PI/4.
IF( B(J).EQ.0.AND.B(J+1).EQ.0) PHASE(KP)=PHASE(KP-1)-3*PI/4.
ELSE
B(1)=1
B(2)=1
PHASE(KP)=PI/4.
ENDIF

S(KP)=CMPLX(COS(PHASE(KP)),SIN(PHASE(KP)))
IF(PHASE(KP).GT.(2.*PI)) PHASE(KP)=PHASE(KP)-2*PI
IF(PHASE(KP).LT.(-2.*PI)) PHASE(KP)=PHASE(KP)+2*PI
109 CONTINUE

*** NOW S(K) REPRESENTS A COMPLEX VECTOR ACCORDING TO THE DAT

```

*** GENERATE A RAYLEIGH DISRIBUTED RANDOM VARIABLE

```
ISEED = 8743
NQ = NNR + 10
CALL RNNOA(NQ,RALY1)
ISEED = 76206
CALL RNNOA(NQ,RALY3)
ISEED = 9867
CALL RNNOA(NQ,RALY2)
```

```
DO 534 KJI = 1,NNR
ALPHA(KJI) = (ABS(RALY1(KJI))**2. + ABS(RALY2(KJI))**2.)**0.5
534 CONTINUE
```

*** GENERATE 2 INDEPENDENT GAUSS RANDOM VAR : GAUS1 AND GAUS2

```
ISEED = 123456
CALL RNNOA(NNR,GAUS1)
ISEED = 45876
CALL RNNOA(NNR,GAUS2)
ES = 1.
EB = .5*ES
DO 667 IZ = 20,20,2
N0 = (EB)/(10.**((REAL(IZ)/10.)))
```

***ADJUST THE NOISE VARIANCE

```
DO 19 IV = 1,NNR
GGAUS1(IV) = (N0/2.0)**.50* GAUS1(IV)
GGAUS2(IV) = (N0/2.0)**.50* GAUS2(IV)
19 CONTINUE
```

*** RR IS A COMPLEX VECTOR REPRESNTING THE RECIEVED SIGNAL

```
RR(1) = S(1)
RPHASE(1) = PI/4.
KX = 0
DO 400 I = 2,NNR
RR(I) = ALPHA(I)*S(I) + CMPLX(GGAUS1(I),GGAUS2(I))
*****
```

```
IF( MOD(MH,300).NE.0) THEN
READ(5,12) C1(I),C2(I)
ELSE
C1(I) = C1(I-1)
C2(I) = C2(I-1)
ENDIF
```

```

IF( I.GT.3) THEN
RR(I) = RR(I) + ( C1(I)*S(I-1) + C2(I)*S(I + 1) )
ELSE
RR(I) = S(I)
ENDIF
400 CONTINUE

SUM = 0
DO 404 I = 3, NR/4
C*****EQUALIZWER

V(1) = RR(I-2)
V(2) = RR(I-1)
V(3) = RR(I)
V(4) = RR(I + 1)
V(5) = RR(I + 2)
QX1 = 0
DO 978 KA = 1, JV
978 QX1 = QX1 + CC(KA)*V(KA)

c NOW WE FIND RR IS CLOSEST TO WHICH X
C L WILL REPRESNT THE CLOSEST VECTOR #
MIN = 1E6
DO 500 KJ = 1, 16
U(KJ) = QX1 - XX(KJ)
ZX = CABS(U(KJ))
IF(ZX.LT.MIN) THEN
MIN = ZX
L(I) = KJ
ENDIF
500 CONTINUE
C*****
C CALCULAT THE ERR
IF(I.LT.10000) THEN
ER = S(I) - QX1
ELSE
ER = XX( L(I) ) - QX1
ENDIF
C UPDATE THE COFF
DO 979 KA = 1, JV
REV = REAL( V(KA))
AMV = AIMAG( V(KA)) * (-1)
VC(KA) = CMPLX(REV, AMV)

```

```

979  CC(KA) = CC(KA) + DELTA * ER * VC(KA)
SUM = SUM + CABS(ER)
SUM2 = SUM / REAL(I)

```

```

404  CONTINUE

```

```

*** DEMODULATE
RB(1) = 1
RB(2) = 1
*** RPHSE IS THE PHASE OF THE RECEIVED SIGNAL
RPHASE(I) = ANGL(REAL(R1(I)), AIMAG(R1(I)))
IF ( RPHASE(I).LT.0) RPHASE(I) = RPHASE(I) + 2.*PI
DE = RPHASE(I) - RPHASE(I-1)
IF(DE.LT.0) DE = DE + 2.*PI
IF(DE.GE.0.AND.DE.LT.PI/2.) THEN
RB(KX + 1) = 1
RB(KX + 2) = 1
ENDIF
IF(DE.GE.PI/(2.0).AND.DE.LT.PI/1.) THEN
RB(KX + 1) = 0
RB(KX + 2) = 1
ENDIF
IF(DE.GE.PI.AND.DE.LT.3*PI/2.) THEN
RB(KX + 1) = 0
RB(KX + 2) = 0
ENDIF
IF(DE.GE.3*PI/(2.0).AND.DE.LT.2.*PI) THEN
RB(KX + 1) = 1
RB(KX + 2) = 0
ENDIF
404  CONTINUE

```

```

DEMODULATE:

```

```

*** NOW WE COMPARE THE SENT BITS B() WITH RECIVED ONES RB()
*** COUNT IS THE TOTAL ERROR RATE
*** CCC IS THE ERROR RATE AFTER EQUALIZER TRAINING IS FINISHE
KKK = 0
COUNT(II) = 0
CCC = 0
DO 700 I = 1, NR, 2
KKK = KKK + 1
IF(B(I).NE.RB(I).OR. B(I+1).NE.RB(I+1)) THEN
COUNT(II) = COUNT(II) + 1.
IF(I.LT.1000) GOTO 700

```



```
CCC=CCC + 1.  
ENDIF  
700 CONTINUE  
TT=(COUNT(I1))/(REAL(NNR))  
ERR=CCC/(REAL(NNR)-500.)  
WRITE(6,*)IZ + 10,TT  
667 CONTINUE  
STOP  
END
```

```
REAL FUNCTION ANGL(XC,YC)  
PI=4.*ATAN(1.)  
IF(YC.EQ.0) THEN  
IF(XC.LT.0) ANGL=PI  
IF(XC.GT.0) ANGL=0  
ELSE  
IF (XC.EQ.0) THEN  
IF(YC.GT.0) ANGL=PI/2.  
IF(YC.LT.0) ANGL=-PI/2.  
ELSE  
ANGL=ATAN(YC/XC)  
ENDIF  
ENDIF  
IF(XC.LT.0.AND.YC.GT.0) ANGL=ANGL + PI  
IF(XC.LT.0.AND.YC.LT.0) ANGL=ANGL-PI  
RETURN  
END
```

REFERENCES

Muhammad Abulma'atti. "Effects of Amplifier Nonlinearities on Error Rate in PSK Systems." Seventh Colloquium on Microwave Comm.: 538-541, 1982.

..... "A Non-linear Model for Microwave GaAs FET Amplifiers", Int. J. Electronics: 239-246, Vol. 57, No. 2, 1984.

F. Adachi and M. Sawahashi. "Performance Analysis of Various 16 Level Modulation Schemes under Rayleigh Fading Channels". Electronic Letters: 1579-1581, 13th August 1992.

F. Adachi and O. Koji. "BER Performance of QDPSK with Postdetection Diversity Reception in Mobile Radio Channels". IEEE Trans. on Vehicular Technology: 237-249, February 1991.

A.H. Aghvami. "Performance Analysis of 16-ary QAM Signaling through two-link Nonlinear Channels in Additive Gaussian Noise." IEEE Proceedings: 403-406, July 1984.

Yoshihiko Akaiwa. "Highly Efficient Digital Mobile Communications with Linear Modulation Method." IEEE Journal on Selected Areas in Communications: 89-895, June 1987.

Oreste Andrisano and Giorgio Corazza. "Adjacent Channel and Coherent Interference in CPFSK Systems with Nonlinear Transmitters and Limiter-discriminator Detection." Com-36: 544-552, May, 1988.

Oreste Andrisano and Nicola Ladisa. "On the Spectral Efficiency of CPM Systems over Real Channel in the Presence of Adjacent Channel and Cochannel Interference: A Comparison Between Partial and Full Response Systems." IEEE Trans. on Vehicular Technology: 89-100, May, 1990.

Sirikiat Ariyavisitakul. "Characterizing the Effects of Nonlinear Amplifiers on Linear Modulation for Digital Portable Radio Communications." IEEE Trans. on Vehicular Technology: 383-389, November, 1990.

H. Baher. "Analog & Digital Signal Processing" Wiley 1992.

Philip Bello. "Characterization of Randomly Time-Variant Linear Channels." Com-12: 360-393, December, 1963.

R. Blum and M.C. Jeruchim. "Modeling Nonlinear Amplifiers for Communication

- Systems." IEEE Conference on Telecommunication: 1468-1472, 1989.
- Raymond Bowers and Alfred Lee. *Communications for a Mobile Society*. Sage Publications 1978.
- Rudi de Buda. "Coherent Demodulation of Frequency-Shift Keying with Low Deviation Ratio." *Com-20*: 429-435, June, 1972.
- F.J. Casadevall et al. "Performance Analysis of QAM Modulations Applied to the LINC Transmitter, *IEEE Trans. on Vehicular Technology*, Vol. 42, 1993, pp. 399-406.
- Y.C. Chow, A.R. Nix and J.P. Mceehan. "Analysis of 16-APSK Modulation in AWGN and Rayleigh Fading Channel." *Electronics Letters*: 1608-1610, 13 August, 1992.
- Yoshimaso Daido, Sadao Takenaka, Eisuki Fukuda, Toshiak; and Hiroshi Nakamora. "Multilevel QAM Modulation Techniques for Digital Microwave Radios." *IEEE Journal on Selected Areas in Communications*, SAC-5(3): 336-341, April 1987.
- Philippe Dapuis, Michel Joindot, Alain Leclert and Dominiue Soufflet. "16 QAM Modulation for High Capacity Digital Radio System." *IEEE Trans. on Comm. Com-27(12)*: 1711-1781, December 1979.
- M.S. El-Hennaey and M.Y. Zaidan. "Performance of Data-driven Echo Cancellers and a New Simplified Structure." *Int. J. Electronics*: 47-64, Vol. 73, No. 1, 1992.
- David Falconer and Jack Salz. "Optimal Reception of Digital Data over the Gaussian Channel with Unknown Delay and Phase Jitter." *IEEE Trans. on Information Theory*: 117-125, January, 1977.
- Stefan Fochtel. "A Novel Approach to Modeling and Efficient Simulation of Frequency-Selective Fading Channels." *IEEE Journal on Selected Areas in Communications*: 422-431, April 1993.
- Victor Fung, Theodore S. Rappaport and Berthold Thoma. "Bit Error Simulation for $\pi/4$ DQPSK Mobile Radio Communications using Two-Ray and Measurement-Based Impulse Response Models." *IEEE Journal on Selected Areas in Communication*: 393-405, April 1993.
- F.D. Garber and M.B. Pursley. "Performance of Binary FSK Communications over Frequency-Selective Rayleigh Fading Channels." *IEEE Trans. on Comm.*: 83-89, January 1989.

..... "Performance of Differentially Coherent Digital Communications over Frequency-Selective Fading Channels." *IEEE Trans. on Comm.*: 21-31, January 1988.

A. Ghorban and M. Sheikhan. "The Effect of Solid State Power Amplifiers Non-linearities on MPSK and M-QAM Signal Transmission." *IEEE Conference on Telecommunication*: 193-197, 1986.

William Gosling. "A Simple Mathematical Model of Co-Channel and Interference in Land Mobile Radio." *IEEE Trans. on Vehicular Technology*: 361-364, November 1980.

Hans Guren and Nilo Holte. "Decision Feedback Sequence Estimation for Continuous Phase Modulation on a Linear Multiple Channel." *IEEE Trans. on Comm.*: 280-284, February 1993.

Masaharu Hata. "Empirical Formula for Propagation Loss in Land Mobile Radio Services." *IEEE Trans. on Vehicular Technology*: 317-325, August 1980.

Simon Haykin. *Digital Communications*. John Wiley & Sons, 1988.

Tricia Hill and Kamilo Feher. "A Performance Study of NLA 64-State QAM." *IEEE Trans. on Comm.*: 821-826, June 1983.

Kenkichi Hirade and Kazuaki Murota. "GMSK Modulation for Digital Mobile Radio Telephony." *IEEE Trans. on Comm.*: 1044-1050, July 1981.

Peter Hoher. "A Statistical Discrete-Time Model for the WSSUS Multipath Channel." *IEEE Trans. on Vehicular Technology*: 461-468, November 1992.

I.K. Hwang et al. "Digital Data Transmission over Nonlinear Satellite Channels, Vol. 41, 1993, *IEEE Trans. on Communications*, pp. 1694-1702.

Mitsuru Ishizaka and Yashaiko Yasudo. "Improved Coherent Detection of GMSK." *IEEE Trans. on Comm.*: 308-311, March 1984.

A. Jones and J. Gardiner. "Performance of GMSK in Nonlinear Channel." *Electronics Letters*: 1605-1607, 13 August 1992.

Chuang Justin. "The Effects of Time Delay Spread on Portable Radio Communications Channels with Digital Modulation." *IEEE Journal on Selected Areas in Communications*. SAC-5(5): 879-888, June 1987.

..... "The Effects of Delay Spread on 2-PSK, 4-PSK, 8-PSK and 16-QAM in Portable Radio Environment." *IEEE Trans. on Vehicular Technology*: 43-45,

May 1989.

Jean-Francois Lemieux, Mohamed S. El-Tanany and H.M. Hafez. "Experimental Evaluation of Space/Frequency/Polarization Diversity in the Indoor Wireless Channel." *IEEE Trans. on Vehicular Technology*: 569-574, August 1991.

William Lee. *Mobile Cellular Telecommunications Systems*. McGraw-Hill, 1989.

William C. Lindsey and Marvin K. Simon. *Telecommunication Systems Engineering*. Prentice-Hall, Inc., 1973.

Chia-Liang Lin and Kamilo Feker. "Bit Error Rate Performance of $\pi/4$ -DQPSK in a Frequency-Selective Fast Rayleigh Fading Channel." *IEEE Trans. on Vehicular Technology*: 558-568, August 1991.

Imberto Mengali. "Joint Phase and Timing Acquisition in Data-Transmission." *IEEE Trans. on Comm. Com-25(10)*: 1174-1185, October 1997.

Kurt Metzger and Rolf Valentin. "An Analysis of the Sensitivity of Digital Modulation Techniques to Frequency-Selective Fading." *IEEE Trans. on Comm. Com-33(9)*: 986-992, September 1985.

James W. Modestino and Kurt Matis. "Interactive Simulation of Digital Communication Systems." *IEEE Journal on Selected Areas in Communication*. SAC-2(1): 51-59, January 1984.

Douglas Morais and Kamilo Feher. "NLA-QAM: A Method for Generating High-Power QAM Signals Through Nonlinear Amplification." *IEEE Trans. on Comm. Com-30(3)*: 517-522, March 1982.

K. Ohno, F. Adachi and K. Kawamura. "Combined Effect of Diversity Reception/Channel Coding on Error Floor due to Delay Spread in DPSK Mobile Radio." *Electronics Letters*: 1131-1133, 4 June 1992.

..... QDPSK Signal Transmission Performance with Postdetection Selection Diversity Reception in and Mobile Radio." *IEEE Trans. on Vehicular Technology*: 795-804, November 1991.

Christoff K. Pauw and Donald L. Shilling. "Probability of Error of M-ary PSK and DPSK on a Rayleigh Fading Channel." *IEEE Trans. on Comm. Com-36(6)*: 755-756, June 1988.

Peyton Z Peebles. *Digital Communication Systems*. Prentice-Hall, 1987.

- John G. Proakis. *Digital Communications*. McGraw-Hill, 1989.
- Theodore S. Rappaport and Victor Fung. "Simulation of Bit Error Performance of FSK, BPSK, and $\pi/4$ DQPSK in Flat Fading Indoor Radio Channels Using a Measurement-Based Channel Model." *IEEE Transactions on Vehicular Technology*: 731-740, November 1991.
- William Rummier. "More on the Multipath Fading Channel Model". *IEEE Trans. on Comm. Com-29(3)*: 346-352, March 1981.
- Saud Al-Semari. "Performance of TCM with Concatenated Codes over Fading Channels." M.Sc. Thesis, King Fahd University of Petroleum and Minerals, Dhahran, Saudi Arabia, 1992.
- Mansoor Shafi. "Statistical Analysis/Simulation of a Three Ray Model for Multipath Fading with Applications to Outage Prediction." *IEEE Journal on Selected Areas on Communications. SAC-5(3)*: 389-404, April 1987.
- K San Shanmugan, Michel C. Jeruchim and Philip Balaban. *Simulation of Communication Systems*. Plenum Press, 1992.
- Curtis Siller, Jr. "Multipath Propagation." *IEEE Communication Magazine*, 22(2): 6-15, February 1984.
- Morvin K. Simon and Charles Wang. "Differential Detection of Gaussian MSK in a Mobile Radio Environment." *IEEE Transactions on Vehicular Technology*: 307-320, November 1984.
- Bernard Sklar. *Digital Communications Fundamentals and Applications*. Prentice-Hall, 1988.
- John I. Smith. "A Computer Generated Multipath Fading Simulation for Mobile Radio". *IEEE Transactions on Vehicular Technology*: 30-31, August 1975.
- Seymour Stein. "Fading Channel Issues in Systems Engineering." *IEEE Journal on Selected Areas on Communications, SAC-5(2)*: 68-89, February 1987.
- Hiroshi Suzuki. "Optimum Gaussian Filter for Differential Detection of MSK." *IEEE Trans. on Comm. COM-29(6)*: 916-918, June 1981.
- Gottfried Ungerboeck. "Channel Coding with Multilevel/Phase Signals." *IEEE Trans. on Information Theory*: 65-67, January 1982.
- Prabodh Varshney and Surinder Kumar. "Performance of GMSK in a Land Mobile

Radio Channel." IEEE Transactions on Vehicular Technology: 607-614, August 1991.

W.T. Webb, L. Hanzo and R. Steele. "Bandwidth Efficient QAM Schemes for Rayleigh Fading Channels." IEE Proceedings-I: 169-175, June 1991.

William J. Weber. "Differential Encoding for Multiple Amplitude and Phase Shift Keying Systems." IEEE Transactions on Comm. COM-26(3): 385-390, March 1978.

K. Wayts and M. Moeneclacy. "BER Performance on Multipath Fading Channels with Random Path Delays." Electronics Letters: 1618-1619, 13 August 1992.

Abbas Yongacoglu, Dimitrios Makrokis and Kamilo Feher. "Differential Detection of GMSK Using Decision Feedback." IEEE Transactions on Comm. COM-36(6): 641-649, June 1988.